The Mechanism of CD24-Mediated Apoptosis in Bone Marrow-Derived Early B-cells.

by

©D. Craig Ayre

A Thesis submitted to the School of Graduate Studies in partial fulfilment of the requirements for the degree of

Master of Science

Department of Biochemistry, Faculty of Science

Memorial University of Newfoundland

May 2014

St. John's Newfoundland

Abstract

B cells are the antibody producing cells of the mammalian immune system and are formed through a differentiation and maturation process in the bone marrow. The glycophosphatidylinositol (GPI)-linked cell surface receptor CD24 causes apoptosis in the earliest B-cell developmental stages. As it has no transmembrane domain, the signal transduction mechanism of CD24 is not well understood and is the focus of this thesis. Using a bioinformatics approach, several genes were identified that are involved in apoptosis, cytoskeletal organization and endocytosis and whose pattern of expression tightly correlated with CD24. In addition, it was shown that extensive crosslinking of CD24 is required to mediate apoptosis in primary B-cells. Moreover, following crosslinking, CD24 protein is rapidly transported to the cell surface and then endocytosed. Lastly, it was observed that CD24 mediates homeotypic adhesion and is closely associated with cell-cell junctions. These data may provide new insight into the mechanism by which GPI-linked receptors activate intracellular signalling pathways.

Acknowledgements

Without question, my first thanks must go to Dr. Sherri Christian, my supervisor. Without her support, motivation, guidance and overabundance of patience I could not have even begun a career in science, let alone accomplish this long-held goal. I know that wherever I go from here, it started with her willingness to say, "Yes."

I am also deeply grateful to my supervisory committee, Dr. Margaret Brosnan and Dr. Martin Mulligan, for their help in steering this project and for their support through this process.

A hard-earned thank you is also due to the entire Christian lab, upon which I inflict myself daily. I have never been more proud to be associated with such fine group of people. They transformed this experience into a true pleasure.

My friends and family have carried me through the best and the worst, have endured much and I have gained much because of you. To my parents and my brother, you are the best. Everything else I can say is insufficient. Finally, my deepest gratitude and admiration must go to my wife Laura. On many days she has become a lab widow as I worked. She encouraged me to leave behind a successful career to follow a childhood dream. Without her continual grace, persistence and love I could never have achieved this goal. Anything I may ever accomplish is thanks to her.

Table of Contents

Table of Contents

Table of Contents

List of Tables

List of Figures

List of Figures

List of Abbreviations

Ab	Antibody
Ag	Antigen
AP1AR	adaptor-related protein complex 1 associated regulatory protein
AP-2	Adapter Protein-2
BCR	B cell receptor
BCR-Abl	Breakpoint cluster Region-Abelson Fusion Protein
CHCHD10	Coiled-coil-helix-coiled-coil-helix domain containing 10
CLP	Common Lymphoid Progenitor
Cyanine	Cy
CytoD	Cytochalasin D
DAMP	Danger Associated Molecular Pattern
DAPI	4',6-diamidino-2-phenylindole
DAVID	Database for Annotation, Visualization and Integrated Discovery
DMSO	Dimethyl sulfoxide
EGFR	Epidermal Growth Factor Receptor
EHD2	Eps Homology 15 Domain Containin 2
EtBR	Ethidium Bromide
FACS	Fluorescent Activated Cell Sorting
FCHO1	FCH Domain Only-1
FITC	Fluorescin Isothiocyanate
FrA	Fraction A
FrBC	Fraction B/C
FrC	Fraction C′
FrD	Fraction D
FrE	Fraction E
FrF	Fraction F
GBAS	glioblastoma amplified sequence
GEF	Guanine Exchange Factor
GLUT4	Glucose Transporter Type 4
GO	Gene Ontoloy
GPI	Glycophosphatidylinositol
HSA	Heat Stable Antigen
HSC	Hematopoietic Stem Cell
HSP2	Heat Shock Protein 2
Ig	Immunoglobin
IgH	Immunoglobulin Heavy Chain
IgL	Immunoglobulin Light Chain
IL-7	Interleukin-7

ImmGen	Immunological Genome Project
ITAM	Immunoreceptor Tyrosine-based Activation Motif
JNK	Jun Amino-Terminal Kinases
LPS	Lipopolysaccharide
MAPK	Mitogen Activated Protein Kinase
mbAb	Membrane Bound Antibody
MCF2L	MCF.2 Cell Line Derived Transforming Sequence-like
MIAME	Minimum Information About Microarray Experiments
MMLV	Moloney Murine Leukemia Virus
MTT	3-(4,5-Dimethylthiazol-2-yl)-2,5-diphenyltetrazolium bromide
N-CAM	Neuronal Cell Adhesion Molecule
PBS	Phosphate Buffered Saline
PC	Plasma Cell
PCR	Polymerase Chain reaction
Peridinin chlorophyll	PerCP
Phycoerythrin	PE
PI	Propidium Iodide
Pre	Precursor
Pro	Progenitor
PTK	Protein Tyrosine Kinase
PTPRC	Protein tyrosine phosphatase, receptor type, C
QS	Quin Saline
RABL5	Rab-Like 5
RMA	Robust Multi-Array Average
RPLPO	Large Ribosomal Protein
RTK	Receptor Tyrosine Kinase
SAPK	Stress-Activated Protein Kinase
SDF-1	Stromal Cell-Derived Factor
SH3GL2	SH3-Domain Containing, Growth Factor Receptor Bound Protein-Like 2
siRNA	Small Interfereing RNA
SL	Surrogate Light Chain
T1	Transitional Stage 1
TCR	T Cell Receptor
TLR	Toll-Like Receptor
TrkA	Insulin Receptor and the Neurotrophin receptor
uPAR	urokinase plasminogen activator receptor
UTR	Untranslated Region
VCAM-1	Vascular Cell Adhesion Molecule-1
VLA-4	Very Late Antigen-4

List of Appendices

CHAPTER 1: INTRODUCTION

1.1 B Cell development

B lymphocytes are an important cell type in adaptive immunity. Their primary function is to produce antibodies (Abs) against foreign macromolecules, termed antigens, as part of the immune response (1). Mammalian B lymphocytes (B cells) arise through a development process that requires stem cells to become committed to the B cell lineage following a highly regulated maturation process in the bone marrow (2, 3). The overall goal of B cell development in the bone marrow is to create a functional B cell receptor (BCR) that is capable of recognizing foreign antigens but cannot bind self-antigen. This process depends on sequential expression of the different components of the BCR as well as other accessory proteins necessary for overall B cell function.

Hematopoietic stem cells (HSC) reside in the bone marrow and give rise to all blood cells, including B cells (3). HSC first become restricted to developing a single cell type, which is termed lineage commitment. HSC's that become lymphoid committed are termed Common Lymphoid Progenitors (CLP), which become further committed to one of the lymphoid cell lines, such as B cells, T cells or Natural Killer cells (3). The defining characteristic of B cells is their expression of the B Cell Receptor (BCR), which is made up of multiple proteins of the immunoglobin (Ig) superfamily (Fig. 1.1). The antigen (Ag) binding portion of the BCR is a heterodimer consisting of two identical heavy chains (IgH) and two identical light chains (IgL), which form the membrane-bound Ab (mbAb) (1). This structure is anchored to the plasma membrane via a transmembrane domain (4). The mbAb forms a complex with CD79α and β (also known as Igα/β), which activates

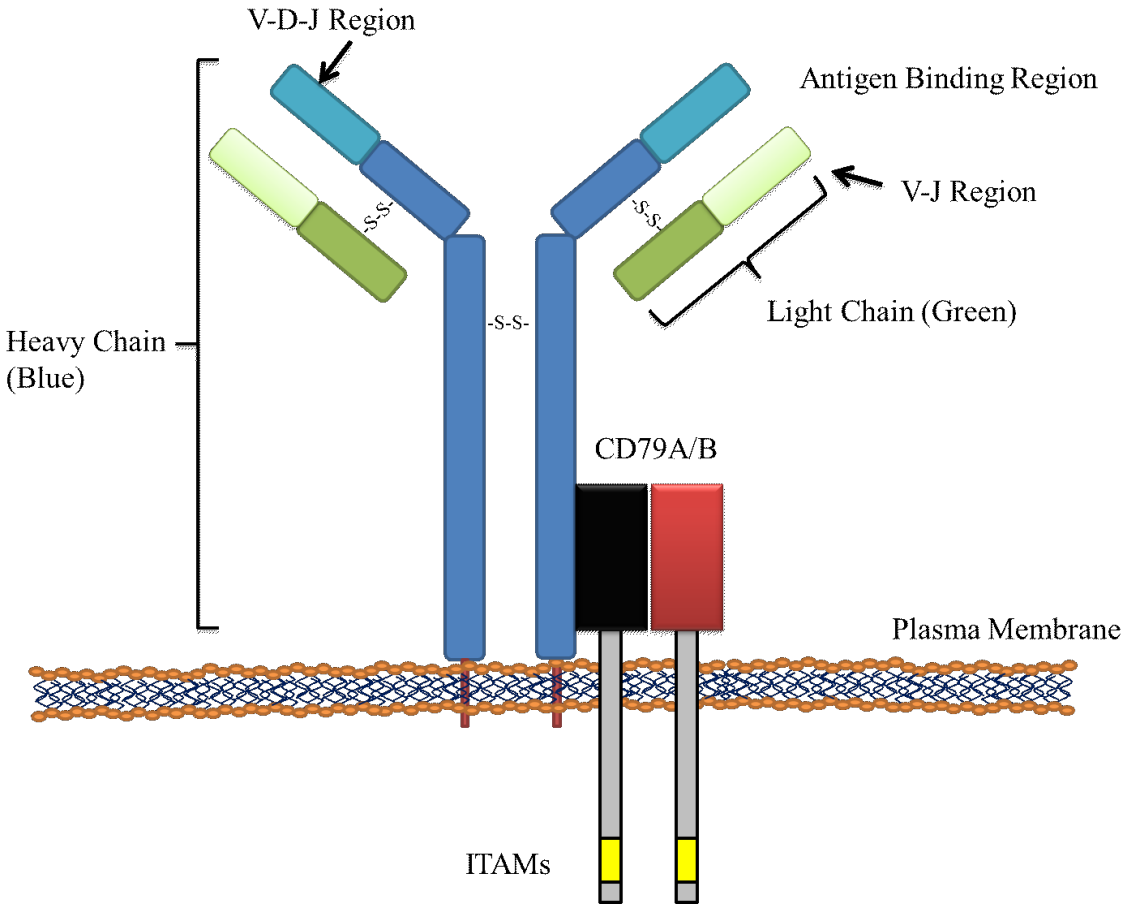

Fig. 1.1: The B cell Receptor. The completed B cell receptor consists of two IgH heavy chains and two IgL light chains bound by disulfide bonds. Antigens are bound by the antigen recognition site defined by the V(D)J segments. Signal transduction occurs through the associated CD75A/B proteins (also known as the Ig α/β) through the immunoreceptor tyrosine-based activation motif (ITAM) structure.

signal transduction pathways in response to binding of the mbAb to antigen (Ag) (4).

The development of B cells is divided into phases that are defined by the successful formation of various BCR components (1). Both the IgH and IgL chains of the BCR are encoded from rearrangement of different gene segments termed Variable (V), Diversity (D), and Joining (J), followed by a Constant (C) region (5). There are two light chain gene loci (termed kappa and lambda) that are composed of several V and J gene segments followed by a constant region. During formation of the light chain, only the kappa or the lambda loci will be expressed. The mature light chain consists of a single V and J gene segment combined with a constant region (5). The heavy chain loci contain V, D and J gene segments and one of 5 possible constant region isoforms, Alpha, Delta, Epsilon, Gamma and Mu. The BCR is mostly commonly expressed as the Mu, and Delta isoforms (IgM and IgD) but can also exist in the other isoforms depending on the cell type and developmental stage (5). These gene rearrangements occur at different times within the B cell maturation process. The earliest developing B cells, termed progenitor (pro-) B cells, begin rearranging the IgH gene, and this process is completed at the final stage of the pro-B cell development phase (6). During this phase the V, D and J gene segments of IgH recombine with a Mu constant region to form the IgH chain. Also during this time, a second structure termed the surrogate light chain (SL) is also formed to serve as a placeholder before the proper IgL chain is formed (6). The expression of the combined IgH/SL protein on the cell surface acts as the pre-B cell receptor and marks the transition of pro-B cells to precursor, or pre-B cells (3, 6). Pre-B cells are now required to complete the formation of the IgL chain and express the completed BCR (consisting of the IgH/IgL structure) on the cell surface. As such, an analogous process to IgH

rearrangement occurs in the light chain genes between the V and J segments and its constant gene (5). After successful generation of the IgH and IgL chains, a BCR is expressed on the cell surface. At this point, the cell is termed immature and is released from the bone marrow into peripheral lymphoid tissues such as the spleen or lymph nodes (2). The antigen recognition site (defined by the V, D and J segments) of the B cell receptor is identical to the antibodies a given B cell can express.

The B cell development process is highly stringent and large numbers of cells are purged via apoptosis at multiple checkpoints (7). Many potential B cell receptors can be generated from the genome, and this process is random. In effect, the number of potentially useful BCRs is dwarfed by the generation of inappropriate receptors. These receptors are subjected to a process termed allelic exclusion. Editing may occur during formation of either the IgH or IgL chains. Initially, IgH or IgL rearrangement occurs on only one of the sets of alleles (one on each parental chromosome). When non-functional IgH chains are formed, B cells are induced to attempt rearrangement from the unused chromosome. Failure a second time to generate a functional BCR results in apoptosis of the pro-B cell. Similarly, the IgL chain can undergo allelic exclusion where failure also results in apoptosis.

Of greater concern to generating non-functional receptors is the formation of BCRs that recognize self-antigen. To become active and produce antibodies, B cells must receive signals through the BCR and other co-stimulatory receptors such as CD40 (8). Recognition of self-antigen would normally occur in the absence of co-stimulation and these B cells would also be purged through apoptosis (8). This process is imperfect,

however and occasionally B cells may survive this selection process, which can lead to the development of autoimmune disease.

B cell development is a delicate balance between receiving appropriate growth and differentiation stimuli, and the induction of apoptosis (6). Indeed, it is at the pro- to pre- B cell checkpoint that CD24 is thought to function, potentially, as a gatekeeper to downstream development (9, 10). Assuming a cell passes these checkpoints immature B cells travel to secondary lymphoid structures and undergo further maturation before entering a quiescent phase as a naïve B cell. It is these naïve B cells that can bind antigens and receive appropriate co-stimulation from T lymphocytes to produce antibodies (1).

1.2 The Hardy fractions

The pro-B and pre-B cell developmental stages have been further refined into more discrete phases with the advent of Fluorescent Activated Cell Sorting (FACS). FACS works on the principle of tagging cell surface proteins typically using antibodies labelled with fluorescent molecules. These antibodies can then be detected by a flow cytometer using lasers at a set wavelength, which excites the fluorophore with the subsequent emission registered by a photomultiplier tube or charged couple device (11). As such, it became possible to delineate cell populations based on the expression of characteristic surface markers, and also to quantify the relative expression of these markers among different samples.

In seminal work, Richard Hardy and colleagues (2, 12) used FACS to subdivide the pro- and pre-B cell fractions into more discrete stages (Fig. 1.2). The earliest marker

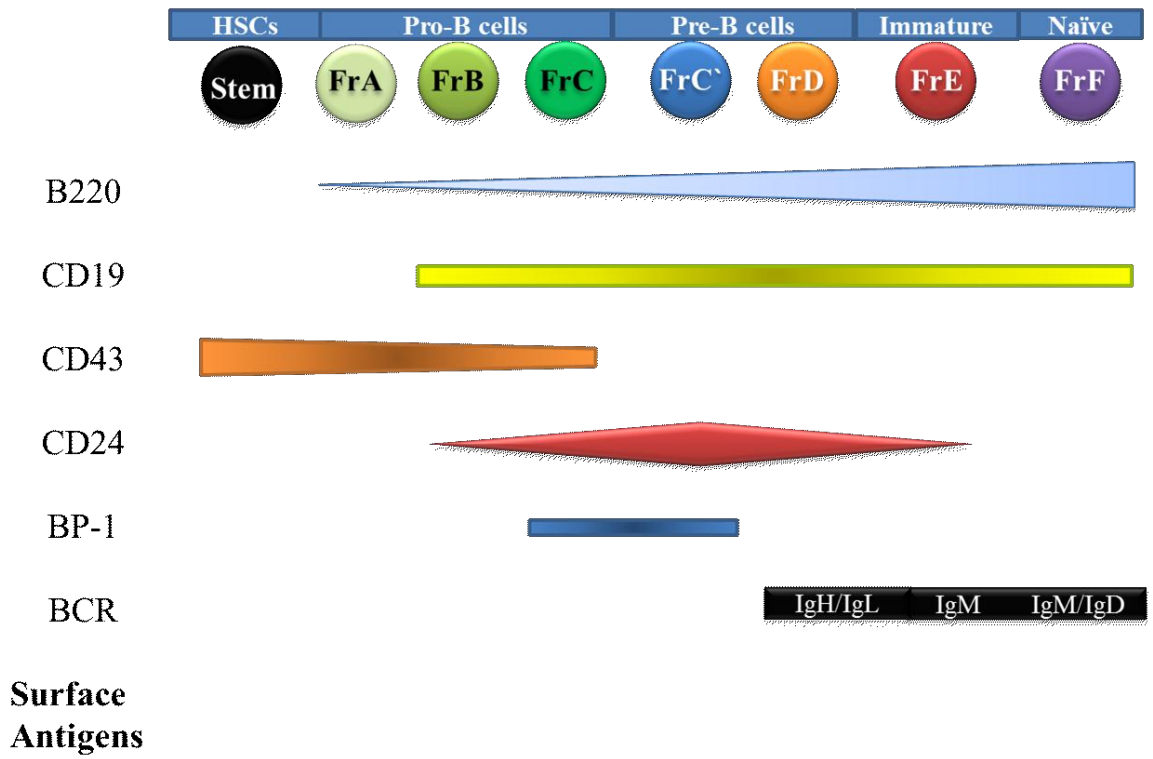

Fig. 1.2: The Hardy Fractions and B Cell Developmental Markers. Fr stands for Hardy Fraction. CD19 and B220 are used as pan-B cell markers in the bone marrow. CD43 expression defines the pro-B cell phase, which is further subdivided by CD24 and BP-1 expression. The development of B cell receptor proteins defines the pre- and immature B cell phases. Adapted from Hardy, et al 1991 (2, 12).

expressed on cells that will become B cells is transmembrane protein B220, also known as protein tyrosine phosphatase receptor type C (PTPRC) or CD45R. Thus, Hardy et al. (2) began by dividing cells into those that express B220 (B220+) from those which did not (B220-). All cells expressing B220 were considered developing B cells, while the rest were excluded. These B220+ cells were similarly subdivided into CD43+ and CD43- populations, corresponding to pro- and pre-B cells, respectively. The CD43+ pro-B cells could be further divided into 3 groups, termed fractions A, B and C using expression of CD24 and BP-1 (Glutamyl Aminopeptidase). Fraction A was CD43+, CD24- and BP-1-; Fraction B; CD43+, CD24+ and BP-1; and fraction C; CD43+, CD24+ and BP-1+ (2). Subsequent experiments proved that these fractions demonstrated a temporal relationship with fraction A being the most immature and giving rise to B and then on to C (2). Hardy et al. (2) also determined that the C fraction contained a subpopulation which had higher expression of CD24 and was subsequently termed C′. Similarly the CD43-, pre-B cells were divided into fractions D, E and F using their relative expression of the IgM isoform of the BCR and B220.

Further research by Hardy and others determined that while B220 is expressed on all bone marrow B cells, it is also expressed in a variety of other isoforms in multiple cell types (13) and cannot unambiguously denote any given cell populations in the absence of other markers (14). Subsequently, CD19 has proven to be a better marker for B cells in the bone marrow as it is expressed on all cells in fractions B through F (3, 15). Although CD19 is not expressed on Fraction A cells, more recent research has found that cells in fraction A are heterogeneous and are not yet fully committed to the B cell lineage (3, 16)

Thus, CD19 expression in the bone marrow now serves as a gold standard marker for in vivo, ex vivo, and in vitro work on bone marrow-derived B cells.

1.3 The CD24 cell surface receptor

As identified by Hardy and others, CD24 (also known as Heat Stable Antigen or Nectadrin) is differentially expressed during B cell development in mice (2, 17). Human CD24 is also differentially expressed between developing and mature B cells (17). It was reported that the highest CD24 expression corresponded to immature developing B cells and upon maturation expression was reduced (17). Later research demonstrated that CD24 expression was not permanently abolished. In peripheral lymphoid tissues mature B cells undergo a brief terminal differentiation before they have the ability to be activated. These cells are termed Transitional B cells and CD24 expression is regained (18) during the earliest part of this process (18). Once mature, B cells lose most or all of their CD24 expression (18, 19).

CD24 was first isolated in 1978 as part of a project to generate rat antibodies against mouse B cell surface proteins (20, 21). The protein was isolated using the antibodies M1/69 and M1/75 and named Heat Stable Antigen (HSA) in accordance with its high thermal stability. The human gene was isolated in 1991 and both the mouse and human CD24 genes were shown to be approximately 240 bp with a long, ~1.6 kb 3' untranslated region (UTR) (Fig. 1.3). The final mature protein is very short, containing 27 or 31 amino acids in the mouse or human version, respectively. The mature protein is also extensively and variably N- and O- glycosylated (22) in a tissue-specific fashion. Thus the final weight of the protein can range from 20 to 80 kDa (23).

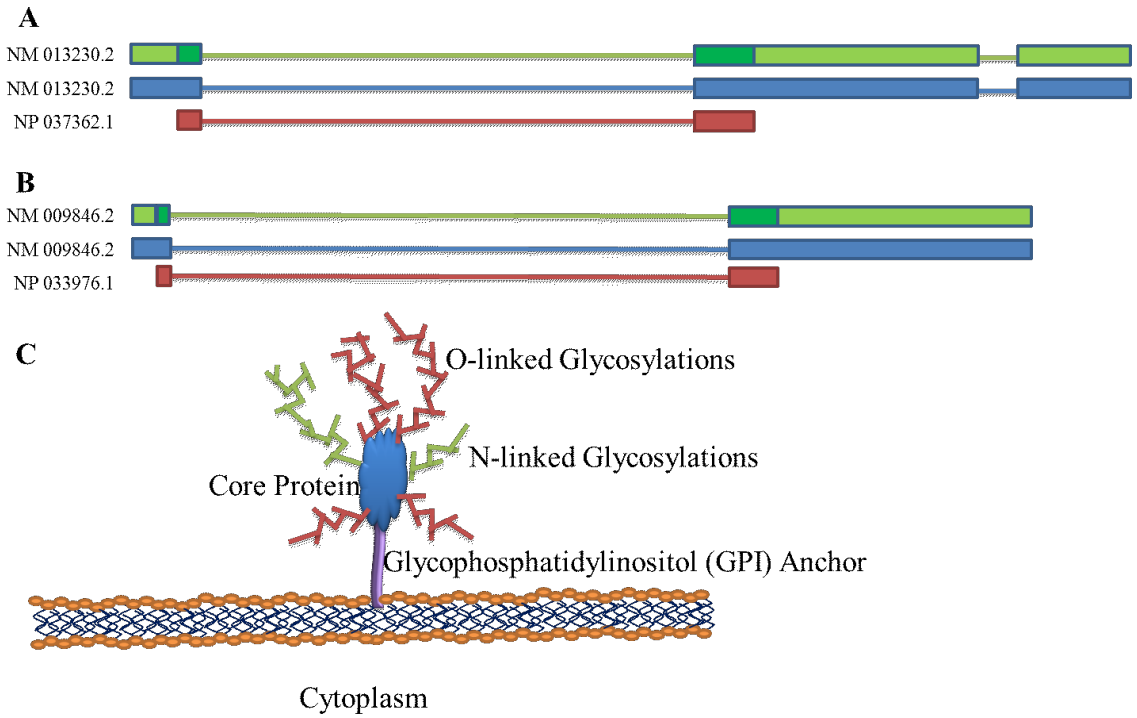

Fig. 1.3: CD24 in Human and Mouse. A. Human CD24 (6q21). Total mRNA transcript 2194 bp B. Mouse CD24A (10 23.01 cM). Total mRNA transcript 1825 bp. Information retrieved from NCIB Entrez ID 12484 (Mouse) and 100133941 (Human). Green lines represent genomic structure with dark green indicating coding regions and light green the 5' and 3' untranslated regions. Exons are denoted by thick lines, introns by thin lines. Blue represents the primary mRNA transcript and red represents the processed mRNA for protein translation. C. Schematic representation of CD24 on the cell surface. The core protein is linked by a GPI anchor. O-linked glycosylations are likely on C and N-terminal regions, with N-linked glycosylations towards the center.

The CD24 protein is bound to the outer leaflet of the cell membrane through a glycosylphosphatidylinositol (GPI) anchor in both mouse and human cells (24). This glycolipid structure could be cleaved using Phospholipase C, which subsequently removed the protein from the membrane (24). This established conclusively that mature CD24 has no transmembrane structure, but left unaddressed questions as to how it might function.

A variety of different CD24 'forms' have been identified due to the differential pattern of glycosylation found on the protein when isolated from various tissues. Therefore it is not unexpected that several potential ligands for the receptor have also been identified. Research into CD24 activity in the small lung cell cancer line SW2 and the breast cancer cell line KS demonstrated a high affinity binding for P-selectin (25, 26), but not the other selectins, suggesting a highly specific affinity (26). CD24 protein isolated by affinity purification interacts with CD171, a cell adhesion molecule also known as L1 and is known to promote neurite outgrowth (20). Finally, in hematopoietic cells, CD24 is known to bind P-selectin and so-called Danger Associated Molecular Patterns (DAMPs) and Siglec G in a trimeric protein moiety (20, 27). CD24 has even been shown to engage in homotypic interactions. This wide range of binding partners and highly variable nature of the post-translational modifications supports the argument that CD24 may participate in an unusually diverse repertoire of physiological functions. Based on this diversity, CD24 may arguably be considered to be a pseudo-family of proteins that share a common protein motif and variable carbohydrate branch 'isoforms'. Despite its first discovery in the late 1970's (21), and its subsequent isolation from a wide range of

cell types, little is known about the underlying role of CD24 in B cell development, and less is known about the mechanism through which it operates.

1.4 CD24 regulates cell survival and adhesion in a cell type dependent manner

CD24 is expressed in a wide variety of cell types and is known to mediate differing processes such as cell adhesion, cell-fate decisions, or participate in cell cycle control and pro-life/pro-death responses depending on the source of the cell type examined. One of its earliest established functions was in cell-cell adhesion between B cells. (28). CD24 is now also known to regulate cell adhesion in developing neuronal tissue (20) while also participating in synaptic transduction (29) and neuronal growth. Other studies have shown that CD24 moderates tumour cell invasiveness and is associated with increased cell proliferation (23). In other studies relating to its role in tumour biology, CD24 has proved to be a valuable biomarker in several malignancies, including carcinomas, sarcomas, lymphoma and leukemia. Shortly after the genomic sequence of CD24 was identified, it was found that CD24 is highly expressed on small lung cell carcinoma (30). CD24 was also highly overexpressed in a majority of hepatocellular carcinoma samples from 79 human samples, but not expressed in non-tumour liver cells (31). In 2002, increased CD24 expression was identified to be a highly significant prognostic indicator of decreased survival time in ovarian cancer (32), non-small cell lung cancer (33) and glioma (34). Moreover, inhibition of CD24 expression in hepatocellular carcinoma and breast cancer cell lines showed a decrease in cellular proliferation (35, 36). Together, these data show CD24 is active in a wide range of cellular contexts.

Research from these diverse fields has consistently demonstrated that CD24 functions as a cell surface receptor, mediates the way cells adhere to neighbouring cells, and moderates the balance between pro-apoptotic and pro-survival signals, As such, it provides context to examine the role of CD24 in B cells as these same functions are dynamically regulated in the bone marrow during B cell development. First, B cell development is critically dependent on receiving and responding to time-appropriate signalling events from external factors, such as Interleukin-7 (IL-7) secreted by stromal cells (37). Second, early progenitor B cells are contact-dependent on the bone marrow stroma but release from the stroma upon transition to the pre-B cell development stage (2, 38). Third, these cells must also tightly regulate the pro-proliferative and pro-apoptotic signals they receive to ensure only appropriate B cells exit the bone marrow (39, 40). We can therefore argue that while the cellular context may be different, the underlying role of CD24 appears to be involved in mediating these pro-survival vs. pro-apoptotic events and thus insight into CD24 is broadly applicable to many disciplines.

It was established early that CD24 was a signalling molecule in B cells (17, 41) but much of the earliest research focused instead on its role in cell adhesion (42). One of the earliest studies on CD24-mediated adhesion examined its role in multiple cell types (28). CD24 was found to be preferentially expressed at the junctions between cells in B lymphocytes, neuroblastoma and neuronal cells. Furthermore, CD24 was isolated from B cell lymphoma cell line ESb 289 in two major isoforms: a large, 40-60 kDa and small 23-30 kDa form. The larger form was shown to have strong homotypic (self) binding properties, and it was shown that blocking CD24 with mouse monoclonal antibody 79 (mAb79) antibodies abolished this (28). The smaller form was suggested to be a cleavage

product from the larger, through removal of specific glycosylations, and did not mediate this binding. This suggested that CD24 can have different roles depending on the form expressed by the cell, although this was not clearly established. Kadmon et al.(28) demonstrated that CD24 functioned in neurons through interactions with L1 and Neuronal Cell Adhesion Molecule (N-CAM) on the same cell (43). The results clearly demonstrated that CD24 actively moderated the signalling response as engagement of both CD24 and L1 together resulted in a 6- to 10- fold increase in intracellular calcium than when they were engaged individually (43).

Despite the evidence for its role in signal transduction, it was over 20 years before an endogenous ligand, other than itself, was identified for CD24. It was hypothesized that the extensive and variable carbohydrate motifs (glycosylations) may be part of the mechanism by which CD24 could mediate different downstream events through multiple ligands (26). Multiple studies have shown that P-selectin, one member of the lectin family of carbohydrate binding proteins normally expressed on endothelial cells and platelets, bound to CD24 (25, 26). This binding was established to be highly specific, as a closely related protein, E-selectin, did not bind (26). Changing the glycosylations by treatment with O-sialoglycoprotein.endopeptidase, which removes O-linked glycosylations from CD24, abrogated this binding (25). These results established that P-selectin was specifically binding to CD24 in humans. Further research has also shown that the CD24-L1 interactions in neuronal cells are dependent on the presence of sialic acid bound to the CD24 protein (44). Removal of the sialic acid abrogated CD24 binding in this cellular context (44). The intracellular signalling events mediated by CD24-ligand binding were not identified at this time, but have been the focus of subsequent work.

Despite evidence that CD24 affects intracellular processes and the discovery of an endogenous ligand, little had been demonstrated with regard to the mechanism of how it signals. While Kadmon et al. (28) showed that CD24 interacted to co-operatively signal with cell adhesion molecules, nothing was known about CD24's intrinsic signalling properties. Evidence that CD24-mediated Src Protein Tyrosine Kinase (PTK) activation in T cells (45) was one of the first results demonstrating that CD24 directly interacts with signalling proteins. Further research in B cells showed that CD24 induces the rapid phosphorylation of the mitogen-activated protein kinases (MAPK) ERK, p38 and Jun amino-terminal kinases (JNK)/Stress-Activated Protein Kinases (SAPK) (46). These findings were the first data to identify a downstream signalling pathway that participates in CD24-mediated regulated of apoptosis. In subsequent studies in colorectal cancer cells, CD24 was shown to regulate ERK activation as a mechanism for controlling cellular proliferation (34, 47). Taken together, these results firmly established that CD24 has an active role in mediating cell proliferative events in multiple cell types, including B cells and cancer cells.

1.5 The role of CD24 in B cell development

CD24 expression in murine B cells has been known since 1978 (21). The first study to demonstrate a role for CD24 in B cell development was not published until 1990 (27). The previously discussed dynamic regulation of CD24 expression, which is highest at the pro- to pre-B cell transition, is strongly suggestive of a functional role at this developmental checkpoint. Research at this time established that CD24 functioned as a cell adhesion molecule (28). Furthermore, Hahne et al. (42) demonstrated that CD24

actively moderated the ability of pre-B cells to attach to bone marrow stroma by altering adhesion of the integrin Very Late Antigen-4 (VLA-4) to Vascular Cell Adhesion Molecule 1 (VCAM-1) and fibronectin (42). In the presence of CD24, VLA-4 binding to VCAM-1 can be inhibited using anti-VCAM-1 antibodies. In the absence of CD24, VLA-4/VCAM-1 binding cannot be blocked, and VLA-4 is also unable to bind to fibronectin (42). Adhesion of B cells to bone marrow stromal cells is a critical requirement for early (progenitor) B cell development (2, 48, 49). Indeed, it has been demonstrated that Fraction A was stromal-contact dependent for survival and that by Fraction C, B cells must release from stroma, but are still dependent on secreted cytokines, most notably IL-7 (2, 50, 51). During bone marrow development, IL-7 is produced by stromal cells and is critical for the early survival of pro-B cells (2, 50, 52). In both pro-/pre- B cell and Transitional B cell developmental time points in which CD24 is highly expressed, B cells must either regulate their interaction with neighbouring cells to receive particular growth or differentiation signals, or they are induced to undergo apoptosis (53, 54). It is thus reasonable to hypothesize that CD24 is actively engaged in this process and that it may potentially serve as a check for receiving developmentally appropriate signals from physical interactions.

While these results provided correlative data for potential CD24 interactions in developing B cells, no specific results had yet established precisely how, or even if, CD24 was functionally important in bone marrow B cell maturation. To establish an unambiguous role for CD24, Wenger et al.(55) developed a novel CD24 knockout mouse strain in embryonic stem cells as a model to study hematopoiesis in the absence of CD24 (55). Mouse strains were made to be either single knockout ($CD24^{-/+}$) or double knockout

($CD24^{-/-}$) where the CD24 gene was removed in one or both homologous chromosomes, respectively. To determine the effect of CD24 knockout on B cell development, lymphocytes from $CD24^{-/-}$ mice were compared to $CD24^{-/+}$ or wild-type mice (55). The number of B220+, BCR+ B cells in the spleen was unaffected (55). Interestingly, in $CD24^{-/-}$ mice the loss of CD24 resulted in a substantial reduction in the number of immature B cells. Specifically, the majority of lost cells corresponded to the B220+/CD43+/BP-1+, Fraction C and C′ cells, but not the earlier or later Hardy fractions (55). These lost cells normally have the highest expression of CD24 in the bone marrow and represent the transition from progenitor to precursor B cells. It is thus reasonable to conclude that CD24 is a key component of the control process by which this transition occurs. Interestingly, this also shows that the loss of CD24 is not a fatal developmental block as normal numbers of B cells are found in subsequent developmental stages (55, 56), suggesting that there is increased proliferation of the cells that progress past the C′ stage to reconstitute the mature B cell population. Follow-up studies in these knockout mice demonstrated that despite the delay in development, the mature B cells were unimpaired in their ability to function (56). These data present two possibilities regarding CD24 activity. Either CD24 is not involved in generating B cells, but perhaps plays a role in their developmental timing or potentially as a quality control checkpoint, or there is some redundancy in the role CD24 plays in B cell development where the loss of CD24 can be compensated.

The work of Wenger et al.(55) and Nielsen et al.(56) demonstrated that CD24 has a functional role in B cell development but did not establish how its effects were mediated. While the use of knockout mice successfully established that CD24 was

involved in B cell development, the use of transgenic mice that constitutively overexpress CD24 first demonstrated that CD24 induces apoptosis in immature B cells (9, 57). The CD24 gene, the T cell receptor (TCR) Vβ promoter and an immunoglobulin gene enhancer were cloned as a unit with multiple copies into an outbred mouse strain to generate mice that constitutively overexpress CD24. As T and B cells share a common lymphoid progenitor, the choice of the TCR Vβ promoter and Ig enhancer ensures that CD24 expression is high in all cells of lymphocyte origin. This construct resulted in a twofold overexpression of CD24 in the thymus, bone marrow, lymph nodes and spleen, representing all the sites of B cell maturation (9).

Immature B cells from these transgenic mice were then used in ex vivo and in vitro assays to identify how CD24 overexpression affects B cell development. One of the first in vitro assays established that CD24 overexpression leads to a profound reduction in the formation of IL-7-responsive B cells (9). Bone marrow cells were isolated from CD24-transgenic mice and cultured in recombinant IL-7 (9) to establish B cell colonies. The responsiveness of CD24-transgenic mice to this assay was decreased (9) demonstrating a loss of IL-7-dependent lymphoid progenitors. This result was highly congruent with the previous data that demonstrated the developmental block at the pro- to pre- B cell transition, as pre-B cells lose their stroma and IL-7 dependency (2), suggesting that CD24 affects maturation of IL-7-dependent cells.

Further categorizing the changes to B cell populations revealed that transgenic mice had significantly lower cell numbers in each Hardy fraction, the numbers of mature, splenic B cells was reduced, and their ability to respond to antigen in the form of membrane proteins from Escherichia coli was attenuated (9).

The loss of B cells in response to CD24 overexpression suggests that an increased level of CD24 artificially causes otherwise viable B cells to be lost. Taken together, the use of knockout and transgenic mice suggests that CD24 is not an absolute requirement for the generation of normal B cells, but is responsible for regulating apoptosis, potentially as a method of "quality control" in B cell development. The data from both the knockout and transgenic mouse studies suggest that CD24 may function to moderate early B cell development through its interactions with the bone marrow environment. In knockout mice, the loss of B cells may be due to their inability to form or regulate appropriate stromal attachment, depriving them of critical growth signals. In transgenic mice, overexpression of CD24 may delay or restrict the ability of these cells to release from the stroma and continue through the maturation process resulting in their elimination.

The most recent work on CD24 activity in B cells has centered on first establishing if CD24 mediates apoptosis, and how this is accomplished. Several studies have examined this question using the transgenic mouse model and in vitro assays using immature B cell lines. Between 1996 and 2006, four major publications demonstrated that CD24 directly induces apoptosis in cells isolated from CD24-transgenic mice and several (but not all) murine and human immature B cells when stimulated with anti-CD24 Abs (19, 46, 57, 58). This technique, known as antibody crosslinking, mimics the interaction of CD24 with an endogenous ligand. Antibody crosslinking is an effective and essential method to stimulate CD24 as the native ligand for CD24 in the bone marrow has yet to be identified. Cells are incubated with a primary Ab that recognizes the receptor and a secondary Ab that recognizes the first Ab, potentially clustering up to 4 receptors given

that each Ab has 2 identical Ag binding sites. Biologically this mimics established B cell signalling methods. For example, stimulating a single BCR is not sufficient to activate B cells, but the simultaneous activation of many receptors by clustering them together in one microdomain results in effective signal transduction (59).

The first publication to directly assess CD24-mediated apoptosis, by Chappel et al. (19), used either bone marrow-isolated B cells that were co-cultured in vitro with stromal cells or cytokines, or mature, splenic-derived B cells. Cells were stimulated using varying doses of the M1/69 anti-mouse CD24 Ab (primary), with or without secondary Ab against M1/69 (19). Engaging CD24 using both primary and secondary Abs resulted in increased apoptosis in the bone marrow-derived B cell cultures (19). This result was the first demonstration of a causal link between CD24 and apoptosis. This effect was restricted to the bone marrow, however, as the mature splenic B cells did not undergo apoptosis. Instead, these cells exhibited a dramatic decrease in proliferation in response to the receptor CD40 that normally will induce proliferation (19).

Building on these results, an in vivo assay of immature B cell apoptosis in the CD24-overexpressing transgenic mice was performed (57). The rate of apoptosis in B220+ cell populations was measured in both transgenic and normal mice. Fresh, uncultured cell isolates from transgenic mice had an apoptotic rate nearly three times that of the normal cells (57). While these transgenic mice showed an exaggerated phenotype compared to normal animals, these results provide substantial support to argue that CD24 directly induces apoptosis in developing B cells resident in bone marrow.

The major unanswered question regarding CD24 activity is the mechanism by which it can induce apoptosis. To that end, the most recent investigations have begun

examining the downstream effects of CD24 antibody crosslinking in human lymphoma cell lines developmentally arrested at the pro- or pre-B cell phase. The first information regarding a signalling method implicated a lipid-raft mediated system (46). Lipid rafts are thought to be signalling platforms in the plasma membrane. They are highly enriched in sphingolipids and cholesterol compared with the rest of the plasma membrane (60). The association of these sphingolipids and cholesterol result in a more stable structure in the membrane, which preferentially associates with proteins such as GPI-linked receptors, including CD24 (60). The components of a lipid raft are not permanent and thus the intracellular signal can be altered by including or excluding particular components (60). CD24 is known to be associated with lipid rafts (46) so attention was focused on other known lipid-raft signalling molecules including the Src-family PTKs. (45, 46, 61). This hypothesis was further reinforced by the previously discussed results that showed CD24 interacts with Src-family proteins in T cells (45).

CD24 crosslinking was demonstrated to selectively engage the Lyn PTK in lipid rafts and CD24 and Lyn co-localized to the lipid raft domains in the membrane (46). This study also produced the first clear data of a downstream signalling event in response to CD24 cross-linking in B cells. Crosslinking of CD24 was then shown to lead to the phosphorylation and activation of several mitogen activated protein kinases (MAPK). Within 3 minutes of cross-linking, high levels of activated Erk and p38 were detected. In the same experiment increased phosphorylated SAPK was found within 18 minutes (46). These results were further validated by subsequent research confirming CD24-mediated phosphorylation of p38, ERK and SAPK in other human lymphoma lines using primary and secondary antibody crosslinking (58). These MAPK proteins are known regulators of

cell survival and apoptosis and thus provide a potential target for future research. It was further demonstrated that this crosslinking causes activation of caspase proteins, which are known downstream mediators of apoptosis (58). Furthermore, Suzuki et al. demonstrated that the BCR may be involved in CD24-mediated signalling through translocation of the pre-BCR into lipid raft domains in response to CD24 cross-linking (46).

Subsequently, it was shown that co-stimulating pre-BCR and CD24 abrogated the induction of apoptosis that normally occurs in response to stimulation of CD24 (58). How these receptors interact is currently unknown, but the pre-BCR is known to provide tonic, resting stimulation to pre-B cells to promote survival and proliferation (6, 58) and likely represents an intrinsic regulatory element in the control of apoptosis in negative selection. While these results are the first conclusive evidence for the downstream signalling of CD24, these cell lines are malignant, and may have altered regulation of pro-proliferative or pro-apoptotic pathways.

1.6 Research Objectives

Research objectives:

1. To determine if WEHI-231 cells are an appropriate model system to investigate the regulation of CD24 expression in B cells.
2. To determine the mechanism through which CD24 mediates apoptosis in bone marrow-derived immature B cells.

To address these two questions I have used a combination of in vitro, bioinformatics, and ex vivo techniques. WEHI-231 cells, a murine immature B cell

lymphoma line, were used to address how CD24 expression is regulated during the transition from immature to mature, antibody-secreting cells. While cell lines cannot perfectly recreate in vivo biological processes, they are advantageous in that they remove much biological variability and simplify the inherent complexity of biological systems.

To address how CD24 signals, bioinformatics data were used as a hypothesis generation tool followed by ex vivo techniques to validate the hypothesized biological functions in primary cells. This ex vivo work generated a highly controlled, homogenous system while preserving the intrinsic organization and regulation of cell signalling pathways.

CHAPTER 2: MATERIALS AND METHODS

2.1 Antibodies and Fluorophores

Rat anti-mouse CD40 (Clone 1C10) was purchased from Abcam (Cambridge, MA). The following antibodies were purchased from Jackson ImmunoResearch (Bar Harbor, ME): μ-chain specific goat anti-mouse IgM (Cat: 115-005-020); goat-anti-rat biotinylated IgG H+L (Cat: 112-065-003); goat-anti-rat IgG (IgH+IgL) (Cat: 112-005-003). The following antibodies were purchased from eBioscience (San Diego, CA): Anti-mouse CD24 functional grade purified (M1/69) rat IgG2b κ; rat IgG2b κ isotype functional grade purified; anti-mouse CD24-FITC (M1/69) rat IgG2b κ; anti-mouse CD19-fluorescin isothiocyanate (FITC) (1D3) rat IgG2a κ; rat IgG2a κ-FITC; anti-mouse CD43-Phycoerythrin (PE) (eBioR2/60) rat IgM; rat IgM κ-PE; rat anti-mouse CD19-PE-Cy5.5 (eBio 1D3) rat IgG2a, κ; rat IgG2a κ (eBR2a)-PE-Cy5.5 Isotype; anti-mouse CD19-Peridinin chlorophyll (PerCP)-Cy5.5 (eBio1D3) Rat IgG2a κ; rat IgG2a κ-PerCP-Cy5.5; anti-human/mouse CD45R (B220)-eFluor660 (RA3-6B2) rat IgG2a κ; rat IgG2a (eBR2a)-eFluor660. Normal rat IgG2a was purchased from Santa Cruz Biotechnologies (Santa Cruz, CA). Streptavidin-FITC was purchased from eBioscience (Cat: 11-4317-87) and Streptavidin-Rhodamine Red X (Cat: S-6366) from Invitrogen (Carlsbad, CA).

2.2 Animal Care

Three-week-old C57BL/6 male mice were obtained from the Quebec facility of Charles River Laboratories (Wilmington, MA) and housed in the animal care facility of Memorial University of Newfoundland. The Institutional Animal Care committee at

Memorial University of Newfoundland approved all animal procedures. Two to three animals were housed per cage in open-topped cages. Animals were sacrificed between 3 and 8 weeks of age by cervical dislocation after isoflurane anaesthesia.

2.3 WEHI-231 culture and treatment

All media and supplements were obtained from Life Technologies (Burlington, ON) unless otherwise indicated. WEHI-231 (ATCC, Manassas, VA), a pre-B cell lymphoma cell line derived from BALB/c x NZB mice, were maintained in Roswell Park Memorial Institute (RPMI) 1640 Media supplemented with 10 % heat-inactivated foetal bovine serum (FBS), 1% antibiotic/antimycotic, 1 % sodium pyruvate and 0.1 % mercaptoethanol (hereafter referred to as RPMI complete media) at 37 °C and 5 % CO_2. Cells were maintained between $2x10^5$ cells/ml to $1x10^6$ cells/ml in 10 ml or 250 mL tissue culture-treated culture flasks. All experiments were performed in complete medium unless otherwise noted.

2.3.1 Viability Assay (MTT)

WEHI-231 cells were plated in 80 μL of RPMI complete media at $3.12x10^5$ cells/mL or $6.25x10^5$ cells/ml in duplicate in a 96-well, flat bottom tissue culture-treated plate. The cells were treated with anti-IgM and anti-CD40 antibodies to a final concentration of 0 to 800 ng/mL and 0 to 1600 ng/mL, respectively (Table 2.1). After 24 h, medium was removed and 90 μL of fresh medium with 10 μL of 5 mg/mL 3-(4,5-Dimethylthiazol-2-yl)-2,5-diphenyltetrazolium bromide (MTT) from Sigma Aldrich

Table 2.1: Anti-IgM and Anti-CD40 antibody concentrations used to determine the optimal conditions to induce or block apoptosis in WEHI-231 Immature B-cells.

anti-IgM / anti-CD40 (ng/ml)[a]					
0/0	50/0	100/0	200/0	400/0	800/0
0/25	50/25	100/25	200/25	400/25	800/25
0/50	50/50	100/50	200/50	400/50	800/50
0/100	50/100	100/100	200/100	400/100	800/100
0/200	50/200	100/200	200/200	400/200	800/200
0/400	50/400	100/400	200/400	400/400	800/400
0/800	50/800	100/800	200/800	400/800	800/800
0/1600	50/1600	100/1600	200/1600	400/1600	800/1600

[a] Numerator is the concentration of anti-IgM, denominator is the concentration of anti-CD40.

(St. Louis, MO) dissolved in phosphate buffered saline (PBS, 100 mM Sodium Phosphate, 1.5 M NaCl) was added. Cells were incubated for 4 h and then 100 µL of 0.04 N HCl in isopropanol was added to solubilize the precipitated formazan product. Absorbance was measured at 570 nm using a Powerwave XS UV/Vis Plate Reader from Biotek (Winooski, VT).

2.3.2 CD24 Expression Analysis

Five million cells at $6.25x10^5$ cells/mL were cultured in RPMI complete media and treated with 400 ng/mL of anti-IgM for 6 or 24 h. To rescue cells from apoptosis, cells were co-stimulated with anti-CD40 at 800 ng/mL along with anti-IgM at the previously stated concentration. Additionally, $5.0x10^6$ cells ($6.25x10^5$ cell/mL) were treated with Escherichia coli lipopolysaccharide (LPS) from Sigma Aldrich (St. Louis, MO) to a final concentration of 3 µg/mL, following the protocol described by Boyd et al. (62) or with LPS/anti-IgM/anti-CD40 for 6 or 24 hours.

Cells were pelleted at 400 x g for 5 min and resuspended in 1 mL TRIzol (Invitrogen). RNA was extracted following the manufacturer's protocol. Extracted RNA was eluted in 10 µL RNAse/DNAse free water and concentration was determined using the Nanodrop 2000 spectrophotometer (ThermoScientific, Wilmington, DE). RNA was checked for integrity by gel electrophoresis in a 1% agarose gel and visualized with ethidium bromide (EtBR). RNA was stored at -80˚C. cDNA was synthesised from 500 ng of RNA from a working stock at 300 µg/mL using the M-MLV RT kit (Invitrogen) following the manufacturer's protocol. Polymerase Chain Reaction (PCR) amplification

from cDNA was performed using using the following primers from IDT (Coralville, IA): CD24: Forward 5'-CTTCTGGCACTGCTCCTACC-3', Reverse 5'-TTTCACGCGTCCTTTAATCC-3'; Ribosomal 18S Subunit: Forward 5'-GACCATAAACGATGCCGACT-3', Reverse 5'-GGCCTCACTAAACCATCCAA-3'; Large Ribosomal Protein (RPLPO): Forward 5'-CGGCCCGTCTCTCGCCAGG-3', Reverse 5'-CAGTGACCTCACACGGGGCG-3'. The number of cycles that showed linear amplification was determined empirically as 32 cycles for CD24 and Ribosomal 18s subunit and 24 cycles for RPLPO. PCR products were run on a 1% agarose gel and visualized with Ethidium bromide (EtBR).

2.4 Bioinformatics analysis

2.4.1 Microarray data

MIAME-compliant microarray data sets were generated by the Immunological Genome Project (ImmGen) (63) from 5-week old C57BL/6 mice using the Affymetrix (Santa Clara, CA) Mouse Genome 1.0ST array (MoGene 1.0ST) platform to profile the expression of 35,556 features. Features included over 28,000 coding transcripts and over 7,000 non-coding and control transcripts. Data files were accessed from the Gene Expression Omnibus (GEO), accession number GSE15907. To determine which genes are differentially expressed during B cell development, arrays for the Multi-lineage progenitor stem cell, Hardy fractions A, B/C, C′, D, E, F, Transitional stage (T)1 and peritoneal-derived plasma cells (PC) were analyzed (Table 2.2). Analysis was performed in R, version 2.15.0 (64) using Bioconductor (65) packages as outlined below. The R-scripts were generated in Tinn-R version 2.3.7.1 (66) before importing into the R

Table 2.2: Mouse Gene 1.0ST array sets from the Immunological Genome Project used to identify differentially expressed genes.

Maturation Stage	Abbreviation	GEO Accession Numbers	GEO File Name
Multilineage Progenitor	MLP	GSM791124 GSM791125 GSM791129 GSM791130	MLP.BM#1 MLP.BM#2 MLP.BM#3 MLP.BM#4
Fraction A	FrA	GSM538351 GSM538352 GSM538353 GSM538354	proB.FrA.BM#1 proB.FrA.BM#4 proB.FrA.BM#5 proB.FrA.BM#8
Fraction B/C	FrBC	GSM538418 GSM476671 GSM399450	proB.FrBC.BM#4 proB.FrBC.BM#2 proB.FrBC.BM#1
Fraction C′	FrC	GSM476669 GSM399452 GSM399453	preB.FrC.BM#1 preB.FrC.BM#2 preB.FrC.BM#3
Fraction D	FrD	GSM476670 GSM399448 GSM399449	preB.FrD.BM#3 preB.FrD.BM#1 preB.FrD.BM#2
Fraction E	FrE	GSM476652 GSM399438 GSM399439	B.FrE.BM#1 B.FrE.BM#2 B.FrE.BM#3
Fraction F	FrF	GSM476653 GSM399440 GSM399441	B.FrF.BM#1 B.FrF.BM#2 B.FrF.BM#3
Transitional Stage 1	T1	GSM538213 GSM538214 GSM538215	B.T1.Sp#1 B.T1.Sp#2 B.T1.Sp#3
Plasma Cell	PC	GSM538198 GSM538199 GSM538200	B.Fo.PC#1 B.Fo.PC#2 B.Fo.PC#3

environment. The annotated R scripts used for all microarray analyses can be found in Appendix A.

2.4.2 Fractions A, C′ and F Differentially Expressed Genes.

Hardy fractions A, C′ and F were used to identify a preliminary list of candidate genes that were differentially expressed during B cell development in bone marrow. Using the Biobase (65) and Oligo (67) packages and the pd.mogene1.1 annotation file (68), the arrays were background corrected and normalized using the Robust Multi-Array Average (RMA) method (69). Differentially expressed genes were identified using the Limma (70) and Affycoretools packages (71).

2.4.3 Differentially Expressed Gene Clustering

Microarray data from bone marrow B cell development stages and several non-immature B cell development stages (Table 2.2) were normalized and background corrected as described in section 2.4.2. The features were annotated using the online Clone|Gene ID converter (72). The edited annotated text file was imported into Genesis 1.7.6 (73). A principle component analysis (PCA) was performed to determine how closely the technical microarray replicates correspond with one another and to identify potential batch effects in the arrays. The 35,556 features were filtered using the 3759 features identified to be differentially expressed between Fractions A, C′ and F. Unsupervised, mutual-information or Euclidian average-linkage clustering was performed using the Genesis program defaults for each setting.

2.4.4 Network Analysis and Biological Annotation

A subset of the 38 CD24 co-clustered genes was used to define a gene network interaction map. Using the online GeneMANIA tool (74) the gene network map was generated using published data from Homo sapiens or Mus musculus after confirming the 38 genes were orthologous. GeneMANIA selected annotation sources according to program defaults. 144 data sources were selected as: 20 co-expression, 2 co-localization, 3 genetic interaction, 6 pathway, 61 physical interaction, 50 predicted and 2 shared protein domain sources. The number of GeneMANIA-supplied genes was set to a maximum of 20. To identify the largest possible network from available data, genes from the cluster were added sequentially in the order given by Genesis in the hierarchical cluster. If a gene disrupted the network established in the previous iteration, it was excluded until no more genes could be added without disrupting the established network. Nineteen co-clustered genes could be successfully mapped into a network. Caspase 7 was also included, based on previously published data linking CD24 and Caspase 7 (58) bringing the total number of user-supplied genes to 20. Thus, the final network contained 20 genes from the CD24 cluster and 20 known interacting genes from GeneMANIA, which were then manually annotated. The Database for Annotation, Visualization and Integrated Discovery (DAVID) online tool (75, 76) was used to identify Gene Ontology (GO) enrichments in the network.

2.5 Bone Marrow B Cell Isolation

Femurs were removed from euthanized male C57/BL6 mice (3-6 weeks of age) and bone marrow was flushed out with Quin saline (QS, 25 mM NaHEPES, 125 mM

NaCl, 5 mM KCl, 1 mM $CaCl_2$, 1 mM Na_2HPO_4, 0.5 mM $MgSO_4$, 1 g/L glucose, 2mM Glutamine, 1 mM Sodium pyruvate, 50 μM 2-Mercaptoethanol, pH 7.2), using a 21-gauge needle. Single-cell suspensions were produced by sieving cells through a 100 μm nylon mesh. The EasySep Mouse B Cell Enrichment kit (Cat. #19754) or the EasySep Mouse B Cell Isolation Kit (Cat. #19854) from StemCell Technologies (Vancouver, BC) were used to enrich bone marrow isolates by removing non-B cells (Table 2.3) following the manufacturer's protocol. Fc-receptors were blocked on the B cells using anti-mouse CD16/CD43 (FcγIII/II receptor).

2.6 Analysis of Cell Death

Primary immature B cells were isolated using StemCell B cell Isolation Kit #19854 (StemCell Technologies, Vancouver, BC) and were plated in flat bottom tissue culture plates at a density of $5x10^5$ cells/mL in RPMI complete medium and were left untreated or treated with 10 μg/mL of M1/69 rat-anti-mouse antiCD24 or matched isotype control antibody in the presence or absence of 5 ug/mL goat-anti-rat secondary antibody. Cells were incubated for 24 h at 37°C and 5% CO_2. After 24 h, cells clusters were photographed under light microscope. Cells were assessed for apoptosis by FACS analysis by staining with AnnexinV-Alexa488 and Propidium Iodide (PI) using the Dead Cell Apoptosis kit (Cat. V13241) from Invitrogen, following the manufacturer's protocol. Briefly, $5x10^5$ cells were washed once in ice-cold PBS. Cells were resuspended in 100 μL, 1X Annexin-binding buffer (50 mM HEPES, 700 mM NaCl, 12.5 mM $CaCl_2$, pH 7.4) containing 5 μL Alexa Fluor 488 Annexin V and 1μL of 100 μg/mL PI and incubated for 15 minutes at room temperature in the dark. Annexin-binding

Table 2.3: Components of the Mouse B cell Isolation Cocktail from StemCell Technologies' Mouse B Cell Isolation Kit (19854).

Protein Target[a]	Cellular Target[b]
CD4	CD4+ T cells, macrophages and granulocytes
CD8a	CD8+ T cells
CD11b	Macrophages, neutrophils, monocytes, granulocytes, NK cells
CD43	Thymocytes, T cells, Fraction A/B/C pro-B cells, Monocytes, Granulocytes
CD49b	Platelets
CD90.2	Pan T cell marker
Ly-6C/G (Gr-1)	Monocytes, Neutrophils, Macrophages, Endothelial cells, CD8+ T-cells, Hematopoietic Cells
TER119	Erythrocytes
CD16/CD32	Fcγ III/II Receptor

[a] Protein targets of antibodies in the selection cocktail.
[b] Cell targets of selection cocktail antibodies.

buffer (400 μL) was added to the cells, which were kept at 4°C in the dark until analyzed by flow cytometry. In parallel, B cell enrichment was determined via analysis of CD19 expression by washing cells three times in FACS buffer (PBS with 1% heat-inactivated FBS), then stained anti-mouse CD19 antibody in 100 μL FACS buffer, followed by three additional washes in FACS buffer. Cells were kept at 4°C in the dark until flow analysis. Flow cytometry data were collected on a FACSCalibur flow cytometer (BD Biosciences, San Jose, CA.) using CellQuest Pro V4.0.2 software (BD Biosciences, San Jose, CA.). Analysis of the results was performed using FlowJo v10.0.5 (Tree Star, Ashland, OR.)

2.7 Analysis of Endocytosis

C57BL/6 mice were sacrificed and immature bone marrow-derived B cells were isolated using B cell isolation kit 19854 as described in section 2.5. Enriched immature B cells ($5x10^5$ cells) were resuspended in 0.5 ml QS and rested at 37°C prior to antibody treatment. M1/69 or isotype control Ab (10 μg) and biotinylated goat-anti-rat secondary Ab (5 μg) in 0.5 mL of QS were pre-incubated at room temperature at least 30 min. Cells and the pre-mixed Abs were incubated for 1, 5, 15, 40 or 60 min at 37°C, as indicated. The untreated control sample was incubated with 1 mL of QS for 60 min at 37°C. Cells were then transferred to 3 mL of ice-cold FACS buffer to halt endocytosis. Cells were left on ice in the presence of pre-mixed Abs for a minimum of 10 min to ensure that the Ab had sufficient time to bind to surface CD24. The untreated control sample was incubated with the pre-mixed Abs for 30 min on ice. Cells were then washed 3 times in FACS buffer followed by incubation with 0.25 μg of streptavidin-FITC, 0.125 μg of anti-mouse

CD19-PerCP-Cy5.5 or both in 100 μL of FACS buffer for 30 minutes at 4°C in the dark. Cells were then washed three times in FACS buffer followed by resuspension in 1% paraformaldehyde in FACS buffer.

To determine if the actin cytoskeleton dynamics were involved in CD24 endocytosis, cells were pre-treated with 1 μM of the F-actin destabilizing agent cytochalasin D (cytoD) dissolved in Dimethyl sulfoxide (DMSO) or DMSO alone as a vehicle control for 30 minutes prior to antibody addition. Cells were analyzed using the BD FACSCalibur and data analysis done using FlowJo v10.0.5 (Tree Star, Ashland, OR.)

2.8 Analysis of CD24 Localization

C57BL/6 mice were sacrificed and immature bone marrow-derived B cells were isolated using B cell isolation kit 19854 as described in section 2.5. Enriched immature B cells ($5x10^5$ cells) were treated as previously described to induce endocytosis, 10μg M1/69 or isotype control Ab pre-incubated with 5 μg of Biotinylated goat-anti-rat secondary antibody in 0.5 ml QS for a total volume of 1 ml in the presence or absence of DMSO and Cytochalasin D as described in section 2.7. Plasma membrane-bound CD24 was stained using 0.5 μg Streptavidin-FITC per $5x10^5$ cells. Cells were fixed in 3.7% paraformaldehyde. Fixed cells were spun onto glass slides using a Shandon Cytospinner centrifuge (Thermo Scientific, Waltham, MA) for 5 min at 1600 x g. Cells were mounted in VectaShield hardset mounting media with 4',6-diamidino-2-phenylindole (DAPI) (Vector Labs, Burlingame, CA). Confocal imaging was done using the Olympus FV1000 system and IX81 inverted microscope (Olympus, Shinjuku, Japan) and FV10-ASW (ver

3.1) software. Imaging was performed using Laser diode (405 nm), and Argon laser (488 nm) with DAPI and FITC bandpass filters. Imaging was done at 40X optical magnification, with digital magnification between 1.5 and 2.9x. Images were taken at 20.0 µs/pixel with sequential excitation of the fluorophores by line.

CHAPTER 3: RESULTS

3.1 CD24 mRNA expression is not dynamic in WEHI-231.

3.1.1 Induction of Growth Arrest and Differentiation in WEHI-231 cells.

WEHI-231 is an IgM+, CD24+ mouse immature B lymphoma cell line thatwas first assessed as a model to examine the regulation of CD24 mRNA expression. CD24 expression is known to decrease when naive B-cells differentiate into antibody-secreting plasma cells. Conditions to stimulate the same differentiation in the WEHI-231 cell line were therefore first established in vitro. In vivo, B cells will normally differentiate into plasma cells upon stimulation of the BCR by exogenous antigens via antigen presenting cells (such as CD4+ helper T cells or dendritic cells) and the CD40 co-receptor through interaction with CD40L. In vitro, this is mimicked using anti-IgM and anti-CD40 antibodies. Stimulation with anti-IgM alone will cause growth arrest and apoptosis in IgM+ immature B cells, while stimulation with anti-CD40 alone will not alter cell survival or differentiation. Stimulation with both anti-IgM and anti-CD40 will, however, induce proliferation and maturation in IgM+ immature B cells. A second method to stimulate maturation is through activation of Toll-like receptors (TLR) via Escherichia coli-derived lipopolysaccharide (62).

To determine the optimal antibody concentration to induce anti-IgM-mediated cell death and anti-IgM/anti-CD40 proliferation, $3.125x10^5$ or $6.25x10^5$ cells/mL were stimulated with varying concentrations of anti-IgM and anti-CD40 antibody for 24h (Table 2.1). Cellular viability was then assessed using the MTT assay, which measures active metabolism through the reduction of a soluble, yellow tetrazolium dye (MTT) to an

insoluble purple formazan precipitate. At $3.12x10^5$ cells/mL, cell viability maximally reduced with 200 ng/mL of anti-IgM. While increasing concentrations of anti-CD40 were capable of partially restoring cell viability it was not rescued to control levels (Fig. 3.1A). At $6.25x10^5$ cells/mL, treatment with 400 ng/mL anti-IgM produced reduced cell viability to a minimum, at 32% of control while 800 ng/mL anti-CD40 co-stimulation was sufficient to restore cell viability to the same level as control (Fig. 3.1B). Therefore, it was decided that WEHI-231 at $6.25x10^5$ cells/mL would be treated with 400 ng/mL of anti-IgM and 800 ng/mL of anti-CD40 to examine what effect this has on the expression of CD24.

3.1.2 CD24 expression is unaffected in stimulated WEHI-231 cells

The mRNA expression level of CD24 was measured by RT-PCR 6 or 24 h after treatment with anti-IgM and/or anti-CD40 (Fig. 3.2). There were no observable changes to CD24 mRNA levels in response to either anti-IgM or anti-CD40 treatment or to the combination at either 6 h or 24 h. Treatment of WEHI-231 cells with 3 μg/mL of LPS has been shown to induce differentiation and maturation (62) and thus CD24 expression was also examined after LPS treatment. Cells were also treated with LPS alone or in conjunction with anti-IgM and anti-CD40 to determine if CD24 expression was regulated in WEHI-231 cells upon differentiation into plasma cells. Similar to the findings with anti-IgM and anti-CD40, no changes in CD24 expression were observed (Fig. 3.3). These results were confirmed by flow cytometry, which also showed no changes in surface protein levels (data not shown). Therefore, WEHI-231 cells do not recapitulate the

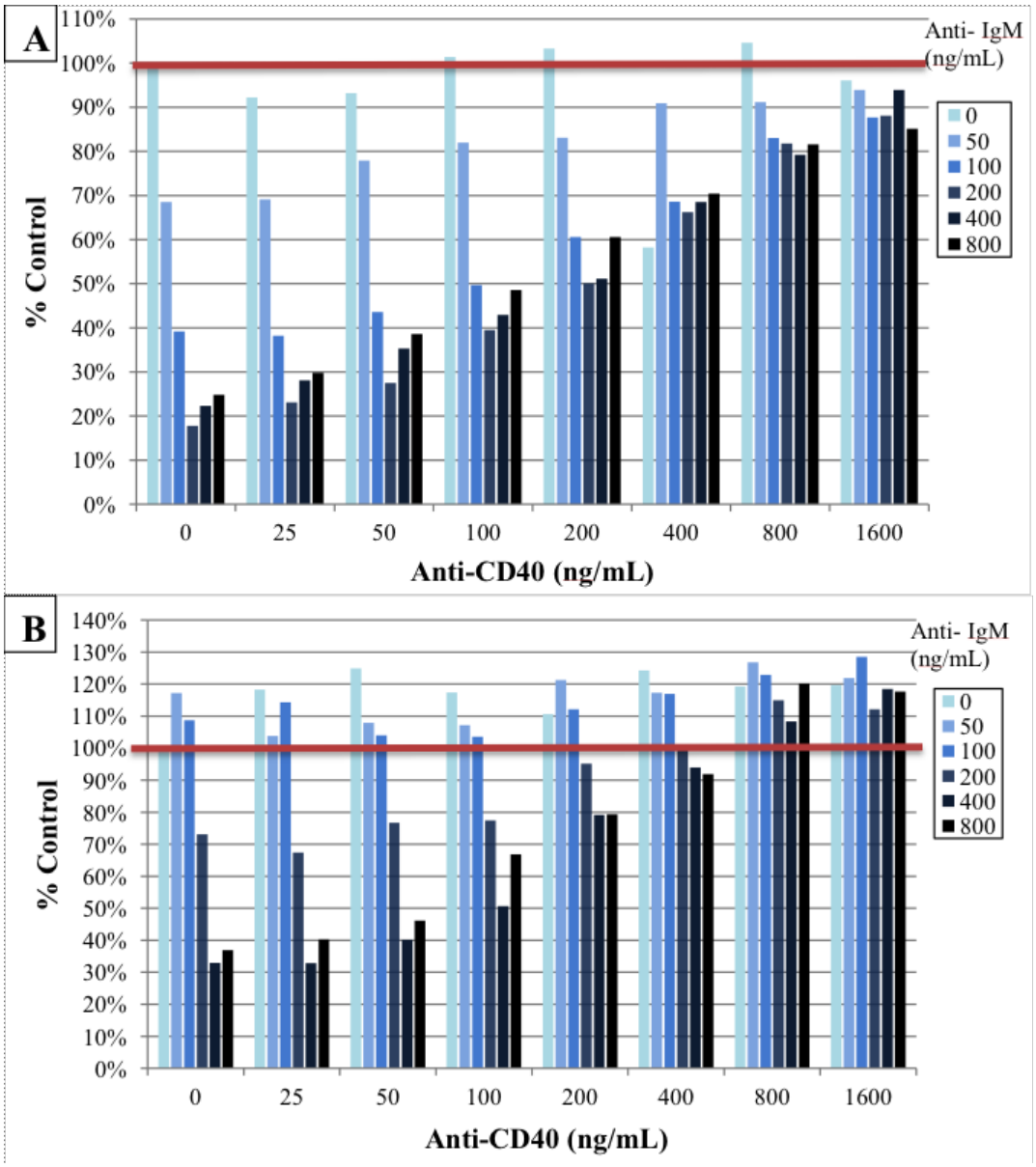

Fig. 3.1: MTT assay to determine anti-IgM/anti-CD40 concentrations required to induce growth arrest and rescue. Control is RPMI-completed media without the addition of anti-IgM or anti-CD40 antibody. A. Antibody stimulation in $2.5x10^4$ cells at $3.125x10^5$ cells/mL. B. Antibody stimulation in $5.0x10^4$ cells at $6.25x10^5$ cells/mL. n=1 with two technical replicates. Values for antibody concentrations informed the optimal treatment conditions in subsequent WEHI-231 experiments.

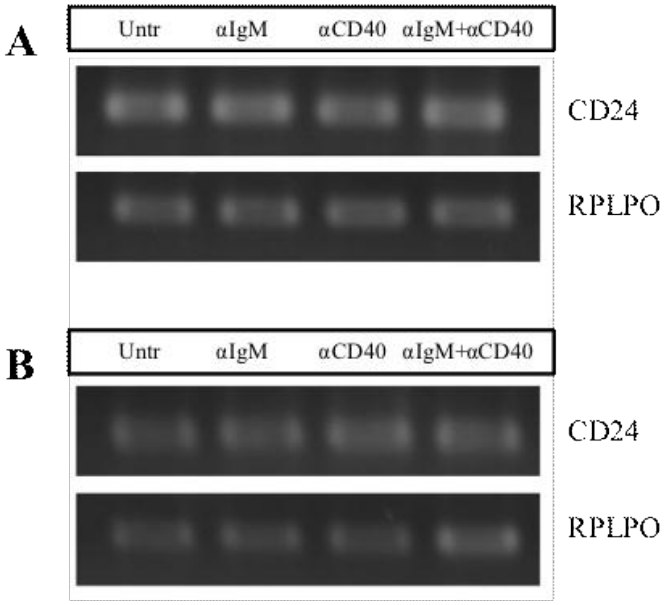

Fig. 3.2: Expression of CD24 mRNA is not affected by antibodies to induce B cell differentiation and activation. WEHI-231 cells were left untreated (Untr), treated with 400 ng/mL anti-IgM (αIgM), treated with 800 ng/mL anti-CD40 or with both anti-IgM and anti-CD40 anti-IgM+anti-CD40 for A. 6h or B. 24h. mRNA was isolated and CD24 expression determined by RT-PCR. RPLPO expression was also determined and used as a loading control. Representative result of 4 independent biological replicates. Both the time points are from the same experiment.

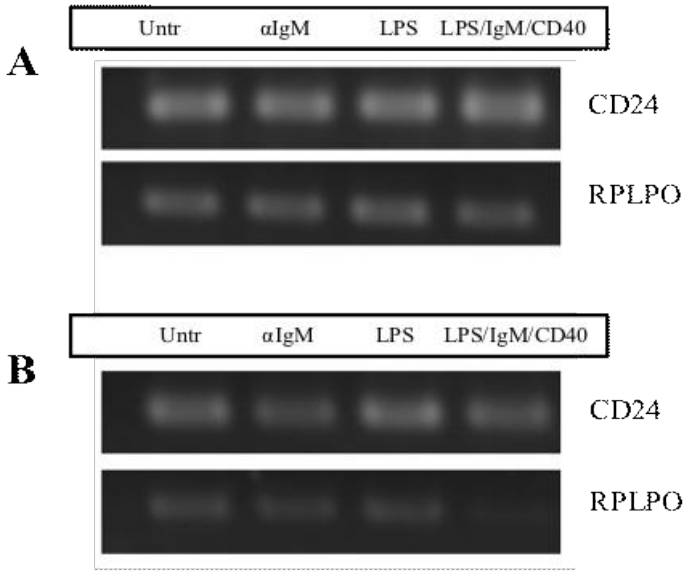

Fig. 3.3: Expression of CD24 mRNA is not affected by LPS stimulation in WEHI-231. Untr is untreated, IgM is 400 ng/mL anti-IgM treatment, LPS is 3.0 μg/mL of LPS and LPS+anti-IgM+anti-CD40 is co-treatment with LPS, anti-IgM/anti-CD40. A. 6h of treatment B. 24h of treatment. CD24 expression was compared against RPLPO as a housekeeping gene. RNA integrity was poor in the LPS/IgM/CD40-treated 24h sample.

changes in CD24 expression in response to maturation observed in primary B cells and are not an appropriate model for investigating the regulation of CD24 expression. Consequently, all further work used primary B cells.

3.2 Bioinformatics-based Identification of Potential CD24 Interactors

3.2.1 Differentially Expressed Genes from Early to Late B-cell Development

Microarray data generated by the Immunological Genome Project was used to identify genes whose expression mirrors that of CD24 through B-cell development in bone marrow. The first analysis focused on Hardy fractions A, C′ and F since these fractions are $CD24^-$, $CD24^+$ and $CD24^-$, respectively, to identify genes whose expression was broadly similar to that of CD24. In total, 3759 unique features were differentially expressed ($p<0.005$). To identify genes with similar expression to CD24 over the entire bone marrow development process, these 3759 genes were analyzed in each Hardy fraction, splenic-derived Transitional B cells and Plasma cells. A Principle Component Analysis revealed that replicates for each of these data sets clustered with the exception of Fractions F and Plasma Cells (Fig. 3.4) and the data were free of batch effects.

3.2.2 Hierarchical Clustering, Network Analysis and Biological Annotation of CD24 Co-expressed Genes

To identify genes that share the closest expression to CD24, unsupervised hierarchical clustering was performed on the 3759 genes identified above (Fig. 3.5). The analysis revealed several distinct groups of gene expression across B cell development (Fig. 3.5A). CD24 resided in a unit of genes that are highly expressed during the late pro-

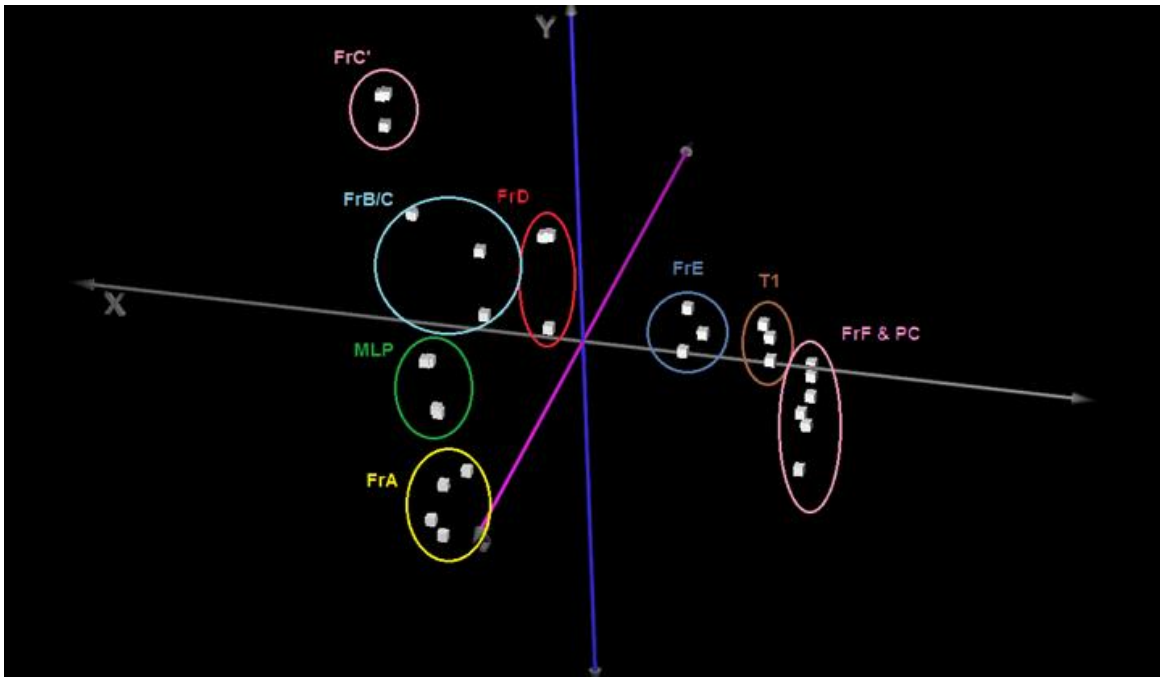

Fig. 3.4: Principle Component Analysis (PCA) of microarray data. Biological replicates are circled. Replicates form distinct clusters with the exception of Hardy Fraction F and Plasma Cells (FrF and PC), which are intermingled. FrA is Hardy fraction A, FrB/C are Hardy fraction B or C cells, FrC' is Hardy fraction C', FrD is Hardy fraction D, FrE is Hardy fraction E, FrF is Hardy fraction F. T1 are Transitional stage 1 B cells, MLP are Multi-lineage Progenitor Stem cells and PC are Peritoneal Plasma Cells.

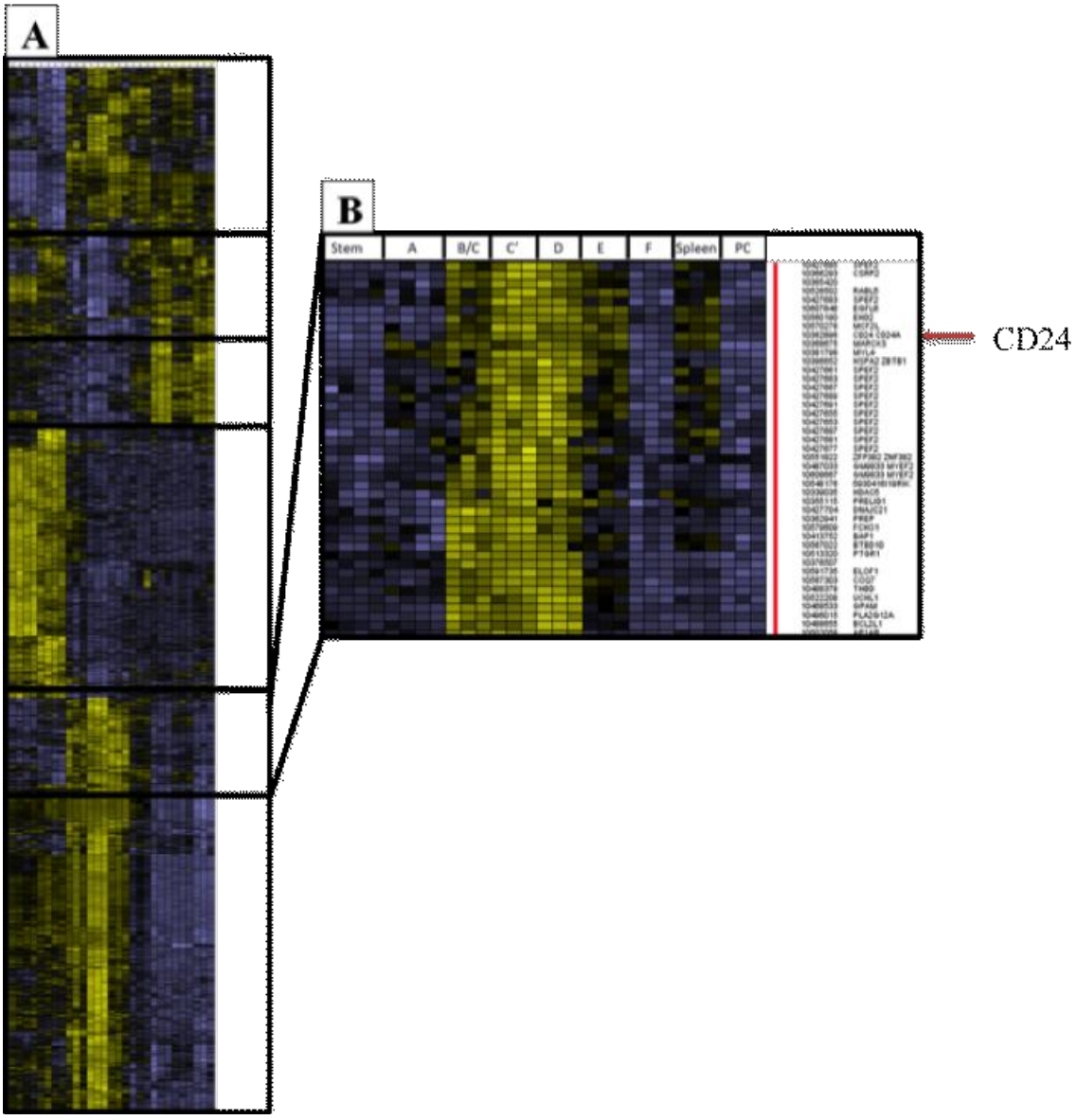

Fig. 3.5: Hierarchical clustering of differentially expressed (DE) genes during B cell development. The total number of DE genes and control features was 3759. Yellow denotes higher expression and blue indicates lower expression. A. Clustering of all DE genes. Boxes outline major 'groups' of co-expressed genes. B. 55 features representing 38 genes co-expressed with CD24.

to early pre- B cell developmental phases, and may be expressed again during splenic maturation. From this, a CD24 co-cluster was identified that contained the features that most closely match CD24's expression (Fig. 3.5B). This cluster contained 55 features, corresponding to 38 individual genes (Table 3.1).

A network interaction map was generated using 19 CD24 co-clustered genes. The full list of 38 genes could not be analyzed due to a lack of published interaction data among them. The 19 selected genes represented those which could form the largest interaction network. Additionally, Caspase 7 was added as it was previously shown to respond to CD24 signalling (58). GeneMANIA-suggested a further 20 genes which interacted heavily with the provided CD24 co-clustered genes according to program defaults (Table 3.2) (74). The addition of the GeneMANIA suggested genes allowed a more complete network interaction map to be generated by identifying potential indirect interactions between the CD24 co-clustered genes. GeneMANIA networked genes according to the following parameters: Co-expression; co-localization; genetic interactions; pathway interactions; physical interactions; predicted interactions and shared protein domains. Due to the larger volume of published data, a more complete network could be constructed using data from Homo sapiens (Fig. 3.6) than Mus musculus. Prior to assessing the biological functions of these genes, it was first established that all 40 of the genes share significant ontology between the two species and that they perform analogous functions

Gene ontology (GO) annotation was used to assign biological significance to the list of 40-networked genes. Using GO, genes are categorized into three hierarchies: biological processes (BP), molecular functions (MF) and cellular components (CC).

Table 3.1: Thirty-eight genes clustering with CD24 identified via unsupervised hierarchical clustering.

Official Gene Symbol[a]	Gene Name
SPEF2	Sperm flagellar 2
CSRP2	Cysteine and glycine-rich protein 2
RABL5	RAB, member RAS oncogene family-like 5
EGFL6	EGF-like-domain, multiple 6
EHD2	EH-domain containing 2
MCF2L	MCF.2 cell line derived transforming sequence-like
CD24	CD24 molecule
MARCKS	Myristoylated alanine-rich protein kinase C substrate
MYL4	Myosin, light chain 4, alkali; atrial, embryonic
HSPA2	Heat shock 70kDa protein 2
ZNF382	Zinc finger protein 382
MYEF2	Myelin expression factor 2
HDAC5	Histone deacetylase 5
PRELID1	PRELI domain containing 1
DNAJC21	DnaJ (Hsp40) homolog, subfamily C, member 21
PREP	Prolyl endopeptidase
FCHO1	FCH domain only 1
BAP1	BRCA1 associated protein-1 (ubiquitin carboxy-terminal hydrolase)
BTBD10	BTB (POZ) domain containing 10
PTGR1	Prostaglandin Reductase 1
ELOF1	Elongation factor 1 homolog (S. cerevisiae)
COQ7	Coenzyme Q7 homolog, ubiquinone (yeast)
THBD	Thrombomodulin
UCHL1	Ubiquitin carboxyl-terminal esterase L1 (ubiquitin thiolesterase)
GPAM	Glycerol-3-phosphate acyltransferase, mitochondrial
PLA2G12A	Phospholipase A2, group XIIA
BCL2L1	BCL2-like 1
AP1AR	Adaptor-related protein complex 1 associated regulatory protein
DCK	Deoxycytidine kinase
P2RX3	Purinergic receptor P2X, ligand-gated ion channel, 3
CAPSL	Calcyphosine-like
GFRA1	GDNF family receptor alpha 1
TIFA	TRAF-interacting protein with a forkhead-associated domain
SMARCA4	SWI/SNF related, matrix associated, actin dependent regulator of chromatin, subfamily a, member 4
GPR12	G protein-coupled receptor 12
DDC	Dopa decarboxylase (aromatic L-amino acid decarboxylase)
TRIM2	Tripartite motif-containing 2
IRS1	Insulin receptor substrate 1

[a] Official gene symbols and names are taken from The Mouse Genome Informatics Database (http://www.informatics.jax.org/mgihome/nomen/) as set by the International Committee on Standardized Genetic Nomenclature for Mice.

Table 3.2: Forty Genes used to perform network and gene ontology enrichment analysis.

Official Gene Symbol[a]	Gene Name
SPEF2[b]	Sperm flagellar 2
AP1AR	Adaptor-related protein complex 1 associated regulatory protein
RABL5	RAB, member RAS oncogene family-like 5
TIFA	TRAF-interacting protein with a forkhead-associated domain
PLA2G12A	Phospholipase A2, group XIIA
COQ7	Coenzyme Q7 homolog, ubiquinone (yeast)
ELOF1	Elongation factor 1 homolog (S. cerevisiae)
GPAM	Glycerol-3-phosphate acyltransferase, mitochondrial
CD24 (CD24A)	CD24 molecule
MCF2L	MCF.2 cell line derived transforming sequence-like
FCHO1	FCH domain only 1
EGFL6	EGF-like-domain, multiple 6
EHD2	EH-domain containing 2
BTBD10	BTB (POZ) domain containing 10
MYEF2	Myelin expression factor 2
MARCKS	Myristoylated alanine-rich protein kinase C substrate
UCHL1	Ubiquitin carboxyl-terminal esterase L1 (ubiquitin thiolesterase)
HSPA2	Heat shock 70kDa protein 2
BCL2L1	BCL2-like 1
CASP7[c]	Caspase 7, apoptosis-related cysteine peptidase
MTMR2[d]	Myotubularin related protein 2
C5orf22	Chromosome 5 open reading frame 22
TSR1	TSR1, 20S rRNA accumulation, homolog (S. cerevisiae)
HSPBP1	Hsp70-interacting protein
TARDBP	TAR DNA binding protein
DLG5	Discs, large homolog 5 (Drosophila)
MYOF	Myoferlin
BCL2L11	BCL2-like 11 (apoptosis facilitator)
BIK	BCL2-interacting killer (apoptosis-inducing)
PLA2G12B	Phospholipase A2, group XIIB
MARCKSL1	MARCKS-like 1
DYX1C1	Dyslexia Susceptibility 1 Candidate 1
ESD	Esterase D/formylglutathione hydrolase
SH3GL2	SH3-domain GRB2-like 2
TIFAB	TIFA-related protein TIFAB
CCDC14	Coiled-coil domain containing 14
EHBP1	EH domain binding protein 1
MEOX2	Mesenchyme homeobox 2
BAK1	BCL2-antagonist/killer 1
NEDD8	Neural precursor cell expressed, developmentally down-regulated 8

[a] Official gene symbols and names are taken from The Mouse Genome Informatics Database (http://www.informatics.jax.org/mgihome/nomen/) as set by the International Committee on Standardized Genetic Nomenclature for Mice.
[b] Highlighted in grey are genes derived from the CD24 co-expression cluster.
[c] Highlighted in black is Caspase 7 which was included due to its known association with CD24-mediated signalling.
[d] GeneMANIA suggested genes.

Fig. 3.6: Network analysis of 40 CD24 associated genes using GeneMANIA. Coloured boxes indicate the genes that participate in the same pathway or function. Capase-7 is highlighted with * to indicate it was not a clustered gene. Lines represent known associations between genes and are colour coded based on the type of interaction as shown in the legend. Line thickness represents the relative weight associated with that association to the network. Twenty genes (black circles) are co-clustered with CD24 expression during B cell development. 20 genes (grey circles) were selected by GeneMANIA

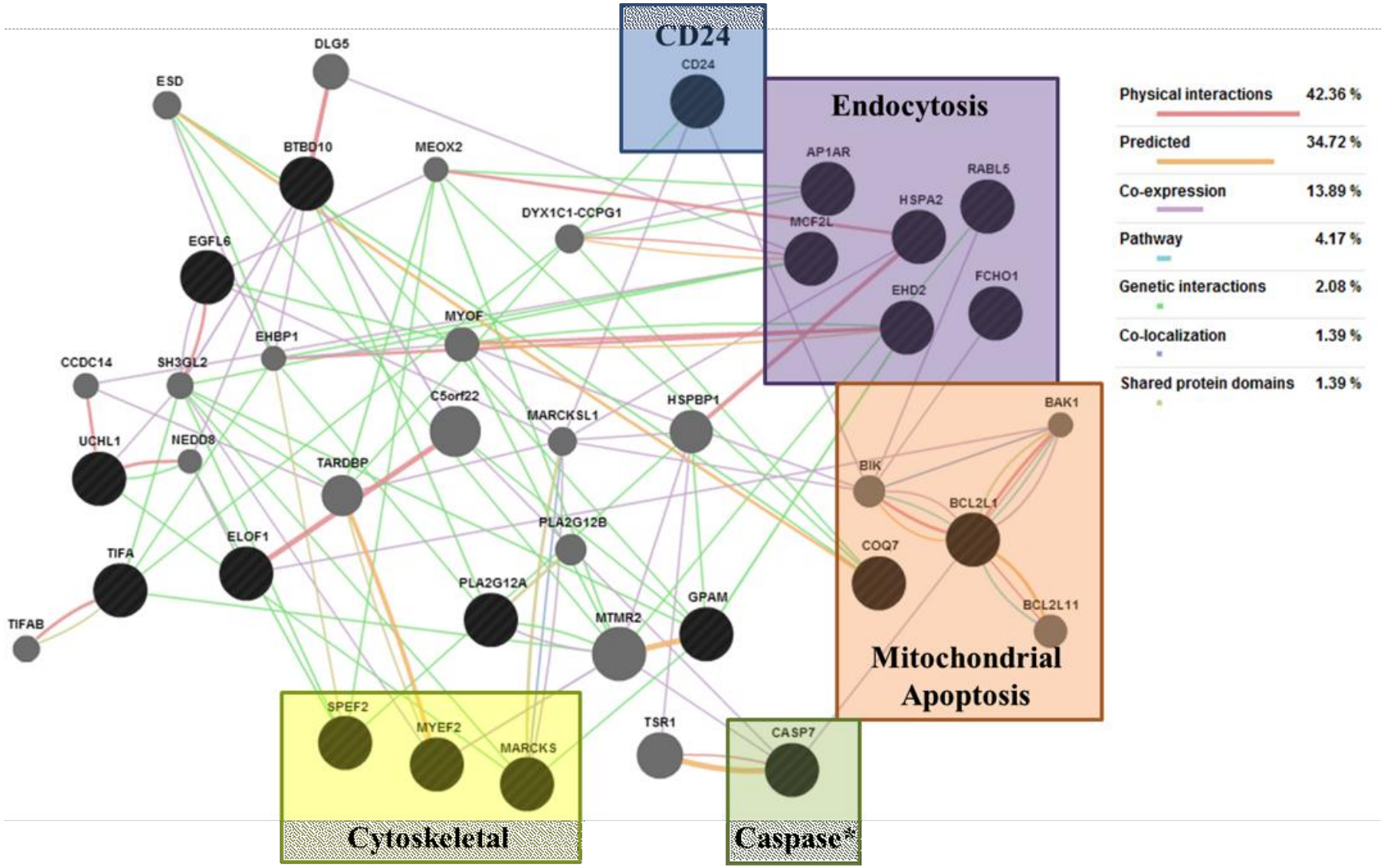
CD24
CD24
Endocytosis
AP1AR
RABL5
HSPA2
MCF2L
EHD2
FCHO1
DLG5
ESD
BTBD10
MEOX2
DYX1C1-CCPG1
EGFL6
MYOF
EHBP1
CCDC14
SH3GL2
C5orf22
MARCKSL1
HSPBP1
UCHL1
NEDD8
TARDBP
PLA2G12B
ELOF1
TIFA
PLA2G12A
GPAM
TIFAB
MTMR2
BAK1
BIK
BCL2L1
COQ7
BCL2L11
Mitochondrial Apoptosis
SPEF2
MYEF2
MARCKS
TSR1
CASP7
Cytoskeletal
Caspase*
Physical interactions 42.36 %
Predicted 34.72 %
Co-expression 13.89 %
Pathway 4.17 %
Genetic interactions 2.08 %
Co-localization 1.39 %
Shared protein domains 1.39 %

.

The categories are further organized by parent and child relationships whereby each hierarchy is subdivided into increasingly specific descriptors. For example, BP includes cell death, followed by programmed cell death, followed by apoptosis. The list of 40-networked genes was assessed using the online Database for Annotation, Visualization and Integrated Discovery (DAVID) tool (75, 76) to determine if there were significant enrichments in any specific ontology. Significant enrichment was found in mitochondrial apoptotic signalling ($p = 3.1 \times 10^{-5}$), and several related subfamilies. In addition, both the ontologies Endocytosis (p=0.076) and Src-Homology (SH3) Domain-containing proteins (p=0.074) trended towards significant enrichment. Various sub-functions in apoptosis, membrane organization and several other gene ontologies were also noted (Appendix B). Manual biological annotation provided additional support that several genes not identified by DAVID participate in mediating apoptosis, endocytosis or in general cytoskeletal organization. Therefore, the network generated by the GeneMANIA analysis was manually annotated to highlight the main functions of mitochondrial apoptosis, endocytosis and cytoskeletal organization (Fig. 3.6). The MCF.2 Cell Line Derived Transforming Sequence-like (MCF2L) GTPase is included in the endocytosis category since it is known to regulate endocytosis (77) even though it is not closely networked with the other endocytosis genes. Furthermore, both CD24 and caspase-7 are highlighted for clarity.

As the DAVID software is limited to specific source data to establish ontology enrichments, the list of genes was also manually annotated using PubMed to identify any functions or associations that were not identified electronically. DAVID initially identified CD24, Eps Homology 15 Domain Containing-2 (EHD2) and SH3-Domain

Containing, Growth Factor Receptor Bound Protein-Like 2 (SH3GL2) as participating in, or being associated with, endocytosis. While EHD2 and SH3GL2 are both known endocytosis genes (78, 79) CD24 has not been directly associated with endocytosis in previously published literature. Electronic analysis of CD24 suggested it may participate in endocytosis due to its similarity to other genes (Inferred from Electronic Annotation), and it has been shown to interact with proteins like Src which can modulate vesicle trafficking (29) Subsequent manual annotation identified a further 4 genes that are also associated with various functions in vesicle trafficking and the regulation of endocytosis: Adapter-Related Protein Complex 1 Associated Regulatory Protein (AP1AR), FCH Domain Only-1 (FCHO1), Rab-Like 5 (RabL5), MCF2L and Heat Shock Protein 2 (HSPA2) (77, 80-83). Therefore, combining the results from DAVID as well as the manual curation revealed that 8 of the 19 CD24 co-clustered genes are known to be involved in regulating endocytosis or vesicular transport. Based on these findings, we hypothesize that CD24 is associated with endocytosis in immature B cells.

3.3 Magnetic Enrichment of Bone Marrow B Cells

To functionally validate this hypothesis and determine if CD24 is associated with endocytosis, primary mouse ex-vivo B cells isolated from bone marrow were used. Untouched magnetic separation was used to purify non-stimulated B cells from bone marrow. The two magnetic separation kits that were available from StemCell Technologies for untouched magnetic separation were the mouse B cell enrichment kit (catalogue number 19754) and the mouse B cell isolation kit (19854). As both kits were designed to isolate B cells from splenic tissue, it was first necessary to determine if they

were also able to enrich developing B cells from the bone marrow. Analysis of the populations recovered after isolation revealed that results with the B cell enrichment kit (19754) were highly variable and only provided a 45.6% pure population of B cells with a standard error rate of 6.4% (n=6). By comparison, results with the B cell isolation kit (19854) averaged 89.6% CD19+ B cells with a standard error of 0.96% over 21 isolations (Tables 3.3 and 3.4). It was therefore determined that the Mouse B cell enrichment kit (19754) was unsuitable for isolating B cells from bone marrow, but that the B cell isolation kit (19854) was well adapted for this role. All subsequent B cell isolations thus relied on this kit.

The relative abundance of B cell fractions immediately following sacrifice, immediately after magnetic isolation using kit 19854, and also after 20 hours in tissue culture were assessed. Unenriched bone marrow had 24.6% B220+ cells and 21.1% CD19+ cells when labelled singly with their respective Abs (Fig. 3.7A and B). When expression of both B220 and CD19 was investigated by incubating with both Abs simultaneously, there was 32.0% (5.57% + 26.4%) B220+ cells and 26.6% (0.24% + 26.4%) CD19+ cells (Fig. 3.7C). The increase in positive staining cells was potentially due to a slight interaction between the fluorophores, or natural variation in the biological samples. Overall, there were 26.4% B220+/CD19+ cells, representing Hardy fractions B through F. Of the B220+ cells, 17.4% were CD19- (Fig. 3.7C) representing Hardy fraction A. More than two thirds of the total cell population did not express either the B220 or CD19 B cell markers indicating a large number of non-B cells were present in the unenriched bone marrow.

Table 3.3: Comparison of the StemCell Technologies Mouse B cell Enrichment Kit (19754) and the Mouse B cell Isolation Kit (19854).to enrich B cells from bone marrow.

StemCell Kit Cat. Number	Date of experiment	Mouse age (weeks)	Number of Cells used in Magnetic Separation	% Isolation from Unenriched Bone marrow[a]	B cell purity by CD19 expression[b]
19754	25 Oct 12	3.5 weeks	$1.00x10^8$	57.5%	23.9%
19754	06 Nov 12	5 weeks	$1.00x10^8$	32.5%	30.5%
19754	22 Nov 12	3 weeks	$1.00x10^8$	20.0%	48.3%
19754	26 Nov 12	4 weeks	$1.00x10^8$	35.25%	65.3%
19754	28 Nov 12	4 weeks	$1.00x10^8$	26.50%	49.0%
19754	03 Dec 12	3 weeks	$1.00x10^8$	22.75%	56.8%
19854	12 Dec 12	3.5 weeks	$1.00x10^8$	33.0%	85.5%
19854	17 Dec 12	3 weeks	$1.00x10^8$	27.5%	80.0%
19854	19 Dec 12	4 weeks	$1.50x10^8$	18.0%	90.4%
19854	16 Jan 13	3 weeks	$8.0x10^7$	15.5%	84.3%
19854	21 Jan 13	4 weeks	$8.0x10^7$	22.0%	91.8%
19854	23 Jan 13	4 weeks	$8.0x10^7$	22.5%	91.8%
19854	04 Feb 13	2 weeks	n.d.	n.d.	84.4%
19854	08 Feb 13	3 weeks	$8.725x10^7$	26.1%	88.5%
19854	12 Feb 13	5 weeks	$6.775x10^7$	24.0%	92.4%
19854	13 Feb 13	5 weeks	$77x10^{67}$	25.8%	92.4%
19854	22 Feb 13	6 weeks	$9.54x10^7$	17.6%	83.5%
19854	26 Feb 13	5 weeks	$90x10^{67}$	20.9%	89.0%
19854	27 Feb 13	5 weeks	$5.49x10^7$	32.3%	90.7%
19854	5 Mar 13	6 weeks	$8.0x10^7$	28.8%	85.5%
19854	7 Mar 13	6 weeks	$6.27x10^7$	21.2%	90.4%
19854	17 Mar 13	3 weeks	$6.19x10^7$	21.3%	90.2%
19854	26 Mar 13	4 weeks	$8.0x10^7$	26.9%	94.3%
19854	15 Apr 13	7 weeks	$8.0x10^7$	15.3%	91.3%
19854	23 Apr 13	4 weeks	$9.38x10^7$	19.2%	96.0%
19854	25 Apr 13	4 weeks	$8.0x10^7$	25.0%	91.5%
19854	30 Apr 13	5 weeks	$9.3x10^7$	23.0%	98.0%

[a] % Isolation from unenriched bone marrow is the number of isolated cells from total bone marrow cells used.
[b] B cells were identified by their expression of CD19 as assessed by FACS.

Table 3.4: Summary of B cell enrichment using the StemCell Technologies B Cell Enrichment Kit (19754) and the B cell Isolation Kit (19854).

Kit	Average CD19+	St. Deviation	St. Error	Variance	n
19754	45.6%	15.7%	6.4%	2.5%	6
19854	89.6%	4.4%	0.96%	0.19%	21

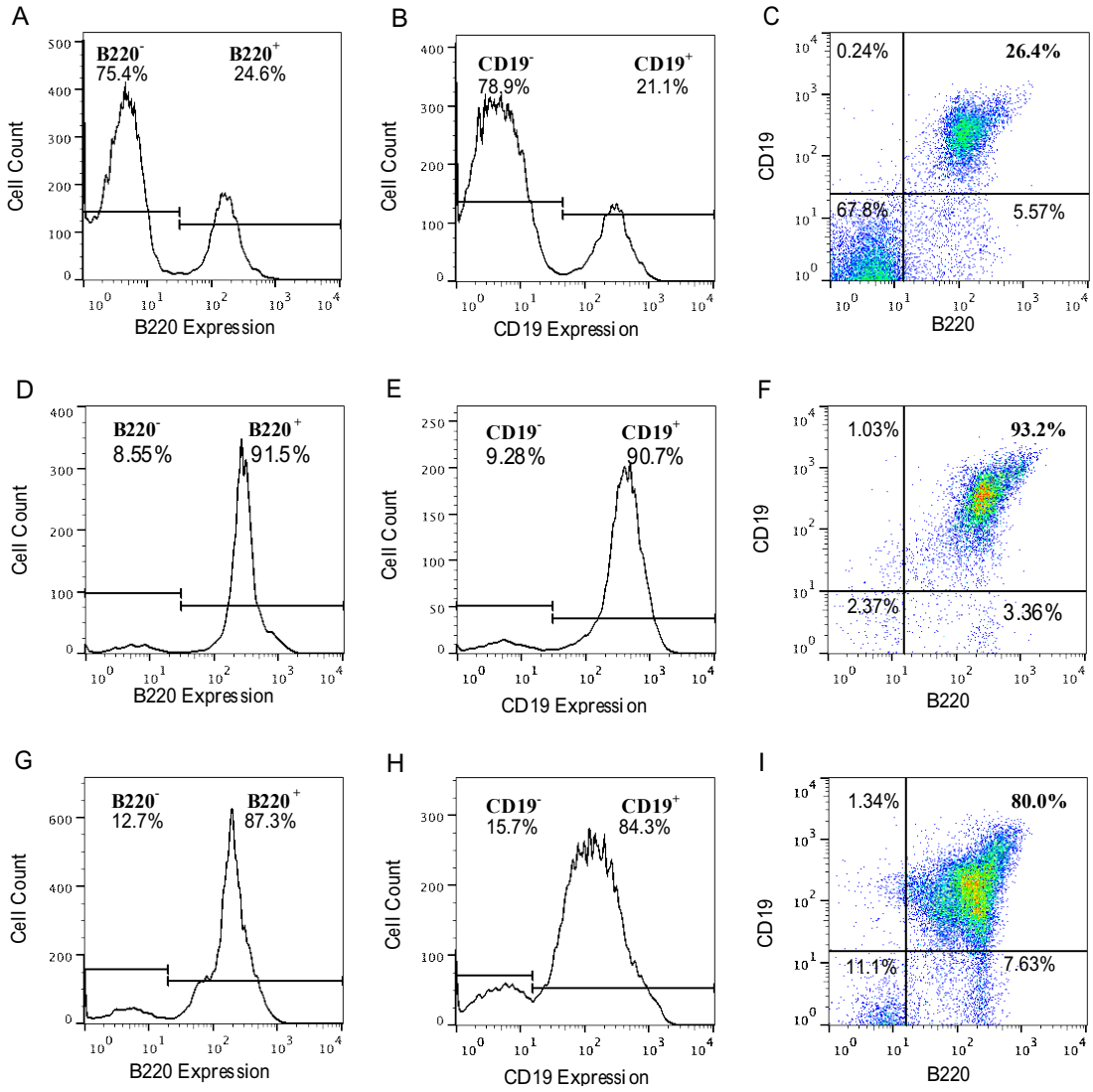

Fig. 3.7: Isolation of B cells from mouse bone marrow using untouched magnetic separation. Unenriched bone marrow (A, B and C) was compared with magnetically isolated B cells either uncultured (D, E and F) or cultured for 20h in RPMI complete media (G, H, and I). B cell isolates. B220 and CD19 expression were used to determine B cell purity. Lineage committed B cells belonging to Hardy fractions B-F express both CD19 and B220 and are identified in C, F and I in the upper-right quadrant.

The induction of apoptosis required B cells to be cultured in tissue media for varying times. To determine how overnight incubation may affect the isolated B cells, the relative populations of B220 and CD19+ cells were assessed immediately after isolation, and after 20 hours in tissue culture. Immediately after isolation, a substantial number of non-B cells were successfully removed with 91.5% of the cells expressing B220 and 90.7% expressing CD19 (Fig. 3.7D and E). When cells were co-labelled with anti-B220 and anti-CD19, there were 96.6% (3.36% + 93.2%) B220+ cells and 94.2% (1.03% + 93.2%) CD19+ cells (Fig. 3.7F). The cell population contained 93.2% B220+/CD19+ cells indicating they were Hardy Fractions B through F. In the B220+ cell population, 3.5% of the cells were CD19- (Fig. 3.7F), representing Hardy fraction A. The total non-B cells were substantially reduced to less than 4%.

After 20 h in culture there were 87.3% B220+ cells and 84.3% CD19+ cells (Fig. 3.7G and H). When co-labelled with both anti-B220 and anti-CD19 Abs there were 87.6% (7.63% + 80.0%) B220+ cells and 81.3% (1.34% + 80.0%) CD19+ cells (Fig. 3.7I). The cell population contained 80.0% B220+/CD19+ cells representing Hardy fractions B through F. Of the B220+ cell population, 8.7% did not express CD19 and were thus Hardy fraction A cells. There were 11.1% B220-/CD19- non-B cells. As B cells are not viable for long-term culture without growth factor supplementation and co-culturing with stromal cells, this change in population distribution was likely due to the loss of cells in the culture. Overall, the results demonstrated that the magnetic isolation kit 19854 was well suited to the isolation of immature bone marrow B cells and that these isolated cells were able to be cultured for short periods in RMPI 1640 complete media.

3.4 Antibody Crosslinking of CD24 Induces Apoptosis in Primary B Cells.

Next, antibody clustering experiments were performed on the isolated, enriched B cells ex vivo to determine if clustering of CD24 induces apoptosis in primary developing B cells. After incubation with antibody for 24 hours, B cell cultures were assessed for the proportion of apoptotic verses viable cells. Apoptosis was measured using FITC-labelled AnnexinV and Propidium Iodide (PI) co-staining. B cells in early apoptosis are positive for AnnexinV, but negative for PI whereas those in late apoptosis are both AnnexinV+ and PI+. Cells undergoing non-apoptotic or necrotic cell death are AnnexinV- but PI+. An average of 28.03% of control-treated samples were apoptotic, with 20.5% of those cells early apoptotic, and 79.5% of cells late apoptotic (Fig. 3.8). Treatment with M1/69 anti-CD24 in the absence of secondary antibody showed a slight, but non-significant increase in apoptotic cells compared with isotype. However, treatment with M1/69 and anti-M1/69 secondary antibodies to cluster CD24 resulted in a significant increase in the number of apoptotic cells (while no significant changes in necrosis were noted). On average, 59.5% of cells were apoptotic, with 35.5% early apoptotic and 64.5% late apoptotic. These results conclusively demonstrated that antibody crosslinking of CD24 induces apoptosis in primary B cells ex vivo.

3.5 Surface Expression of CD24 is Dynamically altered in response to Antibody-mediated Clustering

3.5.1 CD24 is rapidly externalized prior to endocytosis

The results from the bioinformatics analysis suggested that CD24 could be associated with endocytosis. To determine if CD24 is endocytosed in response to

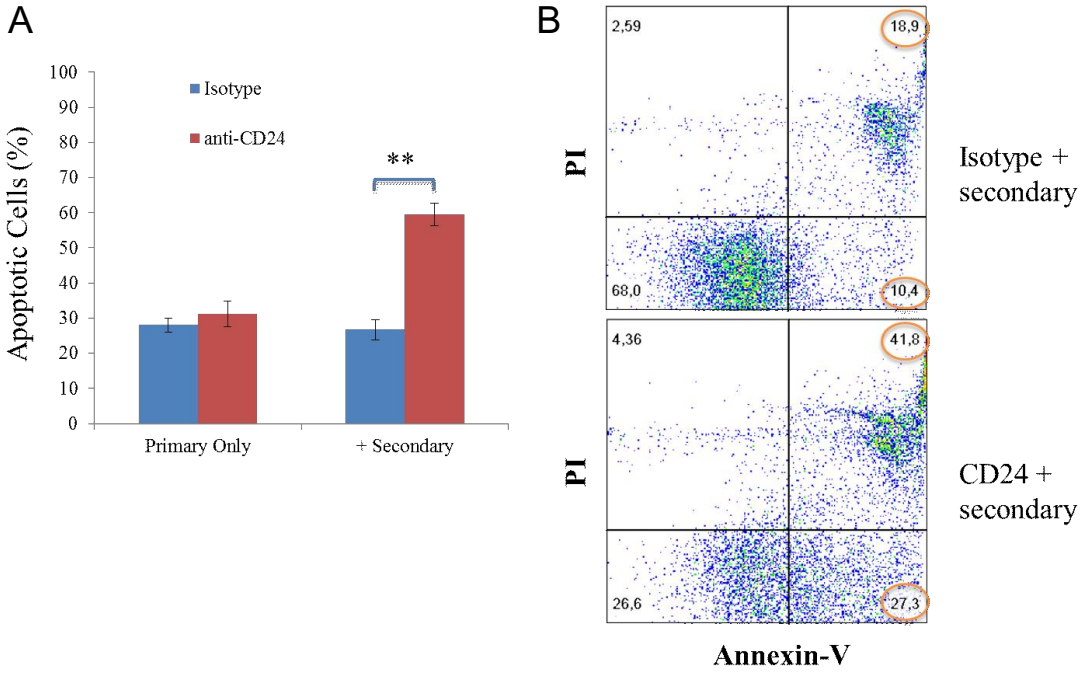

Fig. 3.8: Antibody mediated crosslinking of CD24 causes significant increases in apoptosis in bone marrow-derived, immature ex vivo B cells. Cells were incubated for 24h after addition of M1/69 anti-CD24 antibody or the isotype control antibody in the presence or absence of secondary antibody. Apoptosis was determined via Annexin V-FITC and Propidium Iodide staining. Statistical significance was determined using a paired Students' t-test. n=3 **p<0.005. A. Average induction of apoptosis (n=4). B. Representitive experiment showing proportion of early vs. late apoptotic cells.

antibody crosslinking and clustering, the expression of CD24 protein on the cell surface was examined. B cells were incubated with pre-mixed M1/69 anti-CD24 and a biotinylated anti-M1/69 secondary antibody for 1 to 60 minutes at 37˚C along with untreated control samples which were incubated for 60 minutes at 37˚C without antibody addition. Only biotinylated Ab remaining on the cell surface could bind streptavidin-FITC, and thus, only surface CD24 is detected. Unexpectedly, there was a significant increase in CD24 surface expression from 0 to 15 minutes followed by a decrease in cell surface expression (Fig. 3.9).

To determine if the changes to surface CD24 expression were statistically significant, the number of cells in each log unit of fluorescence intensity was analyzed at each time point (Fig. 3.10A and B). After 60 minutes at 37˚C, untreated control samples had an average of 93% of cells expressed CD24 (as indicated by relative fluorescence intensity above 10^1). Additionally, there was no change in the fluorescent intensity between untreated control samples and those incubated with antibody for 1 min In untreated control samples the largest population, with 62.7% of the total cells at this time point, had a fluorescent intensity between 10^2 and 10^3 and 2.6% had fluorescence above 10^3. Within 15 minutes of Ab-mediated crosslinking, there was a substantial change in the population distribution of CD24 expression. At this time, the number of cells with fluorescence intensity between 10^3 and 10^4, increased significantly from 2.6% to 34.8%. A total of 53.6% of the cells had a fluorescence intensity between 10^1 and 10^3. At this time, however, an increase in the population of cells lacking CD24 surface expression appeared, as 11.6% of the cells fell below 10^1. By 60 minutes, the number of cells with a fluorescence intensity below 10^1 increased significantly from 3.04% at 5 minutes

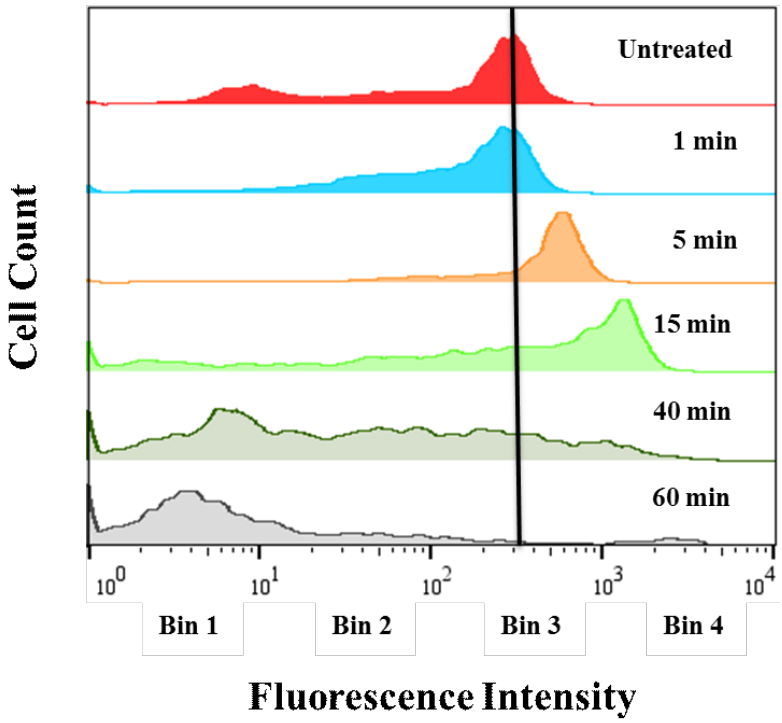

Fig. 3.9: CD24 surface expression is dynamic after antibody crosslinking in bone marrow-derived, immature ex vivo B cells. Cells were incubated for the indicated times in M1/69 anti-CD24 antibody in the presence of biotinylated secondary antibody. CD24 was stained with streptavidin-FITC for FACS analysis. Vertical line indicates modal CD24 expression of the control sample. Bins are demarked as 1 log unit of fluorescence intensity. Representative results shown from n=4 replicates.

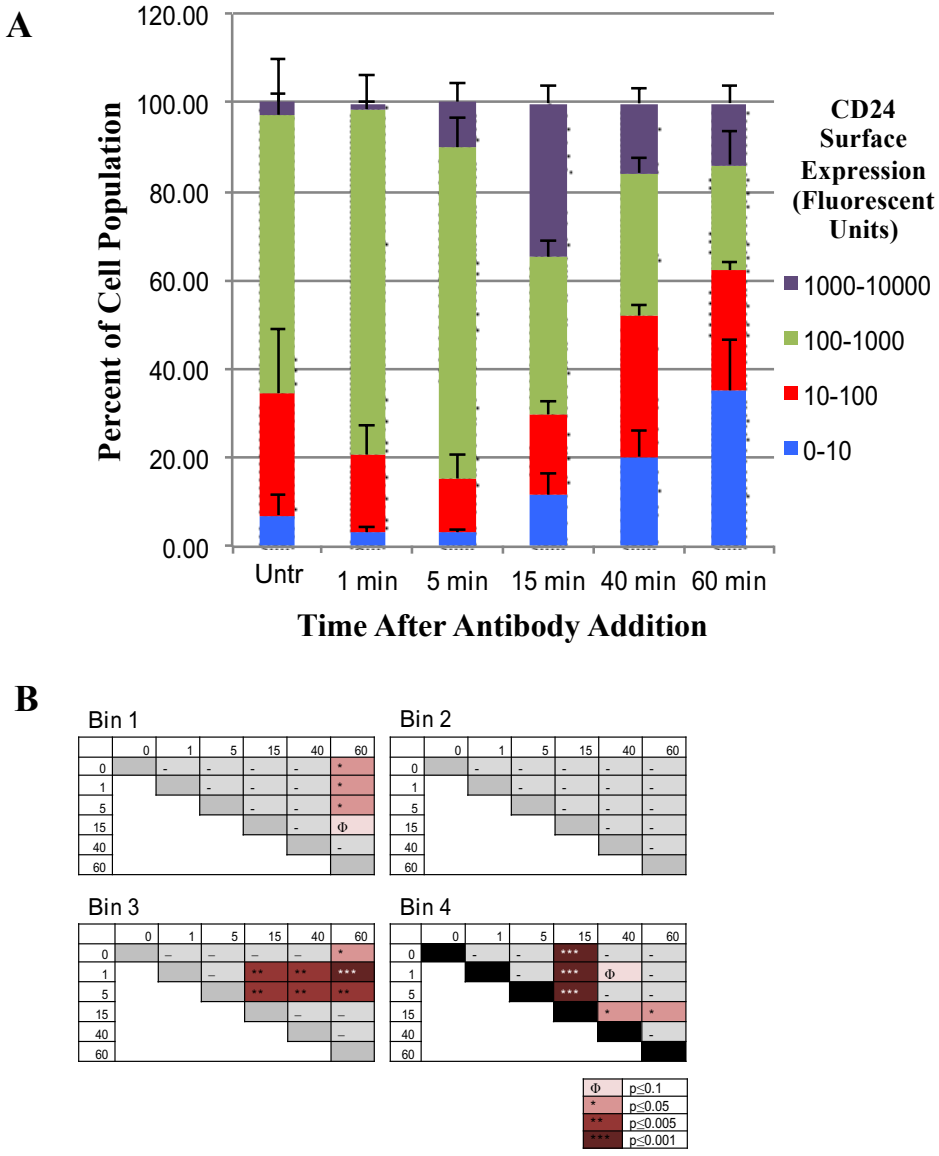

Fig. 3.10: A. CD24 surface expression after antibody crosslinking. Fluorescence intensity was binned over four log units: blue, 0-10; red, 10-100; green, 100-1000; purple, 1000-10000. Untr is untreated control sample. B. Heat map of all significant changes in CD24 expression across the four bins of fluorescent intensity. Significance was determined using a 1-way ANOVA followed by a TukeyHSD post-hoc analysis. n=4

to 35.0%. At both 40 and 60 minutes, however, 15.7% and 13.8% of cells, respectively, retained higher levels of CD24 on the cell surface with fluorescence above 10^3. As this method is specific for surface CD24 rather than total cell, or intracellular protein, the CD24-negative fraction represented cells that had lost CD24 surface expression at these time points. These results conclusively demonstrated that in response to antibody-mediated crosslinking of CD24, B cells rapidly externalized large amounts of CD24 protein followed by an equally rapid loss of surface expression.

In this experiment, a loss of fluorescent intensity may have been caused by receptor internalization via endocytosis, or by shedding of the receptor from the surface. To determine if CD24 protein was lost from the surface due to endocytosis or receptor shedding, primary and biotinylated secondary antibodies were pre-mixed with FITC-labelled streptavidin and added to isolated B cells for 30 minutes on ice before the 37°C incubation. This resulted in all cell surface CD24 being FITC-labelled thus allowing detection of both surface and any subsequently internalized CD24, but not CD24 that had been shed. CD24 staining increased over the entire 60-minute time course. This can be explained through the increased amount of CD24 expressed on the cell surface during the first 15 minutes of antibody crosslinking. As unbound antibody was not removed prior to incubation at 37°C, any newly externalized CD24 would also be FITC-labelled prior to internalization thus the overall fluorescence increased over time. This confirmed that the loss of surface staining was due to endocytosis rather than receptor shedding since the signal was not lost (Fig. 3.11). Furthermore, this result confirmed that the amount of surface CD24 protein increased in response to antibody clustering.

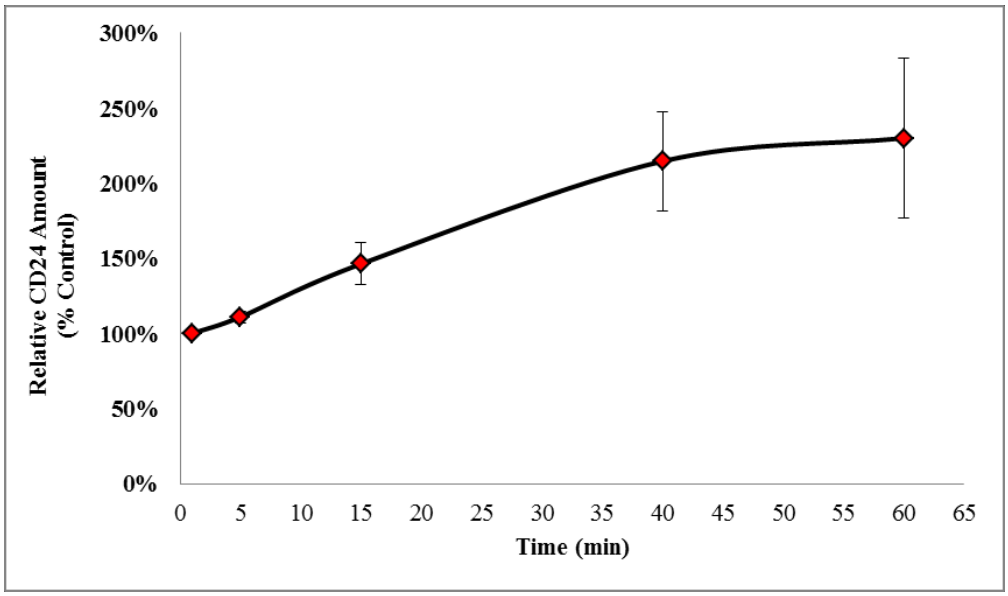

Fig. 3.11: CD24 is internalized and not shed following antibody crosslinking in bone marrow-derived immature ex vivo B cells. CD24 was pre-stained with M1/69 and FITC-labelled secondary antibody for 30 minutes on ice prior to incubation at 37°C for the indicated times, which will detect total surface and internalized CD24. CD24 expression was normalized to 1 minute. Increasing protein expression was detected over the course of 1h. n=4.

3.5.2 CD24 internalization is enhanced by actin depolymerisation

Dynamic actin rearrangement is known to be required for internalization of GPI-linked proteins through receptor-mediated endocytosis (84). To determine if CD24 endocytosis is actin-dependent, cells were pre-treating with Cytochalasin D (CytoD) for 30 minutes before antibody addition. CytoD-mediated loss of actin dynamics did not impair the internalization of CD24 (Fig. 3.12). At 40 minutes, an average of 48% of cells had florescence intensity at 10^1 or lower, indicating a loss of CD24 surface protein. Surprisingly, there was a greater loss of CD24 in CytoD treated cells compared to control treated cells (21.8%), although this difference only trended towards statistically significant (P=0.07). This suggests the dynamics of CD24 surface expression are influenced by actin cytoskeleton depolymerisation.

3.6 CD24 Localization Changes in Response to Antibody Crosslinking

3.6.1 Antibody crosslinking induces dynamic rearrangement of CD24 localization

Confocal microscopy was used to determine if the distribution of CD24 on the cell surface changed during antibody crosslinking (Fig. 3.13). Cell samples were taken during the endocytosis assay previously described. In untreated control samples, CD24 staining was punctate, with several well-defined foci and no obvious polarity. Within 5 minutes of antibody addition, however, cells began to become polarized with respect to CD24 distribution on the cell surface. Cells lost the punctate foci and developed unilateral or bilateral poles of CD24 expression. In this 5-minute interval, substantially larger areas of the cell stained for CD24, as demonstrated by the comparison between the small foci in

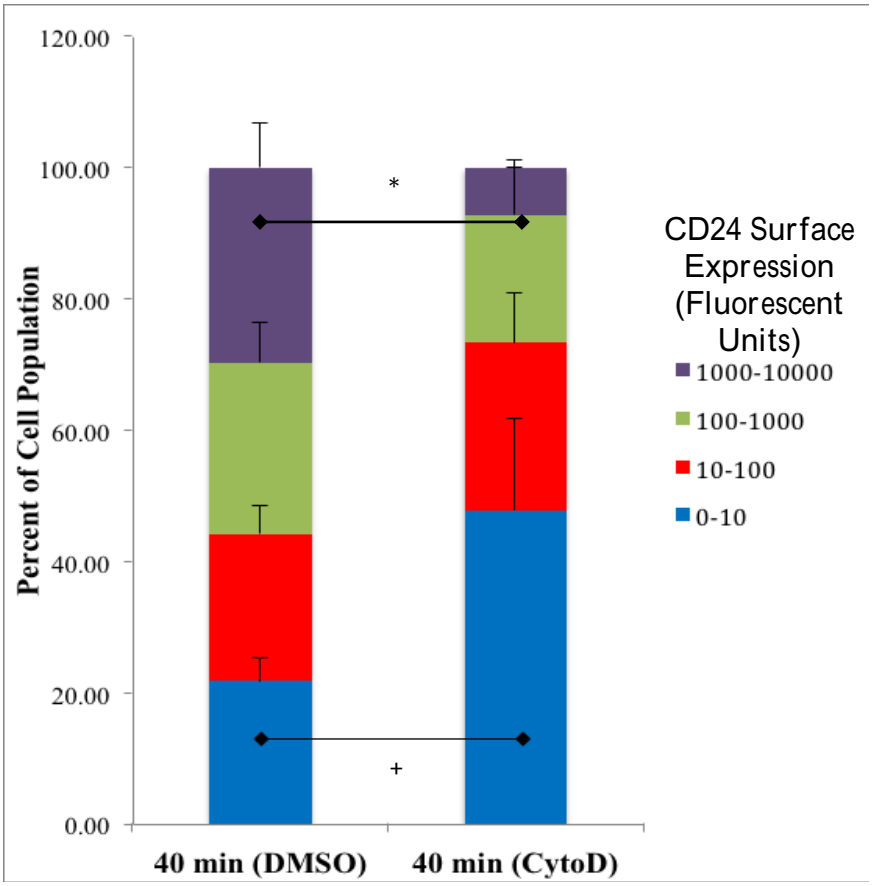

Fig. 3.12: Changes in surface CD24 expression after Cytochalasin D pre-treatment in response to antibody cross-linking. Cells were incubated with antibody for 40 minutes at 37°C. Statistical significance was assessed using a Paired Student's t-test.
*=P<0.05, +=P<0.1. n=3

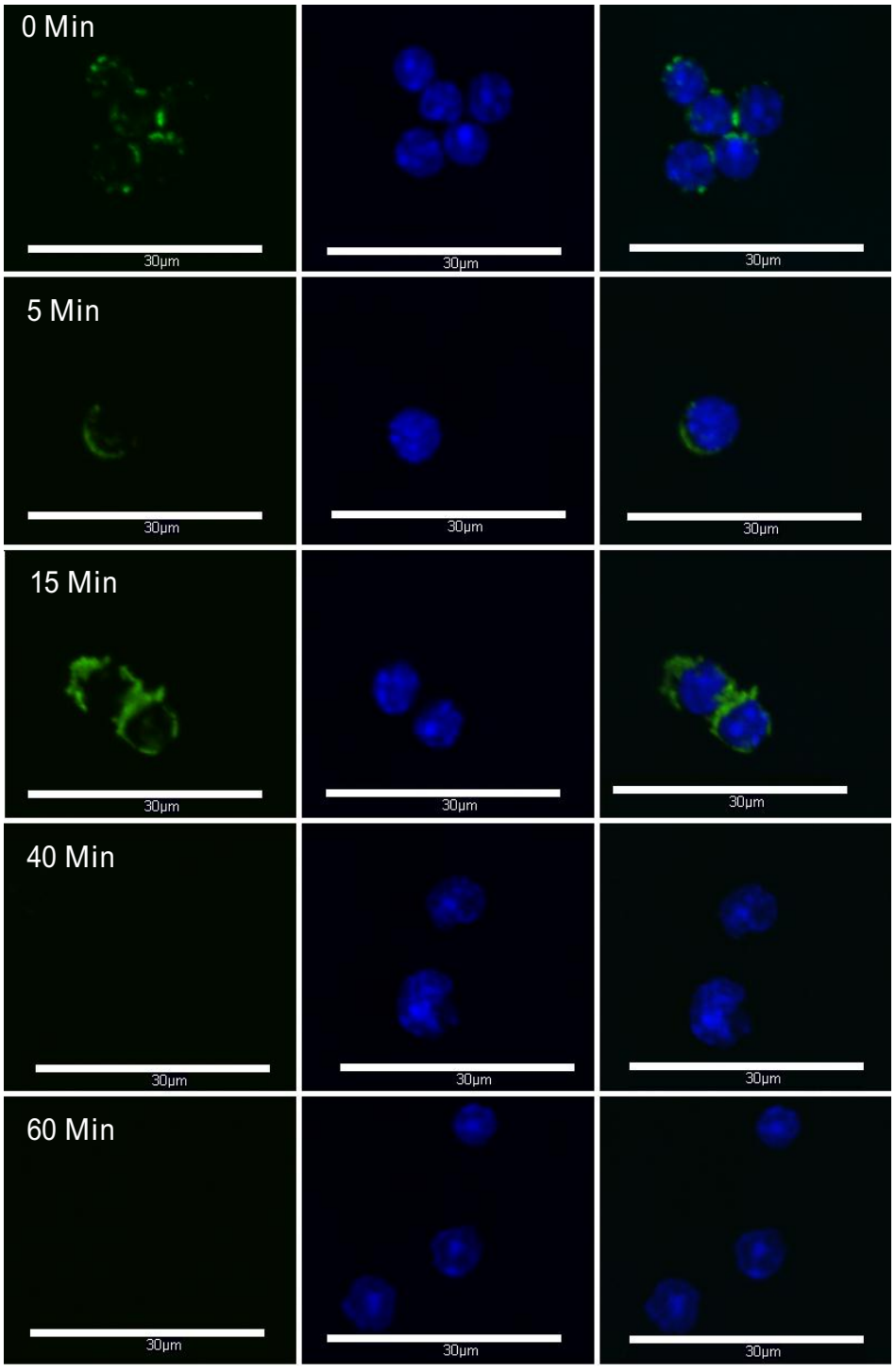

Fig. 3.13: Confocal microscopy analysis of CD24 expression and localization in non-interacting, single B cells in response to antibody crosslinking. Surface CD24 was stained with FITC (green) and cell nuclei were stained with DAPI (blue). Representative images of 3 experiments. Scale bar is 30 µM.

the untreated control sample and the larger 'crescent' at 5 minutes. Cell polarization was also more pronounced at 5 minutes, where the majority of cells had a unipolar expression of CD24. By 15 min, CD24 polarity was maintained and there was an increase in the membrane coverage of surface CD24 expression in single cells, while some developed membrane ruffling. The appearance of a broader pattern of surface staining for CD24 is consistent with the increased protein expression quantified by FACS (Fig. 3.9). In addition, within 15 minutes, two distinct cell phenotypes were observed with a portion of cells forming clusters and others remaining as non-interacting single cells.

At 40 and 60 minutes, single cells lost most, if not all, of their surface CD24 expression (Fig. 3.13). At 40 minutes, single cells returned to a mostly punctate staining, where many cells had only a single area of expression, or lost CD24 expression entirely. By 60 minutes, single cells were predominantly CD24- with very few retaining any measureable expression. These results support the FACS data, as flow cytometry only records the fluorescence of single cells, and any clusters would be disrupted immediately prior to analysis or not analyzed by the software. These data were also congruent with the results from the endocytosis assay, which showed a significant reduction in cells expressing surface CD24, but a small proportion of cells retaining high levels of surface protein.

With respect to each time point, CD24 staining in cell clusters was more intense than in non-interacting single cells and large portions of the cell surface became CD24+ in these clusters (Fig. 3.14). In clustered cells CD24 was localized on the membrane faces between interacting cells after 40 min of anti-CD24 clustering. By 60 min, there was a reduction of staining in clusters. CD24 expression was found on a large fraction of the cell surface in these clustered cells that were present on the interior of clusters,

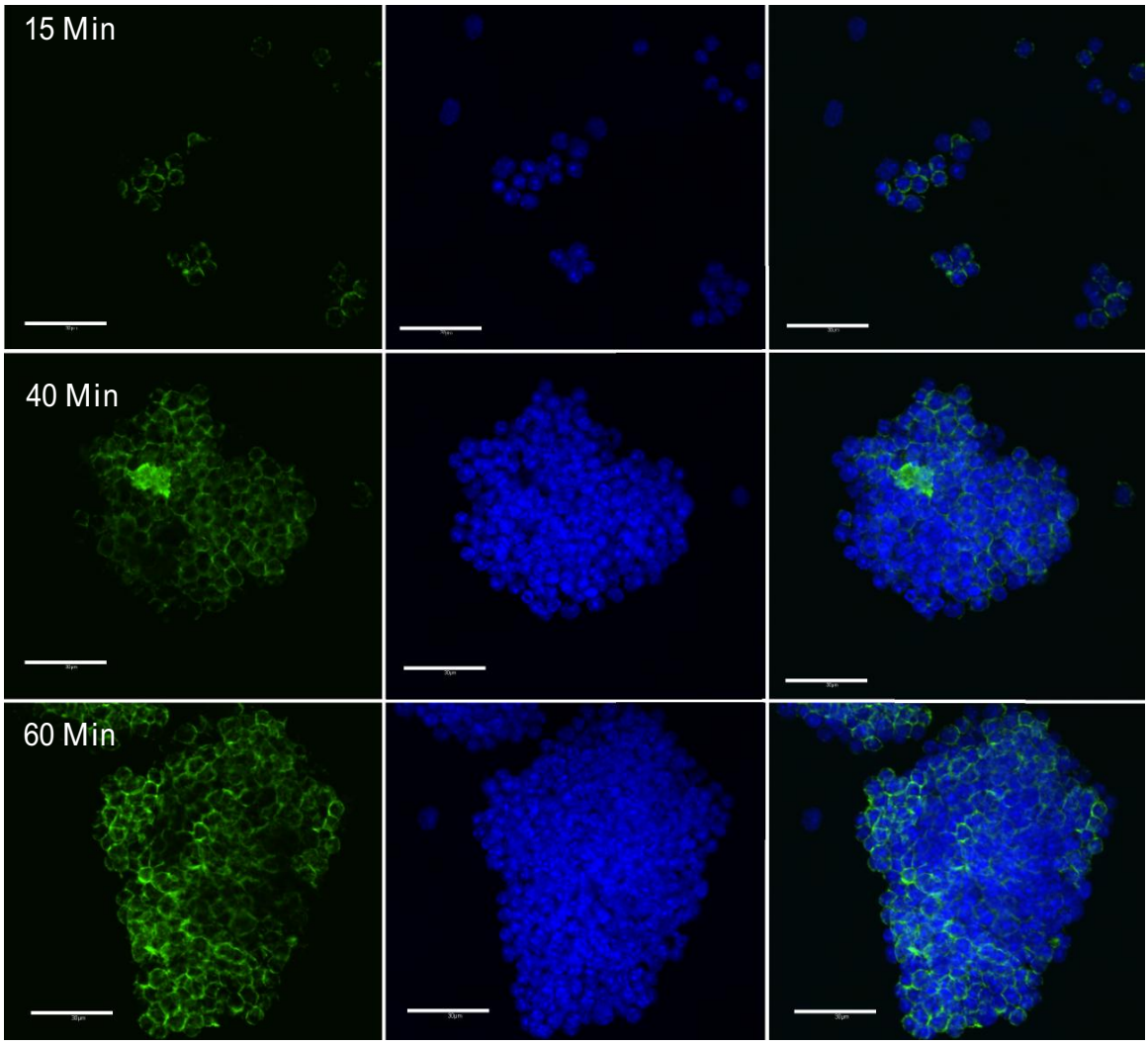

Fig. 3.14: Confocal microscopy analysis of CD24 expression and localization in clustered B cells in response to antibody crosslinking. CD24 was stained with FITC (green) and cell nuclei were stained with DAPI (blue). Representative images of 3 experiments. Scale bar is 30 µM.

however in many cases there was reduced or absent expression on the external face of the outermost cells of the cluster. As described in section 3.5.2, treatment of cells with CytoD tended to increase the internalization of CD24 in B cells. Confocal microscopy was also used to determine how it affected the distribution of CD24 on the cell surface (Fig. 3.15). Cells treated with DMSO as the vehicle control responded similarly to cells treated with anti-CD24 alone: clusters had the highest level of CD24 expression, and single cells had predominately punctate staining with no obvious localization. In comparison, CytoD treated cells had a profound loss of CD24 expression both in single cells and in cells found in clusters (Fig. 3.15). Remarkably, no single cells were found to express CD24 in the images obtained. Even in clusters, CD24 expression was only detected in a minority of cells indicating that CytoD treatment results in an increase in the rate of endocytosis.

These results supported the hypothesis that CD24 is not acting as the anchor for cell adhesion, but is mediating these interactions by regulating other cell adhesion proteins. Furthermore, the CytoD data show that CD24 expression is not permanently maintained in cell clusters. In cells not treated with CytoD the CD24 retained in clusters after it has been lost in single cells is likely due to a change in the rate of endocytosis or exocytosis rather than the abrogation of the process. The results from both the FACS and confocal analysis strongly suggest that altering actin dynamics profoundly augments CD24-mediated endocytosis; however, the precise role of the actin cytoskeleton in regulating this process is unclear.

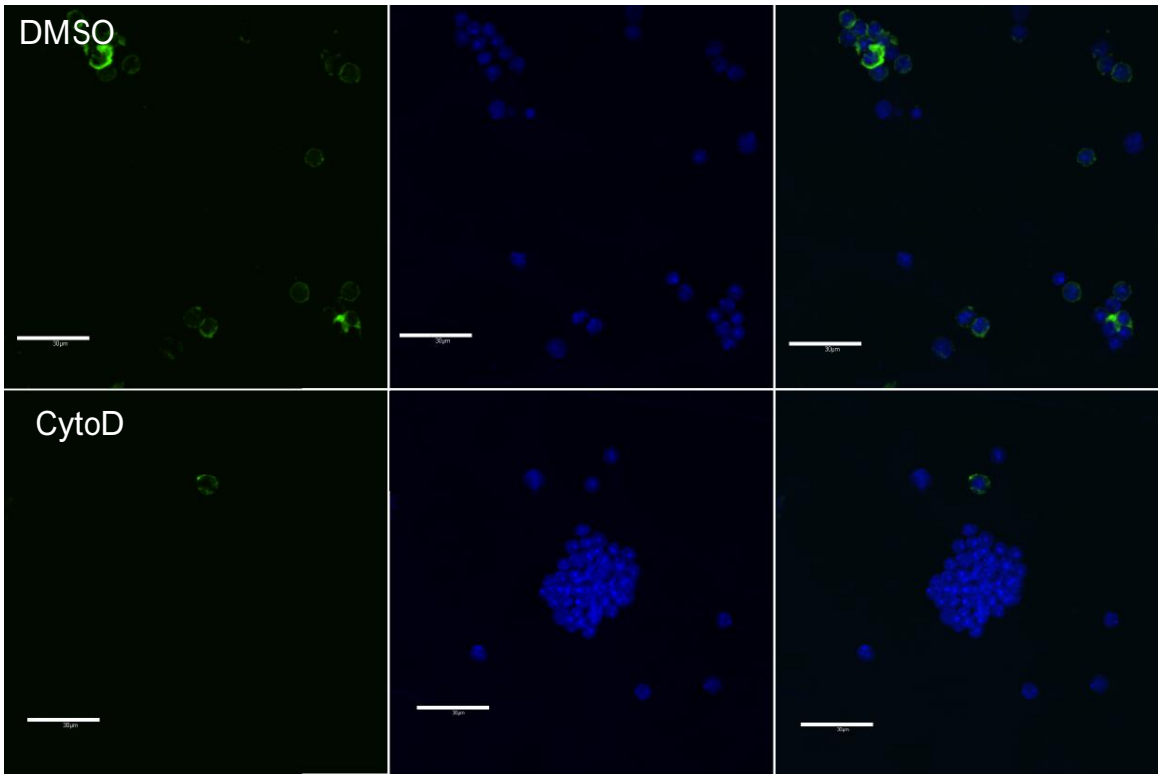

Fig. 3.15: Confocal microscopy analysis of CD24 expression and localization in non-interacting, single B cells pre-treated with DMSO or 1 µM Cytochalasin D in response to antibody crosslinking. CD24 was stained with FITC (green) and cell nuclei were stained with DAPI (blue). Representative images of 3 experiments. Scale bar is 30 µM.

CHAPTER 4: DISCUSSION

4.1 Summary

The purpose of this investigation was to determine if WEHI-231 cells are an appropriate model system to examine CD24 gene regulation in B cells and to determine a mechanism through which CD24 induces apoptosis in bone marrow-derived, immature B cells. Using a bioinformatics-based approach, I identified co-regulated genes to be essential regulators of endocytosis, vesicle trafficking and cytoskeletal organization. From this I hypothesized that engagement of CD24 is associated with endocytosis, and I have shown, for the first time, that primary mouse B cells, isolated from bone marrow using untouched magnetic separation, are susceptible to CD24-induced apoptosis. Using this model, I have shown that CD24 surface expression is dynamic in response to antibody crosslinking, with an initial increase in surface expression followed by endocytosis of CD24. In addition, I have also demonstrated that CD24 protein accumulates in localized membrane regions and is a mediator of homotypic cell adhesion.

4.2 Many transformed B cells do not model CD24 biology

Past studies of CD24 function and regulation in B cells have either used transgenic or knockout animals (56, 57), transformed cell lines (46, 58) or an in vitro long-term cell culture system from bone marrow B cells (19). As a first attempt to follow CD24 expression upon B cell activation in vivo, the expression in the mouse B cell line WEHI-231 was characterized. WEHI-231 cells are classified as an immature (Hardy fraction E) malignant B cell lymphoma (62). Previously it was reported that these cells

are resistant to CD24-mediated apoptosis (19) and indeed, I found that CD24 expression is not dynamically regulated in response to maturation stimulation in WEHI-231 cells. As such, I conclude that both the regulation of CD24 expression and the regulation of downstream function in these cells is deregulated.

The classification of WEHI-231 cells as immature B cells is derived from their high expression of the B-cell receptor in the IgM isoform (62). In normal B cells, CD24 expression is significantly reduced in this fraction (2, 3), whereas WEHI-231 cells express CD24 at high levels more analogous to the pre-B cell Hardy fractions. Indeed, recent research has shown that WEHI-231 cells have characteristics that belong to several different B cell stages. In a recent bioinformatics analysis, it was found that they share similar gene expression patterns to pre-B cells (Hardy fraction C′ or D) (85), while other research has suggested that they are more analogous to mature, transitional B cells or a nonconventional mature B cell (86). This incongruity strongly suggests that WEHI-231 cells may not be truly representative of normally developing B cells and may explain why the underlying system regulating the expression of CD24 appears to be dysfunctional.

In addition to WEHI-231, other immature B cell lines have been developed using both human and mouse systems. The response of these other cell lines to CD24 crosslinking is largely unknown. Research has been done using the human Burkitt's lymphoma lines P32/SH and Namalwa, as well as the Pre-B HPB-NULL, NALM-6, NALM-17 and P30/OHK and the Pro-B NALM-16, NALM-20, NALM-27, LC4-1 and KM-3 cell lines, which demonstrated CD24 crosslinking induces apoptosis in these human cells (46, 56, 58). Thus, other mouse or human cell lines such as CH31 and B104, respectively could be used to investigate the activity of CD24.

Despite their inability to model CD24 activity, the malignant transformation in WEHI-231 cells that renders them insensitive to CD24-mediated apoptosis may serve to help identify potential signalling partners or pathways that can alter a cell's responsiveness to CD24. WEHI-231 cells are resistant to CD24, but they retain their sensitivity to other apoptosis-inducing signals, such as crosslinking of the BCR (85, 86), demonstrating that the underlying apoptotic machinery is still functional in these cells. As the underlying biological transformation that generated the WEHI-231 lymphoma is not known, identifying the disrupted processes would provide insight into the pathways required for CD24 activity. It has been noted that other transformed B cells are also resistant to CD24 mediated apoptosis as well (19); thus any future research into classifying the nature of their transformations can also inform future CD24 research.

One well-documented transformation, which renders B cells insensitive to CD24-mediated apoptosis, is the Abelson transformation (19). Abelson-transformed cell lines have been infected with the Abelson murine leukemia virus (87, 88). This virus encodes the v-Abl gene, which shares a high degree of similarity to the mammalian c-Abl gene (87, 88). The result is a constitutively active form of the Abl non-receptor tyrosine kinase (88). This transformation is also similar to a mutation in humans called the Philadelphia chromosome, caused by a reciprocal translocation between the Breakpoint Cluster Region gene and the c-Abl gene creating constitutively active BCR-Abl fusion protein (89).

In both cases, the malignant transformation is mediated through the Abl tyrosine kinase, which interacts with members of the Ras superfamily of proteins, such as Rho GTPases RAC1 and CDC42 (90, 91). These proteins are known to regulate processes such as cell cycle control, vesicle trafficking, cytoskeletal arrangement and cell polarity

(92, 93). Furthermore, the microarray analysis has shown positive correlations between CD24 expression and several members of the Ras superfamily of proteins. For example, one of the most similar genes with regard to CD24 expression is the Rho GTPase regulator MCF2L that mediates endocytosis, and interacts with both Rac1 and CDC42 (94). CD24 expression is also positively correlated with other GTPase proteins such as the previously discussed RabL5, RHOT2, which regulates mitochondria and apoptosis (95), and a CDC42 regulator involved in cell shape modification (CDC42EP3; CDC42 Effector Protein 3) (96). Thus, the bioinformatics data in conjunction with our knowledge of the WEHI-231 cell line suggest that the induction of apoptosis by CD24 is dependent on members of Ras superfamily. These data are further supported in that Lyn, a Src family tyrosine kinase which was previously discussed to be downstream of CD24 signalling, is upstream of both CDC42 and RAC1 in B cell receptor signalling (97).

From these results, we can conclude that the WEHI-231 cell line is unsuitable for further research with regard to endogenous CD24 activity in healthy, immature B cells. In the future WEHI-231, as well as other transformed B cell lines, could serve as a model system to identify the molecular mechanism for the resistance of transformed cells to undergo CD24-mediated apoptosis.

4.3 Generation of hypothesis that CD24 is associated with endocytosis by bioinformatics analysis

In recent years microarray analysis, and other bioinformatics tools, have produced large caches of gene expression data. Furthermore, the establishment of the MIAME (Minimum Information About Microarray Experiments) protocol ensures that data from

DNA microarray studies are made freely available to the research community. ImmGen is a MIAME-compliant research collaboration that is mapping the transcriptomes of immune relevant cells, including each stage of B cell development.

This valuable resource has allowed the exploration of the relationships between B cell development and CD24 expression to identify potential partners for CD24 function. Specifically, data from the ImmGen database were used as a hypothesis-generating tool using the "guilt by association" theory (98). "Guilt by association" postulates that in biological systems, genes which share similar expression patterns, either through time or under a selection system, are more likely to be involved in the same, or congruent processes, and potentially be under the same transcriptional control (98). While this type of analysis is limited to correlative association, it can suggest previously unknown protein partners or processes for further study. In effect, this technique is used as a screen to select potentially relevant genes from the background population. Individually, the genes may provide targets that can be functionally validated, but this can be time consuming, particularly with large numbers of genes, as each target must be validated individually. Furthermore, many pathways have multiple redundancies, which increase the potential for false negative or false positive results at the functional level. By comparison, grouping genes into functional clusters based on functional relatedness allows biological processes to be validated instead. For example, the screen of ImmGen data revealed EHD2, FCHO1 and RABL5 (among others) as participating in endocytic vesicle formation and trafficking. Blocking or enhancing endocytosis rather than targeting each gene separately can achieve functional validation.

The "guilt-by-association" technique is particularly relevant in identifying underlying gene expression regulatory factors, isolating functional relatedness in poorly understood proteins or pathways, and is used extensively in pharmaceutical target identification. For example, Smith et al. (99) used this approach followed by loss-of-function analysis to identify regulatory elements controlling cytokinesis via central spindle proteins. "Guilt by association" was also used to predict the function of heart tissue-enriched mitochondrial genes Coiled-coil-helix-coiled-coil-helix domain containing 10 (CHCHD10) and glioblastoma amplified sequence (GBAS) (100). Little was known about the function of these genes, but associations suggested they were involved in oxidative phosphorylation, which was later validated (100). Finally Lounkine et al. (101) used "guilt by association" to identify potential side effects from drug testing by identifying pathways which may be affected outside of the intended clinical application. In that study, 656 drugs were studied, and 73 off-target side effects were postulated. The authors noted that half of these were subsequently confirmed in clinical data (101). Moving beyond gene expression and network analysis, this approach provided testable hypotheses through gene ontology enrichment.

In this thesis, potential CD24 partners were identified using unsupervised clustering followed by biological annotation and network analysis. Thirty-eight co-expressed genes were identified out of over 35,000 genes analyzed. The subsequent network analysis and the identification of gene ontology enrichments identified that the three major processes that correlated with CD24 expression to be: mitochondrial apoptosis and apoptotic signalling; cytoskeletal organization; and endocytosis and vesicle trafficking. Identification of endocytosis as a process associated with CD24 formed the

basis of the major hypothesis of this thesis, which is that CD24 signalling is associated with endocytosis. The data presented in this thesis fully support this hypothesis, however, the precise endocytic process through which CD24 is internalized has yet to be established.

The genes whose expression clusters with CD24 expression may provide targets for loss-of-function or gain-of-function studies to determine how the identified genes specifically contribute to CD24 function. For example, EHD2, one of the closest of the co-clustered genes to the expression of CD24, is involved in mediating vesicle internalisation (79). Small Interfering RNA knockdown of EHD2 has been demonstrated in 3T3-L1 mouse adipocytes to disrupt endocytosis (79) and thus represents a valid target in mouse B cells. If disruption of EHD2 also inhibits CD24 endocytosis, it would be strong evidence that CD24 is internalized via a similar process. Alternatively, genes identified in our network could inform target choices to restore sensitivity to CD24-mediated apoptosis, such as in WEHI-231 cells.

4.4 Induction of apoptosis by CD24 clustering in bone marrow derived B cells ex-vivo

To functionally validate the microarray analysis, an ex vivo model system for studying CD24-functionality in immature, bone marrow-derived B cells was first developed. As previously mentioned, prior research on CD24 expression in B cells has used a variety of cell lines, in vitro tissue culturing, transgenic and knockout animals (9, 19, 46, 56, 58). While these systems have provided vital insight for the role of CD24 in B cell survival, they cannot replicate the innate in vivo biology of immature B cells since

genetically altered mice are able to compensate for loss or gain-of-function of CD24, and cell lines or long-term culture methods can change the inherent response of cells. By using untouched magnetic separation, we are able to isolate normal, functional B cells with normal levels of endogenous CD24.

Using bone marrow derived B cells, it was clear that endogenous CD24 induces cell death in wild-type, immature B cells expressing endogenous levels of receptor. The induction of apoptosis requires extensive crosslinking of CD24 on the cell surface, as evidenced by the need for a secondary antibody to induce significant cell death. Previous in vitro studies using mouse pro- and pre-B cells co-cultured with bone marrow stromal cells, as well as human Burkitt's and Acute Lymphoblastic Leukemia cells, demonstrated that addition of primary anti-CD24 antibodies could induce apoptosis, but that adding secondary antibodies to further cluster the receptors increased apoptosis significantly, but was not absolutely required (19, 58, 60). This is in disagreement with the results presented here, which showed that primary antibody alone was not sufficient to induce apoptosis, but that secondary antibody clustering was required. In the study by Chappel et al. (19), the efficacy of apoptosis induction by primary antibody alone was compared to the combined primary/secondary antibody treatments in mouse B-cells derived from bone marrow cell cultures. Their results indicated that primary antibody alone could induce apoptosis and the presence of a secondary antibody potentiated this effect (19). The ability of primary antibody alone to induce apoptosis may be due the amount of CD24 expression the cell surface following this culturing, or possibly due to phenotypic changes in the B cells during the prolonged cell culture. Comparatively, our experiments use B cells directly isolated form bone marrow without tissue culture. Furthermore, Chappel et

al. (19) made extensive use of co-culturing with stromal cells to support B cell populations, which provides a different microenvironment from using a more homogenous isolated population. Subsequent studies in human cell lines, most notably with HPB-Null Pre-B cell acute lymphoblastic leukemia cells used the combined primary and secondary antibody treatment exclusively to induce apoptosis (58). Fundamentally, however, our results as well as the results from both of these previous studies (19, 58) strongly suggest that multiple CD24 receptors must be clustered in order to efficiently activate intracellular activation of pro-apoptotic pathways.

It is also important to note our results have demonstrated that the respond to CD24 crosslinking is specific and requires CD24 to be engaged, and is not a result of either Fc receptor-mediated action or non-specific antibody binding. B-cells express receptors that can bind the constant region of antibodies (Fc receptors), which can modulate immune cell responses (102). During B-cell isolation anti-Fc receptor antibodies were added, which block the ability of these receptors to bind the anti-CD24 or secondary antibodies used to engage CD24. Furthermore, the response to CD24 Ab-mediated crosslinking absolutely requires anti-CD24 antibody because cells incubated with matching isotype antibody with the same secondary antibody did not undergo increased cell death or endocytosis.

The observation that a high level of CD24 clustering is necessary to induce cell death by CD24 is consistent with studies on other lipid raft-associated, GPI-linked proteins. For example, lipid raft clustering brings multiple CD59 proteins into close proximity and initiates downstream signalling (84). This clustering has been shown to recruit between three and nine receptors and leads to the downstream activation of the

Lyn kinase (103). Another example is the GPI-linked urokinase plasminogen activator receptor (uPAR). In human melanoma cells, evidence suggests that uPAR clustering is required for efficient activation and that the receptors will cluster in caveolin-coated invaginations prior to endocytosis (104).

As previously discussed the microenvironment of the bone marrow is critically important in B cell development and thus may play a role in CD24-mediated behaviour in pre- and pro-B cells. Immature B cells are dependent on bone marrow stromal cells for much of their early development (2, 48, 49). Multiple stromal cell lines are available and can mimic the normal stroma in this regard. Thus, our ex vivo system can be modified by culturing stromal cells with the immature B cells to determine if the microenvironment of the bone marrow modifies the response to CD24. Another consideration in replicating the bone marrow microenvironment is that the various cell populations produce and require different growth factors and cytokines to support hematopoietic cell development. For example, early B cells are critically dependent on the hematopoetic growth factor IL-7 (50, 52) and the production of Stromal Cell-Derived Factor (SDF-1), also known as CXCL12, which directs pro-B cell chemotaxis and promotes appropriate stromal attachment (105). CXCL12 is chemotactic for lymphocytes such as B cells. Of further interest, the receptor for this factor is CXCR4, whose function is negatively regulated by CD24 (105). The CXCL12/CXCR4 signalling system is a major regulator in B cell development and directs the earliest B cell precursors to areas capable of supporting their development (106). Thus, a promising avenue for future studies is to examine how the bone marrow microenvironment influences CD24 function and vice versa.

In addition to their support from bone marrow stromal cells, B cell development is highly dependent on the contextual interactions of early B cells with each other (107, 108). For example, research has shown that pre-B cells stimulate maturation through homotypic contact through stimulation of the pre-B cell receptor and that blocking these interactions induces maturation arrest (108). Our results have conclusively shown that CD24 activation causes the rapid formation of B cell clusters, so it is reasonable to conclude that CD24 may be a regulator of these homotypic interactions. Indeed, a second opportunity with this ex vivo system is to further isolate and then selectively combine specific B cell populations (for instance, Pro-B cell, Hardy fraction C′ and Pre-B cell, Hardy fraction D cells) to determine what effect, if any, the local B cell populations have on each other.

4.5 Dynamics of CD24 Surface Expression

This is the first report showing that surface expression of CD24 is dynamic in response to antibody crosslinking. In addition, this work is the first to suggest a mechanism through which CD24 can initiate signalling since CD24 has no transmembrane domain. Previous research has demonstrated that other GPI-linked receptors are endocytosed after crosslinking (84) and that endocytic vesicles can affect intracellular signalling pathways via the endosomal adapter proteins on their surface (109-111). For example, the Eps15 protein, which participates in both clathrin and non-clathrin mediated endocytosis also regulates B cell lymphopoiesis (110). Endosomal coat proteins have also been shown to activate MAPK proteins such as Erk1/2 from endocytic

vesicles (109), which are the same downstream targets of CD24. Thus, endocytosis represents a plausible intial signalling event following CD24 stimulation.

Endocytosis can be divided into two major categories: Clathrin-dependent endocytosis (associated with traditional Receptor-Mediated endocytosis), and caveolin/lipid raft-mediated endocytosis (112, 113). Each process requires unique mediator proteins and results in different downstream events. First isolated in 1975, clathrin is a triskelion-shaped protein, which forms a scaffold around the nascent endocytic vesicles, or endosomes (114, 115). At the plasma membrane, the process of clathrin-mediated endocytosis (CME) can be subdivided into three stages: 1) the formation of the clathrin coat; 2) the invagination of the plasma membrane and; 3) the release of the coated vesicle from the membrane surface (114). The formation of the clathrin coat begins when adapter proteins, such as AP-2, recruit clathrin to the plasma membrane in response to surface receptor signalling (111, 114). The nucleation of clathrin at the membrane then causes invaginations to form (111). During this process, a host of regulatory proteins including, but not limited to, Eps15, Intersectin, Epsin and amphiphysin can bind to the nascent vesicle (111). Finally, scission proteins, such as dynamin release the vesicle from the membrane (111, 114). Research suggests that the initial adapter protein, such as Adapter Protein-2 (AP-2), and the subsequent regulatory proteins are variable and that the specific association of different proteins can direct downstream consequences including signalling from the clathrin coated vesicle, or the trafficking of the endosome (111, 114).

Clathrin-mediated endocytosis was synonymous with receptor-mediated endocytosis signalling for many years (114) and was viewed as a mechanism to resolve or

attenuate a signalling event by the internalization and either degradation or recycling of the receptor (111). However, it has been shown that these endosomes can recruit cytosolic factors and act as signalling platforms (111). For example, clathrin-dependent receptor mediated endocytosis of Receptor Tyrosine Kinases (RTKs) can activate ERK1/2 from endosomes (111). This has been found to be the case for signalling from the Epidermal Growth Factor Receptor (EGFR), the Insulin Receptor and the Neurotrophin receptor (TrkA) and appears to be common to RTKs in general (116). This parallels research showing that CD24 is associated with the protein tyrosine kinase Lyn and can also result in activation of ERK (46). Interestingly, the results from the bioinformatics analysis show that CD24 is co-expressed with mediators of clathrin-dependent endocytosis, such as adaptor-related protein complex 1 associated regulatory protein (AP1AR) (81) and FCHO1 (80).

Lipid raft-mediated endocytosis is another mechanism for endocytosis. In some cases caveolin proteins induce endocytosis by coating membrane invaginations, termed caveolae (113). The nature of lipid raft-mediated endocytosis is complicated in lymphoid cells, including B cells, as they do not express caveolin (117), but can form functional caveolae-like invaginations from clustered lipid rafts in a cholesterol-dependent manner (84). Caveolin-coated and lipid raft-derived caveolae retain the same physical and functional properties (113). As such, it is becoming increasingly common to discuss caveolin/lipid raft endocytosis as one type of endocytosis (113). Caveolin appears to be a vesicle-stabilizing protein that delays the scission of the vesicle from the membrane (113). One theory is that caveolin creates a stabilized signalling platform whereas the lipid rafts are used as a more rapid, transitional signalling system (113, 118). Indeed,

research has shown that caveolin itself is dispensable for endocytosis as the endocytosis of cholera toxin B by the ganglioside GM1 receptor can occur in the presence or absence of the caveolin protein (119).

The release of endosomes from the plasma membrane into the cytoplasm, a process known as vesicle scission, is the next step in endocytosis. The protein dynamin, or dynamin-family proteins, are essential for scission, regardless if the endosomes have formed through clathrin- or caveolin/lipid raft-mediated events (113). Dynamin is a GTPase, which acts as a scission motor to release the endosome after it has formed (113). Thus, regardless of how cargo is targeted for endocytosis, the action of dynamin, or a closely related protein, is essential for any downstream internalization (113, 120). As such, we may hypothesize that despite lacking caveolin, GPI-linked receptors may still be endocytosed by lymphocytes through lipid raft-mediated invaginations followed by a release from the membrane by dynamin.

Research in B cells on the GPI-linked CD59 cell surface receptor may serve as a model for the action of CD24 (84). CD59 is a known negative regulator of the compliment membrane attack complex (121). Like CD24, CD59 endocytosis was only observed after lipid raft clustering. Furthermore this internalization could be blocked using nystatin, a cholesterol-chelating agent that results in the disruption of lipid rafts (84) but clathrin-mediated endocytosis was unaffected (84). This strongly supports the contention that lipid rafts themselves can be mediators of endocytosis. Moreover, CD59 was internalized through uncoated caveolae (84). Unlike what was observed for CD24, CD59 internalization was blocked when cells were treated with Cytochalasin H, an actin-destablizing agent similar to CytoD (84). This suggests that dynamic actin rearrangement

is necessary for internalization of CD59, but that the inhibition of actin dynamics actually enhanced internalization of CD24. Another possibility is that the actin cytoskeleton is required to regulate the localization of CD24 on the cell surface, as well as its interactions with other surface proteins. Thus the addition of Cytochlasin D may disrupt these associations leading to the inappropriate or untimely internalization of CD24.

Future work is necessary to determine the precise method by which CD24 is internalized. The results from our bioinformatics assay were the first to suggest that CD24 may function through endocytosis. Several of the genes identified are involved in vesicle trafficking or serve as regulatory or adaptor proteins and are thus applicable to both clathrin and caveolin/lipd-raft –mediated endocytosis. Despite this, one of the genes with the closest co-expression pattern to CD24 is EHD2, which has recently been shown to be specific to caveolae internalization. Guilherme et al. (79) reported in 2004 that EHD2 links endocytosis to the actin cytoskeleton. Subsequent research has shown that EHD2 regulates endocytosis in a similar manner to caveolin, by delaying the release of caveolae from the cell surface into the cytosol. (122). Given the lack of caveolin expression in lymphocytes (117), it is possible that EHD2 may act as a substitute for caveolin function. As previously discussed, EHD2 knockdown has been accomplished in mouse cell lines opening the possibility for loss-of-function studies in isolated immature B cells. As such, understanding the role that EDH2 plays in mediating CD24 internalization is a priority for future studies.

Future research could also use pharmacological inhibition of endocytosis to identify the mechanism for endocytosis of CD24 in B cells. There are several methods for selectively disrupting caveolin-, lipid raft-, and clathrin-mediated endocytosis. The first

hypothesis to test would be that CD24 is internalized via a lipid raft-mediated mechanism, given that other GPI-linked receptors are known to function in this manner and the co-expression of CD24 and EHD2. Inhibition of lipid-raft-mediated endocytosis has been accomplished using the cholesterol sequestering agents filipin or nystatin through selective depletion of cholesterol via methyl-β-cyclodextran, and by inhibiting cholesterol synthesis with enzymatic inhibitors (123).

In addition to demonstrating that CD24 is endocytosed, this is the first study to observe that CD24 protein expression increases on the cell surface in response to antibody-mediated crosslinking. Moreover, this is the first time that CD24 has been implicated in regulating its own expression. The increase in CD24 protein may be due to either a rapid increase in the formation of new protein or due to the fusion of CD24-containing exosomes with the plasma membrane. Further research is required to determine exactly how the increase in CD24 occurs. To help identify the mechanism, the level of expression of surface CD24 can be compared with the level of expression of internal CD24 that can be detected after membrane permeabilization followed by FACS and confocal analysis. If CD24 is pre-formed and resides in vesicles, it will be fluorescently labelled and thus detectable prior to exocytosis. Total cell staining would then show no increase over time whereas surface staining would increase. If CD24 is newly translated, however, both total cell and surface staining would increase during the first 15 minutes after antibody crosslinking.

The regulation of CD24 surface expression is analogous to that of the glucose transporter type 4 (GLUT4) receptors. During signalling in response to insulin, GLUT4 signals into the cell and is endocytosed from the cell surface. This initial signalling causes

the release of stored GLUT4 from pre-formed vesicles. In sustained signalling, the GLUT4 receptors are endocytosed and recycled to the surface to maintain signalling (124).

The effect of CytoD on CD24 endocytosis has also raised new questions of the role that the actin cytoskeleton plays in regulating CD24 surface expression. CytoD disrupts actin dynamics by capping actin filaments, by preventing the addition of G-actin monomers, and by promoting the dissociation of filamentous actin (125). In clathrin-dependent endocytosis, this serves to halt vesicle internalization (126). Indeed, the use of cytochalasin H was shown to block the endocytosis of CD59 in T cells. The original hypothesis was that CytoD would prevent CD24 internalization due to the loss of dynamic actin reorganization. Given the disparity between CD24 and CD59 endocytosis, it is likely that there are unknown roles for the actin cytoskeleton in mediating endocytic events from lipid rafts. Interestingly, when polarized endothelial cells are treated with CytoD, both clathrin-dependent and -independent endocytosis is inhibited from the apical membrane, but endocytosis from the basolateral membrane surface is enhanced (127, 128). Given the appearance of a polar distribution of CD24 following stimulation, it is possible that the antibody-treated B cells become polarized and thus the rate of CD24 endocytosis is increased from this face in response to CytoD. In order to fully validate the observed increase in CD24 endocytosis in the presence of a disorganized actin cytoskeleton, the cells would need to treateded with other inhibitors of actin dynamics, such as latrunculin A, which binds to monomeric actin (129), preventing it from forming filaments. If polymerized actin is required in mediating endocytosis, latrunculin A will inhibit internalization. Latrunculin A has been used to examine the relationship between

BCR signalling and the underlying actin network of B cells (59). After treatment with Latrunculin A, the B cell actin cytoskeleton was substantially disrupted and MAPK phosphorylation was induced, suggesting that cytoskeletal reorganization is a component of downstream signalling events following antigen recognition (59).

In addition to the change in overall surface expression, the distribution of CD24 on the cell surface was also altered in response to antibody stimulation. Furthermore, there was a difference in the distribution of CD24 if B cells were non-interacting single cells or in clusters suggesting that the downstream effect of CD24 activation is dependent on the existence of cell-cell interactions. Within 5 minutes of stimulation, CD24 distribution changes from punctate to highly organized and polarized. These polarized faces appear to serve as areas for cell to cell contact and indeed, within 40 minutes in interacting cells, CD24 expression appears to be intensified and is uniform around the cell membrane. Interestingly, over the same time course, CD24 expression is reduced or even completely lost in non-interacting cells.

The confocal data further support the FACS analysis that demonstrated the endocytosis of CD24, but further suggested that single cells respond differently than cell clusters. As FACS analysis can only provide information on single cells and not clusters, we can thus be certain that CD24 is endocytosed rapidly from single cells, but that it may play other, as yet unknown, roles in cell clusters. Furthermore it is unknown if CD24 expression is promoted or enhanced through clustering, or if clustering stabilizes CD24 proteins at the cell surface, changes the rate of loss, or alters the balance between endocytosis and replacement at the cell surface. We may thus hypothesize that CD24 may

be important in establishing interactions between B cells and is lost in the event these cell to cell interactions are not established or maintained.

Given its known role as a cell adhesion molecule (28), it may appear that following stimulation, CD24 is redirected to the cell surface to mediate the formation of these clusters; however the evidence that CD24 is endocytosed following crosslinking makes this unlikely. It is more likely that CD24-mediated signals cause changes in other cell adhesion molecules, which cause stable aggregates to form. CD24 has previously been shown to cause changes in pre-B cell adhesion through altering the VLA-4 adhesion molecule (42). In CD24+ cells, VLA-4 shows blockable binding to endothelioma cells with anti-VCAM-1 antibodies and it can bind to fibronectin. In $CD24^{-/-}$ cells, VLA-4 is unable to bind fibronectin and the binding to the same endothelioma cells cannot be blocked (42). This conclusively shows that CD24 mediates cell adhesion events without necessarily participating as the adhesion molecule itself. CD24 has also been shown to regulate Integrin β1 incorporation into lipid rafts and to promote tumour invasiveness in breast cancer cells (10). In both these examples, CD24 signalling is associated with changes in cell-cell adhesion, but through altering other adhesion molecules. The observation that CytoD results in a more rapid and pronounced loss of surface CD24 compared with control treatments but that the cells do not lose their ability to cluster supports the hypothesis that the cell-cell adhesion is mediated by other receptors. If CD24 was required for mediating this adhesion, CytoD would be disruptive. Instead, CytoD appears to alter CD24 expression and localization at later times without altering the cells' ability to form clusters. These results also raise new questions for the role of CD24 in B cell development since it is unknown if these cell aggregates are related to the induction

of apoptosis, or if they are a secondary event. Therefore, future studies should determine if homotypic B cell adhesion is necessary for the induction of apoptosis. To do this, cells would be treated with antibodies against the cell adhesion molecule VLA-4. These antibodies would interfere with the ability of B cells to form clusters and thus could separate the induction of apoptosis from the formation of cell clusters to determine if these events are linked.

While much of the mechanism remains unclear, the discovery that CD24 is endocytosed following receptor stimulation can now serve as a starting point for determining the precise signal transduction machinery responsible for inducing apoptosis and mediating B cell adhesion.

4.6 Conclusions and Future Directions

The objectives of this thesis were to determine how cell surface CD24 expression may be regulated, and to identify a mechanism through which CD24 mediates apoptosis. To address these questions, a bioinformatics approach was used to identify potential protein partners in mediating CD24 activity through a 'guilt-by-association' approach. An ex vivo model was then developed to study CD24 biology in bone marrow derived B cells. Using this model, it was demonstrated that extensive clustering of CD24 is required to mediate apoptosis in B cells. Furthermore, it was shown that surface CD24 protein expression is dynamic and self-regulatory in response to antibody stimulation.

In addition, the localization of CD24 was found to change in a highly coordinated fashion in response to antibody crosslinking. Prior to stimulation, CD24 resided in small, discrete foci distributed around the cell. After stimulation, CD24 surface expression

rapidly increased and became polarized. Interestingly, CD24 appears to have a context-dependent expression pattern where single cells lose surface expression rapidly after polarization whereas interacting cells retain expression for a prolonged time. Finally, endocytosis of CD24 appears to be delayed by the presence of a dynamic actin cytoskeleton.

Taken together, these data along with published work suggest that clustering of CD24 results in a complex sequence of events culminating in apoptosis that can be delineated as follows:

1. Extensive crosslinking via primary and secondary antibodies induces the protein of CD24 from small foci to larger membrane microdomains. These microdomains are increasingly pronounced at areas of cell-cell contact.
2. CD24 crosslinking stimulates a rapid increase in the amount of protein on the cell surface, which is then followed by the endocytosis of the CD24 receptor.
3. CD24 stimulates the formation of cell clusters. These cell clusters promote the retention of CD24 on the cell surface by decreasing the rate of endocytosis or recycling the CD24 protein back to the cell surface. Previously published data lend strong support to the suggestion that clustering occurs through other CAMs, such as VLA-4 or Integrin β1.
4. Downstream signalling from CD24 induces apoptosis through alterations in mitochondrial function and the action of caspases.

Not only does this schema of CD24 activity correspond with our results, it is also applicable to the behaviour reported in the previously discussed studies. Furthermore,

several new avenues of research have been identified in response to this investigation. First, the rapid increase in CD24 surface expression in response to stimulation has not previously been shown. It is unknown if this increase is due to changes in CD24 transcription and translation, or if it results from the mobilization of stored intracellular protein. Furthermore, if clustering of CD24 recruits sequestered vesicles, there is a strong possibility that other surface receptors or signalling molecules are co-recruited to the cell surface. Second, the mechanism through which CD24 mediates B cell adhesion is unknown. It is possible that CD24 itself is responsible for the formation of cell clusters; however, previous research (42) has shown that CD24 can induce changes in other cell adhesion molecules. It is unknown if endocytosis or cell-cell adhesion are linked to the mediation of apoptosis or if these outcomes are separate. Together, these data have identified likely mechanisms used to induce signalling by CD24 and have offered new insight and a new research pathway to explore the role that CD24 plays in B cell development.

CHAPTER 5: REFERENCES

1. LeBien, T. W., and T. F. Tedder. 2008. B lymphocytes: how they develop and function. Blood 112: 1570-1580.
2. Hardy, R. R., C. E. Carmack, S. A. Shinton, J. D. Kemp, and K. Hayakawa. 1991. Resolution and characterization of pro-B and pre-pro-B cell stages in normal mouse bone marrow. J. Exp. Med. 173: 1213-1225.
3. Hardy, R. R., and K. Hayakawa. 2001. B cell development pathways. Annu. Rev. Immunol. 19: 595-621.
4. Dal Porto, J. M., S. B. Gauld, K. T. Merrell, D. Mills, A. E. Pugh-Bernard, and J. Cambier. 2004. B cell antigen receptor signaling 101. Mol. Immunol. 41: 599-613.
5. Tonegawa, S. 1983. Somatic generation of antibody diversity. Nature 302: 575-581.
6. Meffre, E., R. Casellas, and M. C. Nussenzweig. 2000. Antibody regulation of B cell development. Nat. Immunol. 1: 379-385.
7. Lu, L., and D. G. Osmond. 1997. Apoptosis during B lymphopoiesis in mouse bone marrow. J. Immunol. 158: 5136-5145.
8. Tsubata, T., J. Wu, and T. Honjo. 1993. B-cell apoptosis induced by antigen receptor crosslinking is blocked by a T-cell signal through CD40. Nature 364: 645-648.
9. Hough, M. R., M. S. Chappel, G. Sauvageau, F. Takei, R. Kay, and R. K. Humphries. 1996. Reduction of early B lymphocyte precursors in transgenic mice overexpressing the murine heat-stable antigen. J. Immunol. 156: 479-488.
10. Runz, S., C. T. Mierke, S. Joumaa, J. Behrens, B. Fabry, and P. Altevogt. 2008. CD24 induces localization of beta1 integrin to lipid raft domains. Biochem. Biophys. Res. Commun. 365: 35-41.
11. Bonner, W. A., H. R. Hulett, R. G. Sweet, and L. A. Herzenberg. 1972. Fluorescence activated cell sorting. Rev Sci Instrum 43: 404-409.
12. Hardy, R. R., K. Hayakawa, D. R. Parks, L. A. Herzenberg, and L. A. Herzenberg. 1984. Murine B cell differentiation lineages. J. Exp. Med. 159: 1169-1188.
13. Hermiston, M. L., Z. Xu, and A. Weiss. 2003. CD45: a critical regulator of signaling thresholds in immune cells. Annu. Rev. Immunol. 21: 107-137.
14. Nikolic, T., G. M. Dingjan, P. J. Leenen, and R. W. Hendriks. 2002. A subfraction of B220(+) cells in murine bone marrow and spleen does not belong to the B cell lineage but has dendritic cell characteristics. Eur. J. Immunol. 32: 686-692.
15. Tung, J. W., D. R. Parks, W. A. Moore, L. A. Herzenberg, and L. A. Herzenberg. 2004. Identification of B-cell subsets: an exposition of 11-color (Hi-D) FACS methods. Methods Mol Biol 271: 37-58.
16. Rumfelt, L. L., Y. Zhou, B. M. Rowley, S. A. Shinton, and R. R. Hardy. 2006. Lineage specification and plasticity in CD19- early B cell precursors. J. Exp. Med. 203: 675-687.
17. Duperray, C., J. M. Boiron, C. Boucheix, J. F. Cantaloube, T. Lavabre-Bertrand, M. Attal, J. Brochier, D. Maraninchi, R. Bataille, and B. Klein. 1990. The CD24

antigen discriminates between pre-B and B cells in human bone marrow. J. Immunol. 145: 3678-3683.
18. Chung, J. B., M. Silverman, and J. G. Monroe. 2003. Transitional B cells: step by step towards immune competence. Trends Immunol. 24: 343-349.
19. Chappel, M. S., M. R. Hough, A. Mittel, F. Takei, R. Kay, and R. K. Humphries. 1996. Cross-Linking the Murine Heat-Stable Antigen Induces Apoptosis in B Cell Precursors and Suppresses the Anti-CD40-Induced Proliferation of Mature Resting B Lymphocytes. J. Exp. Med. 184: 1639-1649.
20. Fang, X., P. Zheng, J. Tang, and Y. Liu. 2010. CD24: From A to Z. Cell Mol Immunol 7: 100-103.
21. Springer, T., G. Galfre, D. S. Secher, and C. Milstein. 1978. Monoclonal xenogeneic antibodies to murine cell surface antigens: identification of novel leukocyte differentiation antigens. Eur. J. Immunol. 8: 539-551.
22. Kristiansen, G., M. Sammar, and P. Altevogt. 2004. Tumour biological aspects of CD24, a mucin-like adhesion molecule. J Mol Histol 35: 255-262.
23. Kristiansen, G., E. Machado, N. Bretz, C. Rupp, K. J. Winzer, A. K. Konig, G. Moldenhauer, F. Marme, J. Costa, and P. Altevogt. 2010. Molecular and clinical dissection of CD24 antibody specificity by a comprehensive comparative analysis. Lab. Invest. 90: 1102-1116.
24. Kay, R., P. M. Rosten, and R. K. Humphries. 1991. CD24, a signal transducer modulating B cell activation responses, is a very short peptide with a glycosyl phosphatidylinositol membrane anchor. J. Immunol. 147: 1412-1416.
25. Aigner, S., Z. M. Sthoeger, M. Fogel, E. Weber, J. Zarn, M. Ruppert, Y. Zeller, D. Vestweber, R. Stahel, M. Sammar, and P. Altevogt. 1997. CD24, a mucin-type glycoprotein, is a ligand for P-selectin on human tumor cells. Blood 89: 3385-3395.
26. Sammar, M., S. Aigner, M. Hubbe, V. Schirrmacher, M. Schachner, D. Vestweber, and P. Altevogt. 1994. Heat-stable antigen (CD24) as ligand for mouse P-selectin. Int. Immunol. 6: 1027-1036.
27. Liu, Y., G. Y. Chen, and P. Zheng. 2009. CD24-Siglec G/10 discriminates danger-from pathogen-associated molecular patterns. Trends Immunol. 30: 557-561.
28. Kadmon, G., M. Eckert, M. Sammar, M. Schachner, and P. Altevogt. 1992. Nectadrin, the heat-stable antigen, is a cell adhesion molecule. J. Cell Biol. 118: 1245-1258.
29. Jevsek, M., A. Jaworski, L. Polo-Parada, N. Kim, J. Fan, L. T. Landmesser, and S. J. Burden. 2006. CD24 is expressed by myofiber synaptic nuclei and regulates synaptic transmission. Proc Natl Acad Sci U S A 103: 6374-6379.
30. Jackson, D., R. Waibel, E. Weber, J. Bell, and R. A. Stahel. 1992. CD24, a signal-transducing molecule expressed on human B cells, is a major surface antigen on small cell lung carcinomas. Cancer Res. 52: 5264-5270.
31. Huang, L. R., and H. C. Hsu. 1995. Cloning and expression of CD24 gene in human hepatocellular carcinoma: a potential early tumor marker gene correlates with p53 mutation and tumor differentiation. Cancer Res. 55: 4717-4721.

32. Kristiansen, G., C. Denkert, K. Schluns, E. Dahl, C. Pilarsky, and S. Hauptmann. 2002. CD24 is expressed in ovarian cancer and is a new independent prognostic marker of patient survival. Am J Pathol 161: 1215-1221.
33. Kristiansen, G., K. Schluns, Y. Yongwei, C. Denkert, M. Dietel, and I. Petersen. 2003. CD24 is an independent prognostic marker of survival in nonsmall cell lung cancer patients. Br. J. Cancer 88: 231-236.
34. Su, N., L. Peng, B. Xia, Y. Zhao, A. Xu, J. Wang, X. Wang, and B. Jiang. 2012. Lyn is involved in CD24-induced ERK1/2 activation in colorectal cancer. Mol Cancer 11: 43.
35. Lee, K. M., J. H. Ju, K. Jang, W. Yang, J. Y. Yi, D. Y. Noh, and I. Shin. 2012. CD24 regulates cell proliferation and transforming growth factor beta-induced epithelial to mesenchymal transition through modulation of integrin beta1 stability. Cell. Signal. 24: 2132-2142.
36. Zheng, J., Y. Li, J. Yang, Q. Liu, M. Shi, R. Zhang, H. Shi, Q. Ren, J. Ma, H. Guo, Y. Tao, Y. Xue, N. Jiang, L. Yao, and W. Liu. 2011. NDRG2 inhibits hepatocellular carcinoma adhesion, migration and invasion by regulating CD24 expression. BMC Cancer 11: 251:251-259.
37. Lu, L., P. Chaudhury, and D. G. Osmond. 1999. Regulation of cell survival during B lymphopoiesis: apoptosis and Bcl-2/Bax content of precursor B cells in bone marrow of mice with altered expression of IL-7 and recombinase-activating gene-2. J. Immunol. 162: 1931-1940.
38. Pelayo, R., R. S. Welner, Y. Nagai, and P. W. Kincade. 2006. Life before the pre-B cell receptor checkpoint: specification and commitment of primitive lymphoid progenitors in adult bone marrow. Semin. Immunol. 18: 2-11.
39. Defrance, T., M. Casamayor-Palleja, and P. H. Krammer. 2002. The life and death of a B cell. Adv. Cancer Res. 86: 195-225.
40. Lu, L., and D. G. Osmond. 2000. Apoptosis and its modulation during B lymphopoiesis in mouse bone marrow. Immunol. Rev. 175: 158-174.
41. Fischer, G. F., O. Majdic, S. Gadd, and W. Knapp. 1990. Signal transduction in lymphocytic and myeloid cells via CD24, a new member of phosphoinositol-anchored membrane molecules. J. Immunol. 144: 638-641.
42. Hahne, M., R. H. Wenger, D. Vestweber, and P. J. Nielsen. 1994. The heat-stable antigen can alter very late antigen 4-mediated adhesion. J. Exp. Med. 179: 1391-1395.
43. Kadmon, G., F. von Bohlen und Halbach, R. Horstkorte, M. Eckert, P. Altevogt, and M. Schachner. 1995. Evidence for cis interaction and cooperative signalling by the heat-stable antigen nectadrin (murine CD24) and the cell adhesion molecule L1 in neurons. Eur. J. Neurosci. 7: 993-1004.
44. Kleene, R., H. Yang, M. Kutsche, and M. Schachner. 2001. The neural recognition molecule L1 is a sialic acid-binding lectin for CD24, which induces promotion and inhibition of neurite outgrowth. J. Biol. Chem. 276: 21656-21663.
45. Sammar, M., E. Gulbins, K. Hilbert, F. Lang, and P. Altevogt. 1997. Mouse CD24 as a signaling molecule for integrin-mediated cell binding: functional and physical association with src-kinases. Biochem. Biophys. Res. Commun. 234: 330-334.

46. Suzuki, T., N. Kiyokawa, T. Taguchi, T. Sekino, Y. U. Katagiri, and J. Fujimoto. 2001. CD24 Induces Apoptosis in Human B Cells Via The Glycolipid-Enriched Membrane Domains/Rafts-Mediated Signaling System. J. Immunol. 166: 5567-5577.
47. Wang, W., X. Wang, L. Peng, Q. Deng, Y. Liang, H. Qing, and B. Jiang. 2010. CD24-dependent MAPK pathway activation is required for colorectal cancer cell proliferation. Cancer Sci. 101: 112-119.
48. Holl, T. M., B. F. Haynes, and G. Kelsoe. 2010. Stromal cell independent B cell development in vitro: generation and recovery of autoreactive clones. J. Immunol. Methods 354: 53-67.
49. Jarvis, L. J., J. E. Maguire, and T. W. LeBien. 1997. Contact between human bone marrow stromal cells and B lymphocytes enhances very late antigen-4/vascular cell adhesion molecule-1-independent tyrosine phosphorylation of focal adhesion kinase, paxillin, and ERK2 in stromal cells. Blood 90: 1626-1635.
50. Fleming, H. E., and C. J. Paige. 2001. Pre-B cell receptor signaling mediates selective response to IL-7 at the pro-B to pre-B cell transition via an ERK/MAP kinase-dependent pathway. Immunity 15: 521-531.
51. Li, Y. S., R. Wasserman, K. Hayakawa, and R. R. Hardy. 1996. Identification of the earliest B lineage stage in mouse bone marrow. Immunity 5: 527-535.
52. Sudo, T., M. Ito, Y. Ogawa, M. Iizuka, H. Kodama, T. Kunisada, S. Hayashi, M. Ogawa, K. Sakai, and S. Nishikawa. 1989. Interleukin 7 production and function in stromal cell-dependent B cell development. J. Exp. Med. 170: 333-338.
53. Hartley, S. B., M. P. Cooke, D. A. Fulcher, A. W. Harris, S. Cory, A. Basten, and C. C. Goodnow. 1993. Elimination of self-reactive B lymphocytes proceeds in two stages: arrested development and cell death. Cell 72: 325-335.
54. Park, S. Y., P. Wolfram, K. Canty, B. Harley, C. Nombela-Arrieta, G. Pivarnik, J. Manis, H. E. Beggs, and L. E. Silberstein. 2013. Focal adhesion kinase regulates the localization and retention of pro-B cells in bone marrow microenvironments. J. Immunol. 190: 1094-1102.
55. Wenger, R. H., M. Kopf, L. Nitschke, M. C. Lamers, G. Köhler, and P. J. Nielsen. 1995. B-cell Maturation in Chimaeric Mice Deficient for the Heat Stable Antigen (HSA/mouse CD24). Transgenic Res. 4: 173-183.
56. Nielsen, P. J., B. Lorenz, A. M. Muller, R. H. Wenger, F. Brombacher, M. Simon, T. von der Weid, W. J. Langhorne, H. Mossmann, and G. Kohler. 1997. Altered erythrocytes and a leaky block in B-cell development in CD24/HSA-deficient mice. Blood 89: 1058-1067.
57. Lu, L., M. S. Chappel, R. K. Humphries, and D. G. Osmond. 2000. Regulation of cell survival during B lymphopoiesis: increased pre-B cell apoptosis in CD24-transgenic mouse bone marrow. Eur. J. Immunol. 30: 2686-2691.
58. Taguchi, T., N. Kiyokawa, H. Mimori, T. Suzuki, T. Sekino, H. Nakajima, M. Saito, Y. U. Katagiri, N. Matsuo, Y. Matsuo, H. Karasuyama, and J. Fujimoto. 2003. Pre-B Cell Antigen Receptor-Mediated Signal Inhibits CD24-Induced Apoptosis in Human Pre-B Cells. J. Immunol. 170: 252-260.
59. Freeman, S. A., V. Lei, M. Dang-Lawson, K. Mizuno, C. D. Roskelley, and M. R. Gold. 2011. Cofilin-mediated F-actin severing is regulated by the Rap GTPase

and controls the cytoskeletal dynamics that drive lymphocyte spreading and BCR microcluster formation. J. Immunol. 187: 5887-5900.
60. Simons, K., and D. Toomre. 2000. Lipid rafts and signal transduction. Nat. Rev. Mol. Cell Biol. 1: 31-39.
61. Zarn, J. A., S. M. Zimmermann, M. K. Pass, R. Waibel, and R. A. Stahel. 1996. Association of CD24 with the kinase c-fgr in a small cell lung cancer cell line and with the kinase lyn in an erythroleukemia cell line. Biochem. Biophys. Res. Commun. 225: 384-391.
62. Boyd, A. W., J. W. Goding, and J. W. Schrader. 1981. The regulation of growth and differentiation of a murine B cell lymphoma. I. Lipopolysaccharide-induced differentiation. J. Immunol. 126: 2461-2465.
63. Heng, T. S., and M. W. Painter. 2008. The Immunological Genome Project: networks of gene expression in immune cells. Nat. Immunol. 9: 1091-1094.
64. Team, R. D. C. 2008. R: A language and environment for statistical computing. R Foundation for Statistical Computing, Vienna, Austria.
65. Gentleman, R. C., V. J. Carey, D. M. Bates, B. Bolstad, M. Dettling, S. Dudoit, B. Ellis, L. Gautier, Y. Ge, J. Gentry, K. Hornik, T. Hothorn, W. Huber, S. Iacus, R. Irizarry, F. Leisch, C. Li, M. Maechler, A. J. Rossini, G. Sawitzki, C. Smith, G. Smyth, L. Tierney, J. Y. Yang, and J. Zhang. 2004. Bioconductor: open software development for computational biology and bioinformatics. Genome Biol 5: R80.
66. Faria, J. C. 2012. Resources of Tinn-R GUI/Editor for R Environment. Universidade Estadual de Santa Cruz, Ilheus, Bahia, Brasil.
67. Carvalho, B. S., and R. A. Irizarry. 2010. A framework for oligonucleotide microarray preprocessing. Bioinformatics 26: 2363-2367.
68. Carvalho, B. 2013. pd.mogene.1.1.st.v1: Platform Design Info for Affymetrix MoGene-1_1-st-v1.
69. Irizarry, R. A., B. Hobbs, F. Collin, Y. D. Beazer-Barclay, K. J. Antonellis, U. Scherf, and T. P. Speed. 2003. Exploration, normalization, and summaries of high density oligonucleotide array probe level data. Biostatistics 4: 249-264.
70. Smyth, G. K. 2005. Limma: linear models for microarray data. In Bioinformatics and Computational Biology Solutions using R and Bioconductor. R. G. a. V. C. a. S. D. a. R. I. a. W. Huber, ed. Springer, New York. 397-420.
71. MacDonald, J. W. 2008. affycoretools: Functions useful for those doing repetitive analyses with Affymetrix GeneChips.
72. Alibes, A., P. Yankilevich, A. Canada, and R. Diaz-Uriarte. 2007. IDconverter and IDClight: conversion and annotation of gene and protein IDs. BMC Bioinformatics 8: 9.
73. Sturn, A., J. Quackenbush, and Z. Trajanoski. 2002. Genesis: cluster analysis of microarray data. Bioinformatics 18: 207-208.
74. Mostafavi, S., D. Ray, D. Warde-Farley, C. Grouios, and Q. Morris. 2008. GeneMANIA: a real-time multiple association network integration algorithm for predicting gene function. Genome Biol 9 Suppl 1: S4.
75. Huang da, W., B. T. Sherman, and R. A. Lempicki. 2009. Bioinformatics enrichment tools: paths toward the comprehensive functional analysis of large gene lists. Nucleic Acids Res. 37: 1-13.

76. Huang da, W., B. T. Sherman, and R. A. Lempicki. 2009. Systematic and integrative analysis of large gene lists using DAVID bioinformatics resources. Nat Protoc 4: 44-57.
77. Leguchi, K., S. Ueda, T. Kataoka, and T. Satoh. 2007. Role of the guanine nucleotide exchange factor Ost in negative regulation of receptor endocytosis by the small GTPase Rac1. J. Biol. Chem. 282: 23296-23305.
78. Verstreken, P., O. Kjaerulff, T. E. Lloyd, R. Atkinson, Y. Zhou, I. A. Meinertzhagen, and H. J. Bellen. 2002. Endophilin mutations block clathrin-mediated endocytosis but not neurotransmitter release. Cell 109: 101-112.
79. Guilherme, A., N. A. Soriano, S. Bose, J. Holik, A. Bose, D. P. Pomerleau, P. Furcinitti, J. Leszyk, S. Corvera, and M. P. Czech. 2004. EHD2 and the novel EH domain binding protein EHBP1 couple endocytosis to the actin cytoskeleton. J. Biol. Chem. 279: 10593-10605.
80. Henne, W. M., E. Boucrot, M. Meinecke, E. Evergren, Y. Vallis, R. Mittal, and H. T. McMahon. 2010. FCHo proteins are nucleators of clathrin-mediated endocytosis. Science 328: 1281-1284.
81. Schmidt, M. R., T. Maritzen, V. Kukhtina, V. A. Higman, L. Doglio, N. N. Barak, H. Strauss, H. Oschkinat, C. G. Dotti, and V. Haucke. 2009. Regulation of endosomal membrane traffic by a Gadkin/AP-1/kinesin KIF5 complex. Proc Natl Acad Sci U S A 106: 15344-15349.
82. Somsel Rodman, J., and A. Wandinger-Ness. 2000. Rab GTPases coordinate endocytosis. J. Cell Sci. 113 Pt 2: 183-192.
83. Umasankar, P. K., S. Sanker, J. R. Thieman, S. Chakraborty, B. Wendland, M. Tsang, and L. M. Traub. 2012. Distinct and separable activities of the endocytic clathrin-coat components Fcho1/2 and AP-2 in developmental patterning. Nat. Cell Biol. 14: 488-501.
84. Deckert, M., M. Ticchioni, and A. Bernard. 1996. Endocytosis of GPI-anchored proteins in human lymphocytes: role of glycolipid-based domains, actin cytoskeleton, and protein kinases. J. Cell Biol. 133: 791-799.
85. Tsapogas, P., T. Breslin, S. Bilke, A. Lagergren, R. Mansson, D. Liberg, C. Peterson, and M. Sigvardsson. 2003. RNA analysis of B cell lines arrested at defined stages of differentiation allows for an approximation of gene expression patterns during B cell development. J Leukoc Biol 74: 102-110.
86. Spillmann, F. J., G. Beck-Engeser, and M. Wabl. 2007. Differentiation and Ig-allele switch in cell line WEHI-231. J. Immunol. 179: 6395-6402.
87. Chung, S. W., P. M. Wong, H. Durkin, Y. S. Wu, and J. Petersen. 1991. Leukemia initiated by hemopoietic stem cells expressing the v-abl oncogene. Proc Natl Acad Sci U S A 88: 1585-1589.
88. Muljo, S. A., and M. S. Schlissel. 2003. A small molecule Abl kinase inhibitor induces differentiation of Abelson virus-transformed pre-B cell lines. Nat. Immunol. 4: 31-37.
89. Advani, A. S., and A. M. Pendergast. 2002. Bcr-Abl variants: biological and clinical aspects. Leuk Res 26: 713-720.

90. Chang, Y. C., S. C. Tien, H. F. Tien, H. Zhang, G. M. Bokoch, and Z. F. Chang. 2009. p210(Bcr-Abl) desensitizes Cdc42 GTPase signaling for SDF-1alpha-directed migration in chronic myeloid leukemia cells. Oncogene 28: 4105-4115.
91. Sahay, S., N. L. Pannucci, G. M. Mahon, P. L. Rodriguez, N. J. Megjugorac, E. V. Kostenko, H. L. Ozer, and I. P. Whitehead. 2008. The RhoGEF domain of p210 Bcr-Abl activates RhoA and is required for transformation. Oncogene 27: 2064-2071.
92. Wennerberg, K., K. L. Rossman, and C. J. Der. 2005. The Ras superfamily at a glance. J. Cell Sci. 118: 843-846.
93. Villalonga, P., and A. J. Ridley. 2006. Rho GTPases and cell cycle control. Growth Factors 24: 159-164.
94. Ieguchi, K., S. Ueda, T. Kataoka, and T. Satoh. 2007. Role of the guanine nucleotide exchange factor Ost in negative regulation of receptor endocytosis by the small GTPase Rac1. J. Biol. Chem. 282: 23296-23305.
95. Fransson, A., A. Ruusala, and P. Aspenstrom. 2003. Atypical Rho GTPases have roles in mitochondrial homeostasis and apoptosis. J. Biol. Chem. 278: 6495-6502.
96. Hirsch, D. S., D. M. Pirone, and P. D. Burbelo. 2001. A new family of Cdc42 effector proteins, CEPs, function in fibroblast and epithelial cell shape changes. J. Biol. Chem. 276: 875-883.
97. Tybulewicz, V. L., and R. B. Henderson. 2009. Rho family GTPases and their regulators in lymphocytes. Nat. Rev. Immunol. 9: 630-644.
98. Wolfe, C. J., I. S. Kohane, and A. J. Butte. 2005. Systematic survey reveals general applicability of "guilt-by-association" within gene coexpression networks. BMC Bioinformatics 6: 227.
99. Smith, K. R., E. K. Kieserman, P. I. Wang, S. G. Basten, R. H. Giles, E. M. Marcotte, and J. B. Wallingford. 2011. A role for central spindle proteins in cilia structure and function. Cytoskeleton (Hoboken) 68: 112-124.
100. Martherus, R. S., W. Sluiter, E. D. Timmer, S. J. VanHerle, H. J. Smeets, and T. A. Ayoubi. 2010. Functional annotation of heart enriched mitochondrial genes GBAS and CHCHD10 through guilt by association. Biochem. Biophys. Res. Commun. 402: 203-208.
101. Lounkine, E., M. J. Keiser, S. Whitebread, D. Mikhailov, J. Hamon, J. L. Jenkins, P. Lavan, E. Weber, A. K. Doak, S. Cote, B. K. Shoichet, and L. Urban. 2012. Large-scale prediction and testing of drug activity on side-effect targets. Nature 486: 361-367.
102. Lydyard, P. M., and M. W. Fanger. 1982. Characteristics and function of Fc receptors on human lymphocytes. Immunology 47: 1-17.
103. Suzuki, K. G., T. K. Fujiwara, F. Sanematsu, R. Iino, M. Edidin, and A. Kusumi. 2007. GPI-anchored receptor clusters transiently recruit Lyn and G alpha for temporary cluster immobilization and Lyn activation: single-molecule tracking study 1. J. Cell Biol. 177: 717-730.
104. Stahl, A., and B. M. Mueller. 1995. The urokinase-type plasminogen activator receptor, a GPI-linked protein, is localized in caveolae. J. Cell Biol. 129: 335-344.

105. Schabath, H., S. Runz, S. Joumaa, and P. Altevogt. 2006. CD24 affects CXCR4 function in pre-B lymphocytes and breast carcinoma cells. J. Cell Sci. 119: 314-325.
106. McLeod, S. J., A. H. Li, R. L. Lee, A. E. Burgess, and M. R. Gold. 2002. The Rap GTPases regulate B cell migration toward the chemokine stromal cell-derived factor-1 (CXCL12): potential role for Rap2 in promoting B cell migration. J. Immunol. 169: 1365-1371.
107. Stoddart, A., H. E. Fleming, and C. J. Paige. 2000. The role of the preBCR, the interleukin-7 receptor, and homotypic interactions during B-cell development. Immunol. Rev. 175: 47-58.
108. Stoddart, A., H. E. Fleming, and C. J. Paige. 2001. The role of homotypic interactions in the differentiation of B cell precursors. Eur. J. Immunol. 31: 1160-1172.
109. Sarkar, S., C. Kantara, and P. Singh. 2012. Clathrin mediates endocytosis of progastrin and activates MAPKs: role of cell surface annexin A2. Am J Physiol Gastrointest Liver Physiol 302: G712-722.
110. Pozzi, B., S. Amodio, C. Lucano, A. Sciullo, S. Ronzoni, D. Castelletti, T. Adler, I. Treise, I. H. Betsholtz, B. Rathkolb, D. H. Busch, E. Wolf, H. Fuchs, V. Gailus-Durner, M. H. de Angelis, C. Betsholtz, S. Casola, P. P. Di Fiore, and N. Offenhauser. 2012. The endocytic adaptor Eps15 controls marginal zone B cell numbers. PLoS One 7: e50818.
111. McPherson, P. S., B. K. Kay, and N. K. Hussain. 2001. Signaling on the Endocytic Pathway. Traffic 2: 375-384.
112. Mukherjee, S., R. N. Ghosh, and F. R. Maxfield. 1997. Endocytosis. Physiol. Rev. 77: 759-803.
113. Nabi, I. R., and P. U. Le. 2003. Caveolae/raft-dependent endocytosis. J. Cell Biol. 161: 673-677.
114. Benmerah, A., and C. Lamaze. 2007. Clathrin-coated pits: vive la difference? Traffic 8: 970-982.
115. Pearse, B. M. 1976. Clathrin: a unique protein associated with intracellular transfer of membrane by coated vesicles. Proc Natl Acad Sci U S A 73: 1255-1259.
116. Wiley, H. S., and P. M. Burke. 2001. Regulation of receptor tyrosine kinase signaling by endocytic trafficking. Traffic 2: 12-18.
117. Fra, A. M., E. Williamson, K. Simons, and R. G. Parton. 1994. Detergent-insoluble glycolipid microdomains in lymphocytes in the absence of caveolae. J. Biol. Chem. 269: 30745-30748.
118. van Deurs, B., K. Roepstorff, A. M. Hommelgaard, and K. Sandvig. 2003. Caveolae: anchored, multifunctional platforms in the lipid ocean. Trends Cell Biol. 13: 92-100.
119. Lakhan, S. E., S. Sabharanjak, and A. De. 2009. Endocytosis of glycosylphosphatidylinositol-anchored proteins. J. Biomed. Sci. 16: 93.
120. Damke, H., T. Baba, D. E. Warnock, and S. L. Schmid. 1994. Induction of mutant dynamin specifically blocks endocytic coated vesicle formation. J. Cell Biol. 127: 915-934.

121. Davies, A., D. L. Simmons, G. Hale, R. A. Harrison, H. Tighe, P. J. Lachmann, and H. Waldmann. 1989. CD59, an LY-6-like protein expressed in human lymphoid cells, regulates the action of the complement membrane attack complex on homologous cells. J. Exp. Med. 170: 637-654.
122. Moren, B., C. Shah, M. T. Howes, N. L. Schieber, H. T. McMahon, R. G. Parton, O. Daumke, and R. Lundmark. 2012. EHD2 regulates caveolar dynamics via ATP-driven targeting and oligomerization. Mol Biol Cell 23: 1316-1329.
123. Ivanov, A. I. 2008. Pharmacological inhibition of endocytic pathways: is it specific enough to be useful? Methods Mol Biol 440: 15-33.
124. Stockli, J., D. J. Fazakerley, and D. E. James. 2011. GLUT4 exocytosis. J. Cell Sci. 124: 4147-4159.
125. Casella, J. F., M. D. Flanagan, and S. Lin. 1981. Cytochalasin D inhibits actin polymerization and induces depolymerization of actin filaments formed during platelet shape change. Nature 293: 302-305.
126. Lamaze, C., L. M. Fujimoto, H. L. Yin, and S. L. Schmid. 1997. The actin cytoskeleton is required for receptor-mediated endocytosis in mammalian cells. J. Biol. Chem. 272: 20332-20335.
127. Gottlieb, T. A., I. E. Ivanov, M. Adesnik, and D. D. Sabatini. 1993. Actin microfilaments play a critical role in endocytosis at the apical but not the basolateral surface of polarized epithelial cells. J. Cell Biol. 120: 695-710.
128. Shurety, W., N. A. Bright, and J. P. Luzio. 1996. The effects of cytochalasin D and phorbol myristate acetate on the apical endocytosis of ricin in polarised Caco-2 cells. J. Cell Sci. 109 (Pt 12): 2927-2935.
129. Yarmola, E. G., T. Somasundaram, T. A. Boring, I. Spector, and M. R. Bubb. 2000. Actin-latrunculin A structure and function. Differential modulation of actin-binding protein function by latrunculin A. J. Biol. Chem. 275: 28120-28127.

CHAPTER 6: APPENDICES

APPENDIX A: Annotated R Scripts

```
# this is the process for creating a gene list to bring to Genesis
# the genes_all.txt file is the full list of expressed genes
# ttaallgenes is the full list of differentially expressed genes at set P.value (if coeff is undefined and n=10,000 to encompass all potential DE genes)

setwd("C:/TinnR/acf_fractions") # set working directory for R session
getwd() # confirm appropriate setting of w.d.
source("http://bioconductor.org/biocLite.R")  #  to access Bioconductor packages if necessary
biocLite("oligo")   # Oligo package is required during background correcting and normalization
biocLite("pd.mogene.1.1.st.v1")  # The pd.mogene.1.1.st.v1 gene id file is the affymetrix platform design information for the MoGene 1.0ST gene array.
```

NORMALIZING AND BACKGROUND CORRECTING

```
library(Biobase)  # load libraries
library(oligo) # load oligo
library(pd.mogene.1.0.st.v1) # load platform design file
celfiles=list.celfiles() # load CEL files
celfiles # call back to confirm CEL files loaded
data=read.celfiles(celfiles) # define data as the readout from the CEL files
data # call back to confirm data is defined properly
hist(data) # histogram plot of gene expression from CEL files (sequentially)
boxplot(data) # boxplot of gene expression (sequentially)
MAplot(data) # MAPlot of gene expression (sequentially)
genes=rma(data, target="core") # define genes as the collected number of unique genes in the microarray by first collapsing any spots which match the same gene into a single function and then normalizing the array based on the RMA algorithm
genes # confirm normalization and definition of genes
hist(genes) # confirm normalization of arrays by histogram
boxplot(genes) # boxplot of normalized gene expression
MAplot(genes) # MA plot of normalized gene expression
write.exprs(genes, file="genes_acf.txt") #for writing all genes in the microarray ExpressionSet data as a txt file.
```

IDENTIFYING DIFFERENTIALLY EXPRESSED GENES

```
library(limma) # load the limma package
library(affycoretools) # load the affycoretools package
design=model.matrix(~0+factor(c(1,1,1,1,2,2,2,3,3,3))) # define the matrix of microarray data sets so that fraction A correspons to 1, fraction C' corresponds to 2 and fraction F corresponds to 3.
colnames(design)=c("FrA", "FrC", "FrF") # give column names to the matrix
design # confirm the matrix design
fit=lmFit(genes, design) # Perform a non-linear least squares fit on the genes according to the matrix
contrast.matrix=makeContrasts(FrC-FrA, FrC-FrF, levels=design) # define the comparisons between fractions A, C' and F
contrast.matrix # confirm the contrast designs
fit2=contrasts.fit(fit, contrast.matrix) # perform the contrasts
fit3=eBayes(fit2) # statistical test on gene changes
results=decideTests(fit3, p.value=0.005)  # only give a positive indication that genes are differentially expressed if they have an adjusted p. value of 0.005 or lower
write.fit(fit3, results, "Maturation") # write the result into a file
ttalldegenes=topTable(fit3, n=10000, adjust="fdr", p.value=0.005) # create a ranked top table of significant gene expression changes with a false discovery rate of 0.005 or lower
# optional addition to top table; Coef 1/2= which comparison, ie: C-A=1 or C-F=2
write.csv(ttalldegenes, file="genes_tt.csv")  # the Top Table is all differentially expressed genes, form All comparisons: ie: all Venn diagram segments between C-A and C-F

########
```

The above procedure was performed two times.
The first analysis was to identify differentially expressed genes from Hardy fractions A, C' and F. The results were collected from the top table.

The second use of R script was to create a normalized gene expression data set for Myeloid Progenitor Stem Cell (MLP), Hardy Fractions A through F, Splenic T1 cells and the Plasma Cell. This script only required use of the normalizing and background correcting scripts with the appropriate CEL files.

APPENDIX B: Gene Ontology Enrichment of CD24 Co-Clustered and GeneMANIA suggested genes by DAVID.

Cell Death Signalling	Enrichment Score: 1.953					
Term	P-Value	Genes	Fold Enrichment	Bonferroni	Benjamini	FDR
Short sequence motif:BH3	5.24E-06	BAK1, BIK, BCL2L1, BCL2L11	112.429	0.001	0.001	0.006
Apoptosis regulator Bcl-2, BH	1.27E-05	BAK1, BIK, BCL2L1, BCL2L11	84.136	0.001	0.001	0.014
SM00337:BCL	2.42E-05	BAK1, BIK, BCL2L1, BCL2L11	66.029	0.001	0.001	0.021
Role of Mitochondria in Apoptotic Signalling	3.06E-05	BAK1, CASP7, BIK, BCL2L1	43.545	0.000	0.000	0.021
GO:0008637~apoptotic mitochondrial changes	3.43E-05	BAK1, CASP7, BCL2L1, CD24	60.191	0.020	0.020	0.050
GO:0008219~cell death	5.16E-04	BAK1, TARDBP, CASP7, BIK, BCL2L1, CD24, MCF2L, BCL2L11	5.190	0.257	0.138	0.756
GO:0016265~death	5.38E-04	BAK1, TARDBP, CASP7, BIK, BCL2L1, CD24, MCF2L, BCL2L11	5.155	0.267	0.098	0.788
GO:0005741~mitochondrial outer membrane	6.94E-04	BAK1, BCL2L1, GPAM, BCL2L11	21.850	0.062	0.062	0.756
GO:0005739~mitochondrion	7.75E-04	BAK1, HSPA2, CASP7, BIK, BCL2L1, COQ7, GPAM, MCF2L, BCL2L11	4.070	0.069	0.035	0.844
GO:0001836~release of cytochrome c from mitochondria	8.47E-04	BAK1, CASP7, BCL2L1	66.640	0.386	0.115	1.236
GO:0031967~organelle envelope	1.02E-03	BAK1, CASP7, BIK, BCL2L1, GPAM, MYOF, BCL2L11	5.550	0.090	0.031	1.109

GO:0031975~envelope	1.04E-03	BAK1, CASP7, BIK, BCL2L1, GPAM, MYOF, BCL2L11	5.533	0.091	0.024	1.127
GO:0031968~organelle outer membrane	1.06E-03	BAK1, BCL2L1, GPAM, BCL2L11	18.908	0.093	0.019	1.148
GO:0005740~mitochondrial envelope	1.14E-03	BAK1, CASP7, BIK, BCL2L1, GPAM, BCL2L11	7.040	0.100	0.017	1.240
GO:0019867~outer membrane	1.18E-03	BAK1, BCL2L1, GPAM, BCL2L11	18.208	0.103	0.015	1.280
GO:0006915~apoptosis	1.23E-03	BAK1, CASP7, BIK, BCL2L1, CD24, MCF2L, BCL2L11	5.424	0.509	0.133	1.796
GO:0012501~programmed cell death	1.33E-03	BAK1, CASP7, BIK, BCL2L1, CD24, MCF2L, BCL2L11	5.344	0.536	0.120	1.938
GO:0043065~positive regulation of apoptosis	1.70E-03	BAK1, BIK, BCL2L1, CD24, MCF2L, BCL2L11	6.509	0.625	0.131	2.470
GO:0043068~positive regulation of programmed cell death	1.75E-03	BAK1, BIK, BCL2L1, CD24, MCF2L, BCL2L11	6.464	0.636	0.119	2.546
GO:0010942~positive regulation of cell death	1.79E-03	BAK1, BIK, BCL2L1, CD24, MCF2L, BCL2L11	6.434	0.644	0.108	2.598
GO:0003006~reproductive developmental process	1.95E-03	BAK1, HSPA2, BIK, BCL2L1, BCL2L11	8.902	0.676	0.106	2.829
GO:0048608~reproductive structure development	2.18E-03	BAK1, BIK, BCL2L1, BCL2L11	14.809	0.716	0.108	3.155
GO:0007005~mitochondrion organization	2.82E-03	BAK1, CASP7, BCL2L1, CD24	13.521	0.804	0.127	4.067
GO:0006917~induction of apoptosis	4.02E-03	BAK1, BIK, CD24, MCF2L, BCL2L11	7.289	0.902	0.163	5.741
GO:0012502~induction of programmed cell death	4.06E-03	BAK1, BIK, CD24, MCF2L, BCL2L11	7.266	0.904	0.154	5.803
GO:0008584~male gonad development	5.14E-03	BIK, BCL2L1, BCL2L11	26.912	0.949	0.179	7.287
GO:0044429~mitochondrial	5.26E-03	BAK1, CASP7, BIK, BCL2L1,	4.957	0.384	0.059	5.597

part		GPAM, BCL2L11				
GO:0042981~regulation of apoptosis	5.28E-03	BAK1, BIK, BCL2L1, DLG5, CD24, MCF2L, BCL2L11	4.061	0.953	0.174	7.480
GO:0043067~regulation of programmed cell death	5.54E-03	BAK1, BIK, BCL2L1, DLG5, CD24, MCF2L, BCL2L11	4.021	0.959	0.172	7.835
GO:0010941~regulation of cell death	5.64E-03	BAK1, BIK, BCL2L1, DLG5, CD24, MCF2L, BCL2L11	4.007	0.962	0.166	7.971
GO:0031966~mitochondrial membrane	6.73E-03	BAK1, CASP7, BCL2L1, GPAM, BCL2L11	6.239	0.463	0.067	7.113
Apoptosis	7.21E-03	BAK1, CASP7, BIK, BCL2L1, BCL2L11	6.311	0.512	0.512	7.707
GO:0016044~membrane organization	7.43E-03	BAK1, BCL2L1, CD24, EHD2, SH3GL2	6.122	0.986	0.202	10.370
GO:0046546~development of primary male sexual characteristics	7.93E-03	BIK, BCL2L1, BCL2L11	21.530	0.990	0.205	11.033
GO:0046661~male sex differentiation	9.92E-03	BIK, BCL2L1, BCL2L11	19.171	0.997	0.239	13.615
GO:0005829~cytosol	1.16E-02	BAK1, CASP7, UCHL1, BCL2L1, GPAM, MCF2L, BCL2L11, SH3GL2	2.957	0.659	0.102	11.981
GO:0008406~gonad development	2.23E-02	BIK, BCL2L1, BCL2L11	12.495	1.000	0.446	28.217
GO:0008624~induction of apoptosis by extracellular signals	2.23E-02	CD24, MCF2L, BCL2L11	12.495	1.000	0.446	28.217
GO:0007283~spermatogenesis	2.51E-02	HSPA2, BIK, BCL2L1, BCL2L11	6.058	1.000	0.472	31.205
GO:0048232~male gamete generation	2.51E-02	HSPA2, BIK, BCL2L1, BCL2L11	6.058	1.000	0.472	31.205
GO:0045137~development of primary sexual	2.82E-02	BIK, BCL2L1, BCL2L11	11.019	1.000	0.497	34.293

characteristics						
GO:0007548~sex differentiation	3.87E-02	BIK, BCL2L1, BCL2L11	9.268	1.000	0.597	43.999
GO:0009628~response to abiotic stimulus	3.96E-02	BAK1, CASP7, BCL2L1, MYOF	5.070	1.000	0.591	44.735
GO:0046907~intracellular transport	4.47E-02	BAK1, UCHL1, BCL2L1, CD24, SH3GL2	3.550	1.000	0.623	48.925
GO:0007276~gamete generation	4.72E-02	HSPA2, BIK, BCL2L1, BCL2L11	4.724	1.000	0.630	50.837
GO:0031090~organelle membrane	5.77E-02	MTMR2, BAK1, CASP7, BCL2L1, GPAM, BCL2L11	2.691	0.996	0.366	47.773
GO:0009314~response to radiation	6.40E-02	BAK1, CASP7, BCL2L1	6.997	1.000	0.731	62.117
GO:0019953~sexual reproduction	6.76E-02	HSPA2, BIK, BCL2L1, BCL2L11	4.074	1.000	0.739	64.224
GO:0032504~multicellular organism reproduction	7.82E-02	HSPA2, BIK, BCL2L1, BCL2L11	3.831	1.000	0.769	69.737
GO:0048609~reproductive process in a multicellular organism	7.82E-02	HSPA2, BIK, BCL2L1, BCL2L11	3.831	1.000	0.769	69.737
GO:0048534~hemopoietic or lymphoid organ development	1.00E-01	BAK1, CD24, BCL2L11	5.382	1.000	0.842	78.857
GO:0002520~immune system development	1.11E-01	BAK1, CD24, BCL2L11	5.070	1.000	0.864	82.215
GO:0006873~cellular ion homeostasis	1.81E-01	BAK1, BCL2L1, CD24	3.742	1.000	0.943	94.642
GO:0055082~cellular chemical homeostasis	1.85E-01	BAK1, BCL2L1, CD24	3.683	1.000	0.944	95.057
GO:0042592~homeostatic process	2.01E-01	BAK1, BCL2L1, CD24, BCL2L11	2.485	1.000	0.951	96.323
GO:0050801~ion homeostasis	2.07E-01	BAK1, BCL2L1, CD24	3.422	1.000	0.952	96.687

GO:0042127~regulation of cell proliferation	2.21E-01	MARCKSL1, BCL2L1, DLG5, CD24	2.371	1.000	0.956	97.447
mitochondrion	2.37E-01	BCL2L1, COQ7, GPAM, BCL2L11	2.312	1.000	0.978	95.029
GO:0019725~cellular homeostasis	2.51E-01	BAK1, BCL2L1, CD24	3.003	1.000	0.971	98.563
GO:0048878~chemical homeostasis	2.87E-01	BAK1, BCL2L1, CD24	2.733	1.000	0.983	99.299
membrane	3.83E-01	EHBP1, BCL2L1, COQ7, BCL2L11, MCF2L, MTMR2, BAK1, MARCKS, BIK, CD24, DLG5, EHD2, GPAM, MYOF, SH3GL2	1.153	1.000	0.987	99.527
GO:0005886~plasma membrane	4.68E-01	MARCKSL1, BCL2L1, DLG5, CD24, MYOF, EHD2, MCF2L, BCL2L11, SH3GL2	1.171	1.000	0.937	99.899
GO:0044459~plasma membrane part	6.47E-01	BCL2L1, DLG5, CD24, EHD2, MCF2L	1.116	1.000	0.967	99.999
cell membrane	6.64E-01	DLG5, CD24, MYOF, EHD2, MCF2L	1.096	1.000	1.000	99.999
GO:0031224~intrinsic to membrane	9.85E-01	BAK1, BIK, MARCKS, BCL2L1, CD24, GPAM, MYOF	0.627	1.000	1.000	100.000
transmembrane region	9.96E-01	BAK1, BIK, BCL2L1, GPAM, MYOF	0.486	1.000	1.000	100.000
transmembrane	9.96E-01	BAK1, BIK, BCL2L1, GPAM, MYOF	0.483	1.000	1.000	100.000
GO:0016021~integral to membrane	9.98E-01	BAK1, BIK, BCL2L1, GPAM, MYOF	0.464	1.000	1.000	100.000

Endocytosis	Enrichment Score: 1.328					
Term	P-Value	Genes	Fold Enrichment	Bonferroni	Benjamini	FDR
GO:0016044~membrane organization	7.43E-03	BAK1, BCL2L1, CD24, EHD2, SH3GL2	6.122	0.986	0.202	10.370
GO:0006897~endocytosis	7.55E-02	CD24, EHD2, SH3GL2	6.361	1.000	0.767	68.432
GO:0010324~membrane invagination	7.55E-02	CD24, EHD2, SH3GL2	6.361	1.000	0.767	68.432
GO:0016192~vesicle-mediated transport	1.15E-01	MARCKSL1, CD24, EHD2, SH3GL2	3.239	1.000	0.865	83.308

SH3 Domain	Enrichment Score: 1.132					
Term	P-Value	Genes	Fold Enrichment	Bonferroni	Benjamini	FDR
domain:SH3	5.05E-02	DLG5, MCF2L, SH3GL2	8.099	1.000	0.924	46.127
IPR001452:Src homology-3 domain	7.35E-02	DLG5, MCF2L, SH3GL2	6.518	1.000	0.978	57.159
SM00326:SH3	1.08E-01	DLG5, MCF2L, SH3GL2	5.115	0.971	0.830	62.537

Dimerization	Enrichment Score: 1.0482					
Term	P-Value	Genes	Fold Enrichment	Bonferroni	Benjamini	FDR
GO:0031090~organelle membrane	5.77E-02	MTMR2, BAK1, CASP7, BCL2L1, GPAM, BCL2L11	2.691	0.996	0.366	47.773
GO:0046983~protein dimerization activity	9.25E-02	MTMR2, BAK1, SPEF2, BCL2L1	3.549	1.000	0.991	65.818
GO:0042802~identical protein binding	1.34E-01	MTMR2, BAK1, BCL2L1, SH3GL2	3.005	1.000	0.991	79.690

Organelle Localization	Enrichment Score: 0.3876					
Term	P-Value	Genes	Fold Enrichment	Bonferroni	Benjamini	FDR
GO:0005730~nucleolus	1.54E-01	TSR1, TARDBP, UCHL1, MYEF2	2.817	1.000	0.666	83.830
GO:0031981~nuclear lumen	3.13E-01	TSR1, TARDBP, CASP7, UCHL1, MYEF2	1.695	1.000	0.885	98.357
GO:0070013~intracellular organelle lumen	4.67E-01	TSR1, TARDBP, CASP7, UCHL1, MYEF2	1.382	1.000	0.945	99.896
GO:0043233~organelle lumen	4.85E-01	TSR1, TARDBP, CASP7, UCHL1, MYEF2	1.351	1.000	0.930	99.930
GO:0031974~membrane-enclosed lumen	5.02E-01	TSR1, TARDBP, CASP7, UCHL1, MYEF2	1.324	1.000	0.923	99.950
GO:0043228~non-membrane-bounded organelle	5.95E-01	TSR1, TARDBP, UCHL1, MYEF2, MARCKS, MYOF	1.136	1.000	0.954	99.995
GO:0043232~intracellular non-membrane-bounded organelle	5.95E-01	TSR1, TARDBP, UCHL1, MYEF2, MARCKS, MYOF	1.136	1.000	0.954	99.995

Cellular Localization	Enrichment Score: 0.3586					
Term	P-Value	Genes	Fold Enrichment	Bonferroni	Benjamini	FDR
GO:0000267~cell fraction	3.57E-01	CASP7, CD24, EHD2, BCL2L11	1.816	1.000	0.908	99.191
GO:0005624~membrane fraction	4.76E-01	CD24, EHD2, BCL2L11	1.823	1.000	0.933	99.914
GO:0005626~insoluble fraction	4.95E-01	CD24, EHD2, BCL2L11	1.758	1.000	0.927	99.943

Metal Ion Binding	Enrichment Score: 0.1408					
Term	P-Value	Genes	Fold Enrichment	Bonferroni	Benjamini	FDR
calcium	2.22E-01	EGFL6, PLA2G12A, PLA2G12B, EHD2	2.395	1.000	0.984	93.775
GO:0005509~calcium ion binding	2.78E-01	EGFL6, PLA2G12A, PLA2G12B, EHD2	2.093	1.000	0.998	97.290
Secreted	8.68E-01	EGFL6, PLA2G12A, PLA2G12B	0.854	1.000	1.000	100.000
metal-binding	8.73E-01	BAK1, ELOF1, PLA2G12A, PLA2G12B, COQ7	0.809	1.000	1.000	100.000
GO:0046872~metal ion binding	8.83E-01	BAK1, EGFL6, ELOF1, PLA2G12A, PLA2G12B, COQ7, EHD2	0.813	1.000	1.000	100.000
GO:0043169~cation binding	8.89E-01	BAK1, EGFL6, ELOF1, PLA2G12A, PLA2G12B, COQ7, EHD2	0.805	1.000	1.000	100.000
GO:0043167~ion binding	8.98E-01	BAK1, EGFL6, ELOF1, PLA2G12A, PLA2G12B, COQ7, EHD2	0.794	1.000	1.000	100.000
GO:0005576~extracellular region	9.22E-01	EGFL6, PLA2G12A, PLA2G12B	0.734	1.000	1.000	100.000
signal	9.71E-01	EGFL6, PLA2G12A, PLA2G12B, CD24	0.592	1.000	1.000	100.000
signal peptide	9.72E-01	EGFL6, PLA2G12A, PLA2G12B, CD24	0.588	1.000	1.000	100.000
GO:0046914~transition metal ion binding	9.85E-01	BAK1, ELOF1, COQ7	0.518	1.000	1.000	100.000

Transcription Factor Activity	Enrichment Score: 0.0934					
Term	P-Value	Genes	Fold Enrichment	Bonferroni	Benjamini	FDR
GO:0003700~transcription factor activity	5.92E-01	MEOX2, TARDBP, MYEF2	1.480	1.000	1.000	99.995
GO:0030528~transcription regulator activity	8.23E-01	MEOX2, TARDBP, MYEF2	0.954	1.000	1.000	100.000
dna-binding	9.04E-01	MEOX2, TARDBP, MYEF2	0.772	1.000	1.000	100.000
GO:0003677~DNA binding	9.61E-01	MEOX2, TARDBP, MYEF2	0.619	1.000	1.000	100.000

Nucleotide Binding	Enrichment Score: 0.07179					
Term	P-Value	Genes	Fold Enrichment	Bonferroni	Benjamini	FDR
GO:0000166~nucleotide binding	6.81E-01	HSPA2, RABL5, TARDBP, MYEF2, EHD2	1.07	1.000	1.000	100.000
nucleotide-binding	8.68E-01	HSPA2, RABL5, EHD2	0.86	1.000	1.000	100.000
GO:0032555~purine ribonucleotide binding	9.00E-01	HSPA2, RABL5, EHD2	0.79	1.000	1.000	100.000
GO:0032553~ribonucleotide binding	9.00E-01	HSPA2, RABL5, EHD2	0.79	1.000	1.000	100.000
GO:0017076~purine nucleotide binding	9.14E-01	HSPA2, RABL5, EHD2	0.75	1.000	1.000	100.000

Appendix B:DAVID Analysis of Gene Ontology Enrichment. Genes are grouped into clusters based on their main function (ie: Cell Death Signalling). The enrichment score for each cluster is the geometric mean of the P value enrichment. Term column designates the Gene Ontology identifier. P-Value is Fisher Exact P score associated significance of enrichment in that function. Genes are given as official gene symbol. Fold enrichment is the ratio of genes involved in a GO term divided by the total number of input genes divided by the total number of genes in the background data set involved in that GO term, divded by the total number of background genes. Bonferroni and Benjamini values are multiple testing corrected P-values and FDR is the false discovery rate.